

University of Montana

## ScholarWorks at University of Montana

---

Graduate Student Theses, Dissertations, &  
Professional Papers

Graduate School

---

2008

### Structure Activity Relationships for Intracellular Loop 2 of the 5HT1A Serotonin Receptor

Brian Patrick Hall  
*The University of Montana*

Follow this and additional works at: <https://scholarworks.umt.edu/etd>

**Let us know how access to this document benefits you.**

---

#### Recommended Citation

Hall, Brian Patrick, "Structure Activity Relationships for Intracellular Loop 2 of the 5HT1A Serotonin Receptor" (2008). *Graduate Student Theses, Dissertations, & Professional Papers*. 920.  
<https://scholarworks.umt.edu/etd/920>

This Dissertation is brought to you for free and open access by the Graduate School at ScholarWorks at University of Montana. It has been accepted for inclusion in Graduate Student Theses, Dissertations, & Professional Papers by an authorized administrator of ScholarWorks at University of Montana. For more information, please contact [scholarworks@mso.umt.edu](mailto:scholarworks@mso.umt.edu).

STRUCTURE ACTIVITY RELATIONSHIPS FOR INTRACELLULAR LOOP 2 OF  
THE 5HT1A SEROTONIN RECEPTOR

By

BRIAN PATRICK HALL

BA Geography, The University of Montana, Missoula, Montana, 2002  
Doctorate of Pharmacy, The University of Montana, Missoula, Montana, 2006

Dissertation

Presented in partial fulfillment of the requirements  
for the degree of

Doctorate of Philosophy  
in Pharmacology/Pharmaceutical Sciences

The University of Montana  
Missoula, MT

May 2008

Approved by:

Dr. David A. Strobel, Dean  
Graduate School

Dr. Keith K. Parker, Chair  
Department of Biomedical and Pharmaceutical Sciences

Dr. Jerry Smith  
Department of Biomedical and Pharmaceutical Sciences

Dr. Kathleen George  
Department of Biomedical and Pharmaceutical Sciences

Dr. John Gerdes  
Department of Biomedical and Pharmaceutical Sciences

Dr. Jean Carter  
Department of Pharmacy Practice

## ABSTRACT

Hall, Brian, Ph.D., May 2008

Pharmacology/Pharmaceutical Sciences

### Structure Activity Relationships for Intracellular Loop 2 of the 5HT1A Serotonin Receptor

Chairperson: Dr. Keith Parker

The human (H) serotonin (5-hydroxytryptamine; 5HT) 1a receptor (R) has been implicated in various physiological processes such as mood regulation, vascular and temperature control, anxiety, depression, and migraine headache. This seven transmembrane domain (7TMD), G protein-coupled receptor (GPCR) is negatively coupled to adenylyl cyclase (AC). This work was designed to better understand the coupling and activation requirements of intracellular loop 2 (ic2) with Gi in Chinese Hamster Ovary (CHO) cells. 10 MER peptides that are derived from the known sequence of the cloned receptor have been used as probes and the current study includes peptides P21 to P27 of ic2 (LDRYWAITDPIDYVKNKRTPRPR), approaching the ic2 carboxy terminus of TMD4 two residues per 10 MER. Peptide ability to uncouple receptor from G protein was determined in agonist inhibition studies using the selective 5HT1aR agonist [<sup>3</sup>H]8-OH-DPAT. Peptides P21 to P23 uncoupled the G protein from the receptor to 50% of control. Peptides P24 to P27 uncoupled the G protein from the receptor to 6-15% of control. Peptide capacity to alter signal transduction was measured using enzyme-linked assays of intracellular cyclic AMP (cAMP) and assays quantifying incorporation of [<sup>35</sup>S]-γ-Guanosine Triphosphate (GTP). Peptides closer to TMD3, but in the C-terminal aspect of ic2, were capable of uncoupling the receptor-G protein, suggesting a role for that region of the native receptor in G protein coupling (and activation). The final peptides in this region, P25 to P27 are relatively inactive with respect to G protein coupling and activation. Thus, we propose that the immediate ic2/TMD4 interface is beyond the receptor segment involved in coupling. Peptides P22-P24 were the most active with respect to stimulation of [<sup>35</sup>S]-γ-GTP incorporation and decreasing cAMP concentration, therefore they were chosen for a thermodynamic binding study. The K<sub>d</sub> for [<sup>3</sup>H]8-OH-DPAT was measured over a range of temperatures, which allowed the calculation of Standard Gibb's Free energy ( $\Delta G^\circ$ ), enthalpy ( $\Delta H^\circ$ ), and entropy ( $\Delta S^\circ$ ). The peptides increased the enthalpy and entropy of the system. These results contribute to structural information about 5HT1aR's interaction with Gi derived from a number of different, but compatible techniques. The developing model for ic2 (and ic3) loop-G protein regulation has implications for developing new therapeutic drugs for serotonergic pathologies such as the affective disorders.

## TABLE OF CONTENTS

Abstract.....	ii
Table of Contents.....	iii
List of Figures.....	iv
List of Tables.....	v
Serotonin Introduction.....	1
Experimental Methods.....	12
5HT1AR Intracellular Loop 2 Signal Transduction.....	18
5HT1AR Intracellular Loop 3 Signal Transduction.....	41
Discussion: H5HT1AR ic2 and ic3 Signal Transduction.....	50
References.....	70
Appendices.....	79
Appendix A: Cannabinoids.....	80
Appendix B: Bacopa.....	94
Appendix C: Cell Volume.....	102

## LIST OF FIGURES

Figure 1: Schematic of Human 5HT1a Receptor.....	4
Figure 2: 5HT1a Receptor High Affinity Ligand Binding.....	7
Figure 3: P11 Agonist 8-OH-DPAT Binding Displacement.....	20
Figure 4: P11 G Protein Activation Activity.....	20
Figure 5: P11 Changes Kd of 8-OH-DPAT at 25 °C and 35 °C.....	21
Figure 6: P21 Concentration Dependent Displacement of Bound 8-OH-DPAT.....	22
Figure 7: Concentration Dependent Changes in 8-OH-DPAT Binding for P23 and P25..	23
Figure 8: P23 Kd Plot at 15 °C and 30 °C.....	26
Figure 9: Van't Hoff plot for P22, P23, and P24.....	28
Figure 10: ic2 Peptide Effect on $\gamma$ -[ <sup>35</sup> S]-GTP incorporated into G <sub>i</sub> .....	31
Figure 11: ic2 Peptide Effect on Forskolin Stimulated cAMP Production.....	33
Figure 12: Low Affinity Versus High Affinity Ligand Binding.....	35
Figure 13: P12 Dependent Displacement of Specifically Bound 8-OH-DPAT.....	44
Figure 14: P12 Stimulated Incorporation of $\gamma$ -[ <sup>35</sup> S]-GTP.....	45
Figure 15: P13 Stimulated Incorporation of $\gamma$ -[ <sup>35</sup> S]-GTP.....	45
Figure 16: P12 and P13 Effect of Forskolin Stimulated cAMP Production.....	46
Figure 17: Isoprene.....	80
Figure 18: Cannabidiol and Serotonin.....	81
Figure 19: Ketanserin Displacement by Hemp Oil at 5HT2a Receptor.....	84
Figure 20: Terpene Components of Hemp Oil Effect on Ketanserin Binding.....	85
Figure 21: Terpene Effect on Ketanserin Binding.....	86
Figure 22: Cannabidiol and THC Displacement of Bound Ketanserin.....	88
Figure 23: Cannabidiol and THC Effect on 8-OH-DPAT Binding.....	89
Figure 24: Cannabidiol Effect on Incorporation of [ <sup>35</sup> S]- $\gamma$ -GTP into G <sub>ai</sub> .....	90
Figure 25: Cannabidiol Effect on Intracellular cAMP Concentration.....	91
Figure 26: Bacopa monniera (Brahmi).....	95
Figure 27: A Comparison of Bacopa Extracted in Water Versus Ethanol.....	96
Figure 28: Effect of Bacopa Extracts on Specific Binding of 8-OH- DPAT.....	97
Figure 29: Effect of Bacopa Extracts on Specific Binding of Ketanserin .....	98
Figure 30: Bacopa Effect on Intracellular cAMP Concentration .....	99
Figure 31: Serotonergic Effect on Cell Volume of Primary Astrocytes.....	106
Figure 32: Serotonin Receptor Population of Primary Rat Astrocytes.....	107
Figure 33: MKC 5HT1a Receptor Binding.....	110
Figure 34: Buspirone Effect on MCK Cell Volume.....	112
Figure 35: Intracellular Loop 2 (ic2) of 5HT1aR.....	114

## LIST OF TABLES

Table 1: ic2 Peptide Mimics.....	21
Table 2: ic2 Peptide Mimic Effect on 8-OH-DPAT Binding.....	23
Table 3: ic2 Peptide Mimic Effect on Kd of 8-OH-DPAT.....	25
Table 4: ic2 Peptide Mimic Effect on Gibb's Free Energy, Enthalpy, and Entropy of 8-OH-DPAT.....	29
Table 5: ic2 Peptide Mimic Effect on $\gamma$ -[ <sup>35</sup> S]-GTP into G <sub>iα</sub> .....	31
Table 6: ic2 Peptide Mimic Effect on cAMP Concentration.....	34
Table 7: ic3 Peptide Mimics.....	42
Table 8: ic3 Peptide Mimic Signal Transduction Data.....	43

## SEROTONIN INTRODUCTION

The molecule, serotonin (5-HT, 5-hydroxytryptamine), was discovered after its effect on vasoconstriction and platelet aggregation during the clotting process was noted (Raymond et al., 1999; De Clerck, 1990). Since that time, it has been shown that serotonin has important roles in multiple biological systems as a neurotransmitter and a paracrine autacoid factor. Serotonergic dysfunction has been implicated in multiple disease states for which treatments have been developed including depression, obsessive-compulsive disorder, migraine headache, and emesis (Cowen, 2000; Pietrobon, 2003; Mann, 2005; Feeney et al., 2007). Reserpine and ergot alkaloids were two of the first agents, which were used clinically. Reserpine was used as an antihypertensive agent, which worked by depletion of the monoamine neurotransmitters (noradrenaline, dopamine, serotonin). Depression was a notable side effect, however, due to the decrease in serotonin levels in the central nervous system (CNS) (Webster et al., 1996). The ergot derivatives, ergotamine and ergonovine, are potent vasoconstrictors used for treating vascular headaches (migraine) and post-partum hemorrhage (McCarthy et al., 1989; Mousa et al., 2007). The involvement of these therapeutic agents in modulating serotonergic transmission was only discovered long after they had been in use. Their efficacy provides clinical evidence of their mechanism of action.

Serotonin is synthesized in a two-step process that begins with the amino acid L-tryptophan. The first, and rate-limiting, step in the conversion is the hydroxylation of L-tryptophan by tryptophan hydroxylase (TPH), followed by the decarboxylation of L-5-hydroxytryptophan by L-aromatic amino acid decarboxylase. The serotonin molecule can then be metabolized in two ways. It can be converted in a two-step process to

melatonin or oxidized by monoamine oxidase (MAO B) with final enzymatic conversion to 5-hydroxyindoleacetic acid (5-HIAA) or 5-hydroxy-tryptophol (Sanders-Bush et al., 2001).

Metabolism of serotonin does not occur in the neuronal synapse; rather it involves the serotonin reuptake transporter (SERT) that clears serotonin from the synapse from which it is either recycled by storage in vesicles or fed into the metabolic pathway. The development of selective SERT inhibitors (fluoxetine, paroxetine, citalopram, escitalopram) led to a revolution in the treatment of major depressive disorder, obsessive compulsive disorder, and panic disorder with fewer side effects than the monoamine oxidase inhibitors (MAOI) and tricyclic antidepressants (TCA) (Taylor et al., 2006).

Following the initial discovery of the serotonin molecule, it was recognized that a receptor protein mediated its actions. Using pharmacological binding assays with [<sup>3</sup>H]-5-HT the specific tissues in which the receptor are expressed were identified (central nervous system, vascular smooth muscle, gastrointestinal tract). However, it soon became apparent by their differing binding affinities for [<sup>3</sup>H]-5-HT that a homogeneous serotonin receptor population did not exist across all tissues. The development of specific agonist and antagonist ligands (8-OH-DPAT, sumatriptan, ketanserin) was the first means available to classify the receptors into distinct subgroups (Hoyer et al., 1994; Peroutka, 1994; Barnes et al., 1999; Schnellmann, 1984).

cDNA cloning and other molecular biology techniques have allowed for a more robust classification system based upon the primary structure of the individual receptor proteins. It has also led to the discovery of new receptor subtypes. There are currently seven recognized families of 5-HT receptors, which include a number of structurally and



pharmacologically distinct receptor subtypes, for a total of 14 known receptors. All of the receptors are 7 transmembrane domain (7TMD) G protein-coupled receptors (GPCRs), except the 5-HT<sub>3</sub> receptor family, which is a ligand-gated ion channel. The 5-HT<sub>3</sub> receptor is structurally related to other ligand gated ion channels such as the nicotinic acetylcholine receptor, GABA<sub>A</sub> receptor, and the glycine receptor, all of which use a disulfide bond (Cys-Cys) to form a gating loop for their respective ion channels (Barnes, 1999).

The linear polypeptide of the seven transmembrane domain receptors passes through the cell membrane in a serpentine fashion seven times (See Figure 1 for example; 5HT1a receptor). The peptide's amino terminus is extracellular and the carboxy terminus is usually intracellular, although it can be inserted into the cell membrane. This creates three distinct regions, which are able to influence the protein's secondary and tertiary structure. These regions are the extracellular loops, which are important for ligand binding, the transmembrane domains, which are important for tertiary structure, and the intracellular loops that are important for coupling to and activation of the G protein (Raymond et al., 1999; Baldwin 1994).

G proteins are heterotrimeric guanosine diphosphate (GDP) binding proteins consisting of  $\alpha$ ,  $\beta$ , and  $\gamma$  subunits. The  $\beta$  and  $\gamma$  subunits are tightly linked to each other to form a dimer. The signal transduction system that is modified by the activation of the receptor and G protein coupled to it depends on its  $\alpha$  subunit. The  $G_\alpha$  subunit is responsible for binding to GDP and guanosine triphosphate (GTP). The 3 most common  $G_\alpha$  subunits are  $G_{\alpha s}$ ,  $G_{\alpha i}$ ,  $G_{\alpha q}$ . All  $G_\alpha$  subunits possess GTPase activity; this means they are able to catalyze the hydrolysis of the  $\gamma$  phosphodiester bond of GTP yielding GDP

and phosphate (Pi).  $G_{\alpha s}$  activation results in increased intracellular cAMP concentrations and protein kinase A (PKA) activity.  $G_{\alpha i}$  activation results in decreased intracellular cAMP concentrations and PKA activity.  $G_{\alpha q}$  activation results in increased inositol triphosphate (IP3) and diacylglycerol (DAG) concentrations as well as increased protein kinase C (PKC) activity. The  $G_{\beta\gamma}$  subunits are regulators of ion conductance into the cell (Gilman, 1987; Stryer, 1986; Dolphin, 2003).

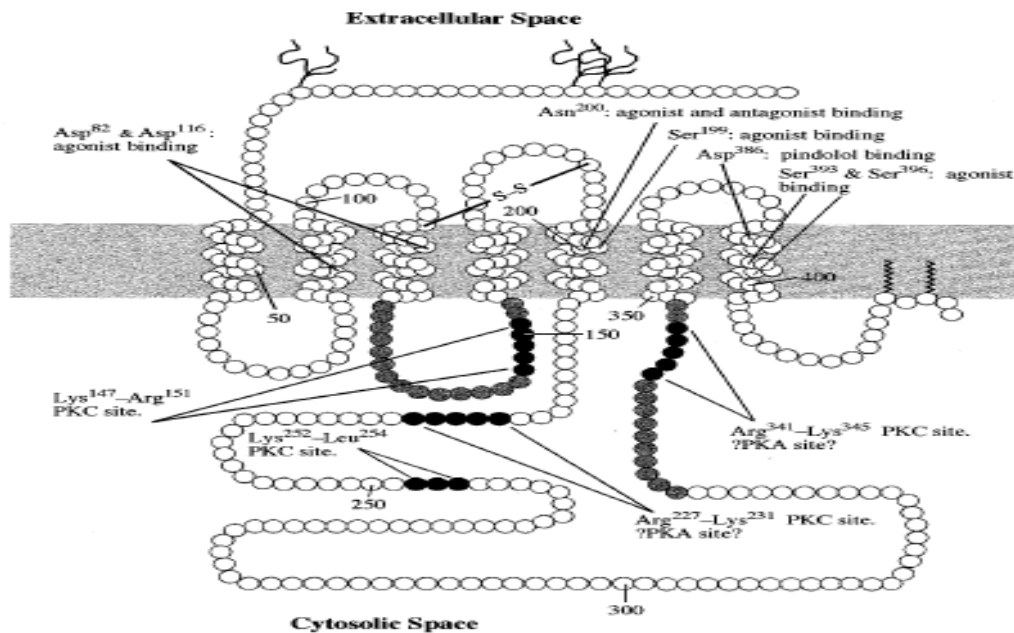


**Figure 1: Schematic of Human 5HT1a Receptor**

A representation of the human 5HT1a receptor protein. From Raymond et al., 1999. Intracellular loop (ic) 2 and 3, shown below the gray cell membrane, are the focus of the following studies. See also Figure 35.

G protein activity is regulated by the guanine nucleotide exchange factors (GEF) family and GTPase activating proteins (GAP) family. GEFs act to promote the exchange of GDP for GTP, which activates the G protein. GAPs increase the rate of hydrolysis of GTP by  $G_{\alpha}$ , which deactivates the G protein (Narumiya, 1996).

Ligand binding to a G protein-coupled receptor is influenced by the receptor's affinity state (in this case 5-HT or 8-OH-DPAT to 5-HT<sub>1A</sub> receptor). The affinity state is referred to as a high affinity or low affinity ligand binding state (Figure 2). The high affinity ligand binding state occurs when the receptor protein has the G protein bound to (coupled) to its intracellular loops. In this state the most robust binding interaction of the ligand or agonist can occur, activating the G protein mediated signal transduction cascade. The low affinity ligand binding state occurs when the receptor protein does not have the G protein bound to (coupled) its intracellular loops. The ligand or agonist is still able to bind to the receptor in this state, but the interaction is less robust, and it is not possible to activate the G protein mediated signal transduction cascade (Maguire et al., 1976; Peroutka et al., 1979).

The sequence of events from ligand receptor binding to activation of the signal transduction cascade is dependent on all of the players being in the right place at the right time. The sequence begins with a ligand finding a receptor coupled to its G protein (which has GDP bound in its  $G_{\alpha}$  subunit), thus in its high affinity state. The ligand binds to the receptor-G protein complex, which induces a conformational change in the receptor protein. This change in shape is transmitted to the G protein, which causes a conformational change in the  $G_{\alpha\beta\gamma}$  subunits. The change in the  $G_{\alpha}$  subunit is of particular interest because it lowers the protein's affinity for the GDP, which up until now has been

bound in its active site. With the  $G_{\alpha}$  active site now unoccupied, it is available to bind a GTP molecule. The GTP-  $G_{\alpha}$  interaction induces another conformational change leading to the dissociation of  $G_{\alpha}$  from  $G_{\beta\gamma}$ . The freed  $G_{\alpha}$  subunit can then, depending on its type ( $G_{\alpha s}$ ,  $G_{\alpha i}$ ,  $G_{\alpha q}$ ), influence changes in its second messenger system (cAMP, IP3 and DAG) and activate various protein kinases. The freed  $G_{\beta\gamma}$  subunit can now interact with ion channels and increase the conductance of ions into the cell affecting the cell's electrical membrane potential (Stryer 1986, Dolphin 2003).



The signal transduction cascade is a complex process involving multiple proteins and cofactors. The complexity of this cascade presents multiple points for possible pathology, and opportunities for intervention. There are two ways in which the system can be changed, mutations in the receptor protein or mutations in the G proteins, to which they couple. Mutations in receptor proteins have been identified as the cause of several diseases. X-linked nephrogenic diabetes insipidus is caused by mutations in the arginine vasopressin receptor (V2); its ligand arginine vasopressin is also known as antidiuretic hormone. This receptor mutation disables the kidneys' ability to reabsorb water in the nephron, causing excessive water loss and low urine osmolality (dilute). An example of disease caused by G protein dysfunction due to a mutation in the  $G_{\alpha s}$  subunit, which inactivates it, is associated with pseudohypoparathyroidism. Pseudohypoparathyroidism leads to the development of resistance to the glycoprotein hormones thyroid stimulating hormone (TSH), luteinizing hormone (LH), follicle stimulating hormone (FSH), and parathyroid hormone (PTH). TSH resistance leads to symptoms of hypothyroidism (loss of hair, bradycardia, hypothermia), LH and FSH resistance leads to reproductive problems, and PTH resistance leads to the loss of calcium homeostasis in the body (Schoneberg et al., 2004; Spiegel et al., 2003).

A group looking for more receptor subtypes in the  $\beta$ -adrenergic receptor family first cloned the 5-HT<sub>1A</sub> receptor from an intronless gene product and is 422 amino acids in length (Fargin et al., 1988). The peptide's carboxy terminus re-inserts into the membrane creating a 4th intracellular loop via palmitoylation at cysteine residues (Raymond et al., 1999). The similar homology between these receptors is evident by the ability of selected  $\beta$ -adrenergic ligands (pindolol, propranolol) to also act as ligands at the

5-HT<sub>1A</sub> receptor (Kuipers et al., 1997; Sprouse et al., 1986), which was found to be due to the conservation of the Asn 385 in the 7<sup>th</sup> transmembrane domain of both receptors (Guan et al., 1992). This was discovered by the generation of receptor clones with point mutations of one amino acid at a time. The 5-HT<sub>1A</sub> receptor is found in neural tissue of the central nervous system at highest concentrations in the hippocampus, septum, frontal cortex, and dorsal raphe nucleus (Lanfumeey et al., 2000).

Following the activation of the 5-HT<sub>1A</sub> receptor in the hippocampus, septum, and frontal cortex by 5-HT or other agonists, the receptor associated neurons are hyperpolarized. In these regions the receptor is found post-synaptically and on serotonergic neuron terminals pre-synaptically. The activation of the receptors in the dorsal raphe nucleus by 5-HT also results in the hyperpolarization of neurons. However, it has the added effect of decreasing the release of 5-HT in the forebrain region. This is likely due to the actions of the 5-HT<sub>1A</sub> autoreceptor (Price et al., 1996). The affect of 5-HT on the release of other neurotransmitters has also been noted. It has been shown that post-synaptic 5-HT<sub>1A</sub> receptors increase the release of acetylcholine in the cortex and hippocampus. The release of noradrenaline is increased in the hypothalamus, hippocampus, frontal cortex, and ventral tegmental area following activation of the 5-HT<sub>1A</sub> receptor. The physiological and behavioral actions mediated by the 5-HT<sub>1A</sub> receptor include hyperphagia, hypothermia, alterations in sexual behavior, and clinical use of 5-HT agonists as anxiolytics and antidepressants (Barnes et al., 1999).

The human 5-HT<sub>1A</sub> receptor is negatively coupled to adenylyl cyclase (AC) by the G<sub>i</sub> protein (Raymond et al., 1992; Fargin et al., 1989). There are 8 isoforms identified for adenylyl cyclase (AC1-AC8). The isoforms are differentially expressed in many tissues,

AC1 and AC8 expressed in neural tissue and AC5 in heart and brain. The isoforms AC1, AC3, AC5 and AC6 are sensitive to inhibition by  $G_{\alpha_i}$ . This selectivity is due to the post-translational N-terminal fatty acylation of  $G_{\alpha_i}$  protein. All known AC isoforms are stimulated to produce cAMP by the diterpine natural product forskolin (FSK) (Simonds, 1999).

The AC enzyme is embedded in the cell membrane which the protein spans 12 times. AC has two catalytic subunits lying along the inside of the cell membrane (Simonds, 1999). Upon stimulation of AC by  $G_{\alpha_s}$ , the catalytic subunits transform adenosine triphosphate (ATP) to cyclic adenosine monophosphate (cAMP). AC cleaves the two terminal phosphates (PPi) off ATP by a nucleophilic attack of the 3' ribose hydroxyl oxygen on the  $\alpha$  phosphate creating cAMP and PPi. The activity of the catalytic subunits is regulated by interactions with  $G_{\alpha_s}$  and  $G_{\alpha_i}$  (Sinha et al., 2006). cAMP is converted to adenosine monophosphate (AMP) by the phosphodiesterase enzyme subtype, inactivating it as a second messenger signaling molecule (Omori et al., 2007).

The 5-HT<sub>1A</sub> receptor selectivity couples to the  $G_i$  protein; it has been shown that this is due to palmitoylation of cysteine residues near the carboxy terminus (Raymond et al., 1999). Activation of the 5-HT<sub>1A</sub> receptor causes the intracellular levels of cyclic adenosine monophosphate (cAMP) to fall. The decreased cAMP production by AC is due to the interaction with the G-protein subunit  $G_{\alpha_i}$ . It is also able to hyperpolarize neurons by opening voltage gated calcium channels (N- and P/Q-types). These channels are opened upon interaction with  $G_{\beta\gamma}$  subunit (Dolphin, 2003).



Understanding the relationship between the receptor protein and its G protein is important to elucidating the mechanism of signal transduction. Which parts of the receptor's intracellular loops are important for coupling to the G protein? Which are important for activation of the G protein? One method of assessing this is the use of peptide mimics of the receptor of interest's intracellular loops. Peptidomimetics (varying in amino acid length of the intracellular loops) have been used to examine G protein coupling and activation in  $\alpha_{2A}$  adrenergic,  $\beta_2$  adrenergic, and  $\delta$  opioid receptor systems (Taylor et al., 1994; Munch et al., 1991; Merkouris et al., 1996).

## EXPERIMENTAL METHODS

### Cell Culture

Chinese hamster ovarian (CHO) cells expressing the human 5HT1aR were cultured in Ham's F-12 medium fortified with 10% fetal calf serum and 200 µg/ml geneticin in 75 or 175 cm<sup>2</sup> flasks. Cultures were maintained at 37 °C in a humidified atmosphere of 5% CO<sub>2</sub>. Cells were subcultured or assayed upon confluency (5–8 days). CHO cells with cloned human 5HT1aR was kindly provided by Dr. John Raymond (Medical University of South Carolina). NIH 3T3 cells expressing the rat 5-HT2aR were cultured under similar conditions in DMEM fortified with 10% calf serum and 200 µg/ml geneticin. These transfected cells were generously provided by Dr. David Julius (UCSF). Both cell lines have been tested for mycoplasma with a PCR kit (ATCC), and are free of contamination.

### Receptor Preparation

Cells were harvested by the removal of culture medium followed by the addition of a 0.25% trypsin solution. Upon the removal of the cell monolayer, an equal volume of ice-cold culture medium was added to the cell-trypsin solution. The resulting cell suspension was centrifuged at low speed (3000 rpm) in ice-cold medium for 10 minutes. The pellet was re-suspended in ice-cold Earle's balanced salt solution followed by centrifugation (3000 rpm) for 10 minutes. The cell pellet was re-suspended in 10 ml of ice-cold binding buffer (50 mmol/l Tris, 4 mmol/l CaCl<sub>2</sub>, 10 µmol/l pargyline, pH 7.4), homogenized with Teflon-glass homogenizer, and centrifuged at 450,000 g at 4 °C. To produce a crude membrane preparation, the pellet was re-suspended in 30 ml of ice-cold

binding buffer, and homogenized, first with Teflon-glass then with a Polytron (setting 4) for 5 seconds. The receptor preparation was stored on ice and assayed within the next 1.5 hour.

#### Assay of Receptor Activity

Binding of the agonist [<sup>3</sup>H]8-OH-DPAT ([<sup>3</sup>H]8-hydroxy-2-(di-*n*-propylaminotetralin)) to H5-HT<sub>1a</sub>R followed well-characterized *in vitro* protocols (Thiagaraj et al., 2007). Radioligands were purchased from New England Nuclear (Boston, Mass., USA). The experimental 1 ml reaction mixtures, in triplicate, were incubated for 30 minutes in a 30 °C water shaker bath. The composition of the 1 ml reaction mixture was:

Experimental controls: 700 µl of receptor preparation; 100 µl of either binding buffer (for total ligand binding) or 10 µM 5HT (final concentration for non-specific ligand binding), 100 µl of the tritiated agent (final concentration of 0.5 nmol/l [<sup>3</sup>H]8-OH-DPAT), and 100 µl of binding buffer in the case of controls.

DPT (dipropyltryptamine) Experiments: 700 µl of receptor preparation; 100 µl of either binding buffer (for total ligand binding) or 10 µmol/l 5-HT (final concentration for non-specific ligand binding), 100 µl of the tritiated agent (final concentration of 0.5 nmol/l [<sup>3</sup>H]8-OH-DPAT), and 100 µl diluted DPT (dipropyltryptamine). In the case of experiments that varied in both DPT concentration and [3 H]8-OH-DPAT concentration, the following radioligand concentrations were used: 0.2, 0.4, 0.6, 0.8, and 1.0 nmol/l. Reactions were stopped by addition of 4 ml of ice-cold 50 mmol/l Tris buffer, pH 7.4, and subsequent vacuum filtration on glass fiber filters (Whatman GF/B). Filters were rinsed twice in 5 ml of ice-cold Tris buffer, dried, and counted in 5 ml of Ecoscint

(National Diagnostics) liquid scintillation fluid in a Beckman LS 6500 instrument.

Homogenates were assayed for protein (Bradford, 1976) to maintain a nominal value of 50 µg protein per filter over weekly assays. Total and non-specific binding tubes were run in triplicate.

Peptide Experiments: 700 µl of receptor preparation; 100 µl of either binding buffer (for total ligand binding) or 10 µmol/l 5-HT (final concentration for non-specific ligand binding), 100 µl of the tritiated agent (final concentration of 0.5 nmol/l [<sup>3</sup>H]8-OH-DPAT), and 100 µl diluted peptide (30 µmol/l). Reactions were stopped and data was gathered as in the DPT experiments above.

#### cAMP Assay

These experiments were a measure of G<sub>ic</sub> regulatory effects on adenylyl cyclase. CHO cells were cultured to confluency in 12- or 24-well plates. Culture medium was aspirated and the cells were rinsed twice in warm serum-free F-12 medium. Cells were then incubated for 20 min at 37 °C in 0.5 ml of serum-free F-12 medium containing 100 µmol/l isobutylmethylxanthine (IBMX) and the following substances (final concentrations) alone or in combination: 30 µmol/l forskolin (FSK)(for all treatments); 1–10 µmol/l 5-HT; 0.1–1 µmol/l DPT or peptide (30 µmol/l). Reactions were stopped by aspiration of medium and addition of 0.5 ml of 100 mmol/l HCl. Following a 10 minute incubation, well contents were removed and centrifuged at 4,000 rpm. The pellets were discarded and the resulting supernatants were diluted in 100 mmol/l HCl, and cAMP was quantified (Thiagaraj et al., 2007) directly in a microplate format by colorimetric enzyme immunoassay using a kit from Assay Designs (Ann Arbor, Mich., USA). Triplicate

independent samples at a minimum were assayed in quadruplicate, yielding an n of 12 for each tested condition.

#### $\gamma$ -S-GTP Incorporation

These experiments were a measure of the activation of the G protein (Thiagaraj et al., 2005). H5-HT1aR membranes from transfected CHO cells were incubated with 5-HT (0.1  $\mu$ mol/l) and/or DPT (0.1–1,000  $\mu$ mol/l) or peptide (30  $\mu$ mol/l), and the following incubation mixture: 20 mmol/l HEPES buffer, pH 7.4 (5 mmol/l MgCl<sub>2</sub>, 1 mmol/l EDTA, 1 mmol/l DTT, 100 mmol/l NaCl, 100  $\mu$ mol/l GDP, 10  $\mu$ mol/l pargyline, 0.2 mmol/l ascorbate, and 0.1 nmol/l [<sup>35</sup>S]- $\gamma$ -S-GTP. The mixtures were incubated for 30 min at 30 °C, and were terminated by dilution in ice-cold buffer. The reaction mixture was filtered on GF/C filters, and rinsed twice in ice-cold buffer, followed by drying and liquid scintillation counting. The negative control (basal incorporation of GTP) was the above mixture minus DPT or peptide or 5-HT. The non-specific binding was determined in the presence of cold  $\gamma$ -S-GTP (10  $\mu$ mol/l). Positive control was H5-HT1aR membranes in the same incubation mixture plus 5-HT. The calculation for specific binding = total binding – non-specific binding; all experimental conditions were run in triplicate.

#### Studies of concentration-dependent inhibition of [<sup>3</sup>H]8-OH-DPAT binding

Concentration-dependency was studied as described for agonist binding assays in membrane bound preparations, except that [<sup>3</sup>H]8-OH-DPAT concentrations were varied in five steps from 0.2 to 1.0 nmol/l, through the K<sub>d</sub> of about 0.6 nmol/l. Peptide concentrations were chosen based upon preliminary information gained from inhibition studies at fixed agonist concentration.

### Peptide Preparation

The peptides were purchased from New England Peptide LLC. These peptides are segments of intracellular loops 2 and 3 of the cloned H5HT1aR. Peptides stored at -20° C were initially dissolved in de-ionized water. Subsequent dilutions of peptides were in binding buffer.

### Thermodynamic Drug-Receptor Binding Assays

Homogenate preparation and binding of the agonist [<sup>3</sup>H]8-OH-DPAT ([<sup>3</sup>H]8-hydroxy-2-(di-n-propylamino)tetralin) to receptors was performed as above. Assays run in triplicate were incubated in a shaker water bath (except for 0° C; ice; 1 hr.) for the following temperature/time combinations: 35° C/15 min.; 30° C/30 min.; 25° C/30 min.; 15° C/45 min. (McGonigle and Molinoff, 1989). Each reaction mixture consisted of 700 µl receptor preparation, 100 µl binding buffer (total binding) or 10 µM 5HT in binding buffer (non-specific binding), 100 µl 0.4, 0.6, 0.8, 1.0, or 2.0 nM [<sup>3</sup>H]8-OH-DPAT, and 100 µl experimental displacing agent (peptide or 100 µl of binding buffer for non-displacement reactions), yielding a total volume of 1 ml. Incubations were terminated with 4 ml ice-cold Tris buffer and rapid filtration over Whatman GF/B glass fiber filters. Two successive ice-cold 5 ml Tris buffer rinses followed. The dried filters were counted in 5 ml of Ecoscint liquid scintillation fluid (National Diagnostics; Atlanta) in a Beckman LS 6500 system.

### Thermodynamic Calculations

Saturation binding analysis was performed for [<sup>3</sup>H]8-OH-DPAT at the H5HT1aR. The following concentrations were used: 0.4, 0.6, 0.8, 1.0 and 2.0 nM. Total and non-specific binding was determined in triplicate, in at least two independent experiments.

Complete experiments were performed at the following Centigrade temperatures: 0, 15, 25, 30, and 35. The same sequence of experiments were conducted in the presence of the following substances: P11 (8  $\mu$ M), P21-P27, and DPT (40 nM). Using reciprocal analysis (Scatchard or a Lineweaver-Burk type double inversion), the  $K_d$ 's were calculated for [ $^3$ H]8-OH-DPAT in every case (Hall et al., 2008). Graphing the inverse  $K_d$  versus reciprocal absolute temperature produces a Van't Hoff plot. The slope of this relationship is then used to calculate the standard enthalpy ( $H^\circ$ ). The standard Gibb's Free Energy ( $G^\circ$ ) was determined from each  $K_d$  at 25°C using an Arrhenius-like calculation:  $\Delta G^\circ = -RT \ln(1/K_d)$ . Having the standard enthalpy and standard free energy, allowed determination of the standard entropy ( $S^\circ$ ) from the Gibb's Free Energy Equation ( $\Delta G = \Delta H - T\Delta S$ ).

#### Data Analysis

All statistics (means, standard errors of the mean (SEM), t tests and ANOVA, Pearson correlation coefficients(r), and graphical procedures (including drug-receptor binding analysis) in the study were conducted with PSI-Plot (Version 7) software (Poly Software International), Prism (version 4.0c), or using a Hewlett-Packard Graphing Calculator, HP48. The apriori  $\alpha$  was 0.05 for all experiments, unless indicated otherwise. Experiments were conducted with a minimum of three independent n, all assayed in triplicate. Most experiments were n = 3-5, in triplicate. In some cases (indicated in figure legends), different n's and multiplicates were used.

## 5HT1AR INTRACELLULAR LOOP 2 SIGNAL TRANSDUCTION

### 5HT1aR Intracellular Loop 2 Introduction

The second intracellular loop (ic2) of the H5HT1aR consists of 21 amino acids between the membrane spanning TMD3 and TMD4. Previous studies have examined the role of ic2 in coupling to the G protein. These studies found, using point amino acid substitution, that Thr149 is necessary for receptor coupling to  $G_{\beta\gamma}$ . This study also found that Tyr144 is most important for activation of the G protein subunits  $G_{i\alpha}$  and  $G_{\beta\gamma}$  (Kushwaha et al., 2006).

To date there have been no diseases identified in humans which are related to either point mutations or deletions in the 5HT1aR. There are, however, reports from other members of the seven transmembrane domain G protein coupled receptor family that mutations in ic2 cause changes in receptor agonist affinity. Studies have shown that the ic2 DRY sequence is highly conserved in all members of the GPCR family. An important point mutation in this sequence is reported in the human gonadotropin releasing hormone (GnRH) receptor that has a serine substituted for the tyrosine (DRS). Replacing the tyrosine in this receptor system showed a 100% increase in agonist binding affinity and a 60% increase in the internalization of the receptor (Arora et al., 1999).

The peptide P11 (Table 1), which consists of the N-terminal side of ic2, was tested previously in our laboratory for activity in H5HT1aR signal transduction (Figures 3, 4, 5). It was observed that as the concentration of P11 was increased, there was a decrease in the coupling of the receptor to the G protein, as evidenced by a decrease in the specific binding of [ $^3$ H]-8-OH-DPAT (Figure 3). This decrease in high affinity ligand binding is hypothesized to be due to P11 acting at the interface between 5HT1aR and G



protein and uncoupling them. This shifts the receptor to its low affinity ligand binding state, which accounts for the remaining [<sup>3</sup>H]-8-OH-DPAT bound to the receptor that was measured in these experiments.

Further experiments were designed to measure the effect of P11 on the signal transduction cascade. To measure the activation of G protein the incorporation of  $\gamma$ -[<sup>35</sup>S]-GTP into G<sub>i $\alpha$</sub>  was measured. G<sub>i $\alpha$</sub>  is a negative regulator of adenylyl cyclase (AC). As a secondary measure of G protein activation, the intracellular concentration of cAMP was measured following AC stimulation with forskolin. These experiments revealed P11 was not able to stimulate either the incorporation of  $\gamma$ -[<sup>35</sup>S]-GTP into G<sub>i $\alpha$</sub>  (figure 4) or decrease the production of cAMP by adenylyl cyclase (data not shown) (Thiagaraj et al., 2007). These data indicate that the portion of ic2 represented by P11 is important for coupling the receptor to G protein, but has no role in G protein activation.

The thermodynamic effect of P11 on the binding of ligand to the receptor was also measured. The observed trend for the K<sub>d</sub> of [<sup>3</sup>H]-8-OH-DPAT was that temperature and K<sub>d</sub> are inversely related, as temperature increases the dissociation constant decreases. The previous data for ic2 peptide P11 is shown; the K<sub>d</sub> is the inverse of the x-intercept of the regression line. The inverse of the y-intercept is the amount of drug specifically bound to the receptor, which shows that more [<sup>3</sup>H]-8-OH-DPAT is bound to the receptor at 35 °C (Figure 5). These data indicate that the entropy of the system drives agonist binding to receptor; the peptide increases the entropy.

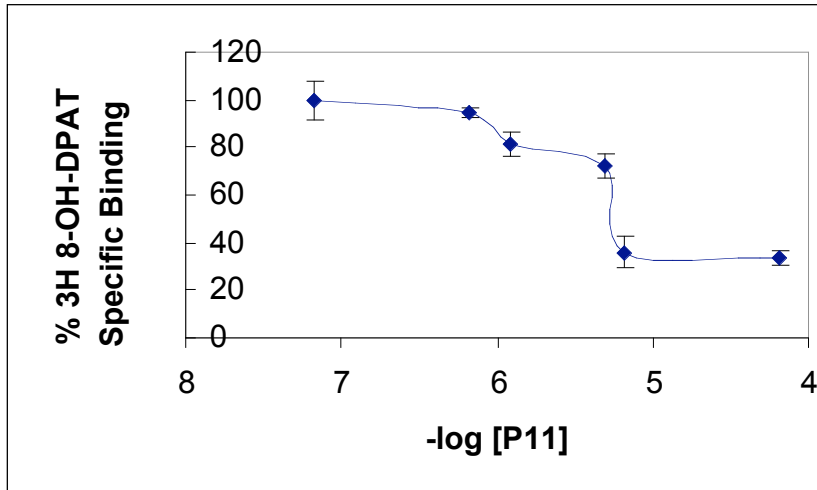


**Figure 3: P11 Agonist 8-OH-DPAT Binding Displacement**  
 Displacement of specifically bound [<sup>3</sup>H]-8-OH-DPAT in membrane preparations of H5HT1aR by the TM3/ic2 peptide probe P11. P11 concentrations are -log(mol/L). P11 IC<sub>50</sub> 7±1 uM. Figure from Thiagaraj et al., 2007.

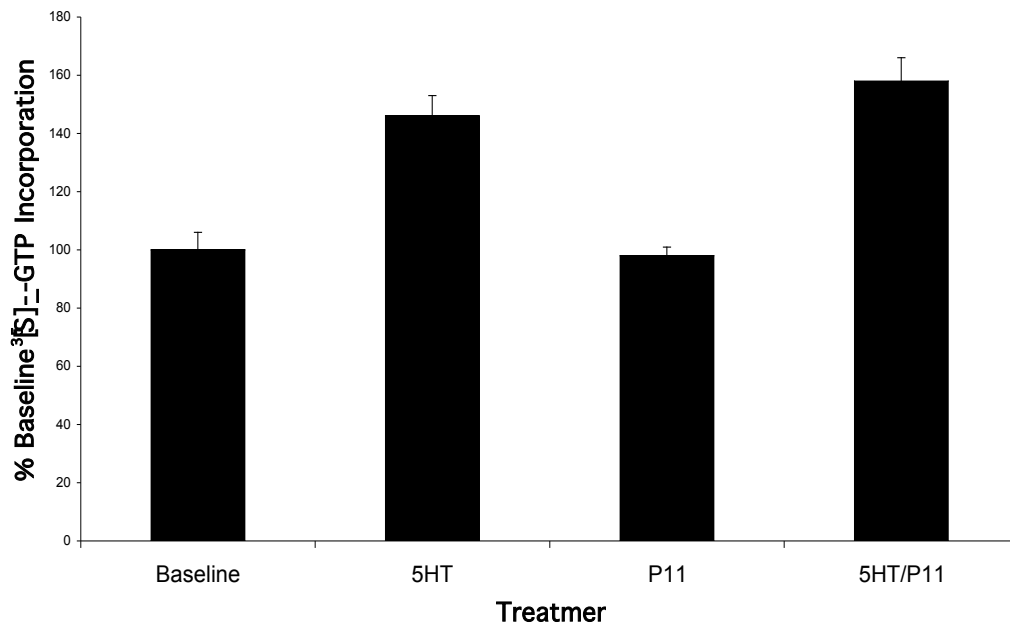


**Figure 4: P11 G Protein Activation Activity**  
 [<sup>35</sup>S]-γ-GTP incorporation into H5HT1aR membranes by 5HT, and P11. Results are mean ±S.E.M. of two experiments, all run in triplicate. Values are expressed as percent of [<sup>35</sup>S]-γ-GTP incorporated in controls (basal) lacking 5HT or P11. [<sup>35</sup>S]-γ-GTP concentration in all conditions is 0.1 nmol/l. 5HT concentration is 1 umol/l. P11 concentration is 0.1 mmol/l. Figure from Thiagaraj et al., 2007  
 Statistics:  
 P < 0.05 for 5HT vs. control, and 5HT/P11 vs. control. All other

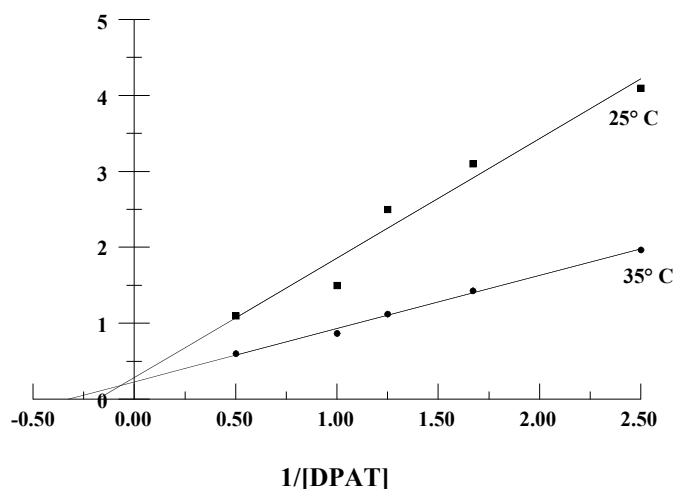


**Figure 5:** P11 Changes  $K_d$  of 8-OH-DPAT at 25 °C and 35 °C  
 Inversion plots of [ $^3\text{H}$ ]8-OH-DPAT binding to membrane preparations of H5HT1aR in the presence of ic2 peptide P11 (8 uM) at 25 °C and 35 °C.  $K_d$  is the inverse of the x-intercept. The inverse of the y-intercept is the amount of drug specifically bound to the receptor. Hall, 2008.  $r$  at 25°C = 0.98;  $r$  at 35°C = 1.00.  
 Regression lines are: 25°C  $y = 15.74x + 2.82$ ; 35°C  $y = 6.85x + 2.82$ .

P11	IALDRYWAITD
P21	LDRYWAITDP
P22	RYWAITDPID
P23	WAITDPIDYV
P24	ITDPIDYVNK
P25	DPIDYVNKRT
P26	IDYVNKRTPR
P27	YVNKRTPRPR

**Table 1:** ic2 Peptide Mimics

The primary amino acid sequences for the H5HT1aR ic2 loop peptide mimics. The receptor's amino terminal is to the left. Sequences for H5HT1aR from Kobilka et al., 1987. P11 is from a previous study by Thiagaraj et al., 2007. Peptides P21 to P27 were utilized to elucidate the role of each segment of ic2 represented to couple receptor to G protein. The peptides' subsequent effect on the signal transduction cascade was also measured by G protein activation and second messenger regulation.

5HT1aR Intracellular Loop 2 Binding Results; HYPOTHESIS: Segments of loop 2 are differentially involved in coupling and activation of G<sub>i</sub>.

The introduction of the peptide mimics of ic2 (Table 1) had varying effects on the specific binding of [<sup>3</sup>H]-8-OH-DPAT to 5HT1aR (Figures 6 & 7, Table 2). The most efficient uncouplers of the receptor and G protein, as evidenced by the decrease in specifically bound agonist versus control are P21-P23. P21-P23 yield values of about 50% (as a percent of control which is 100%) inhibition of specifically bound agonist in the 7-30 uM peptide concentration range. The IC<sub>50</sub> values were calculated for these peptides. The peptides P24-P27 were able to inhibit specific binding of agonist very poorly (6-25% of control) at a 30uM peptide concentration. These peptides were such poor uncouplers that the IC<sub>50</sub> calculation could not be done. The IC<sub>50</sub> data supported the hypothesis by showing that as the peptides progressed from the amino terminus of ic2 towards its carboxy terminus they wane in importance for coupling the receptor to G protein. The peptides closer to ic2 carboxy terminus could not decrease the ligand binding even at their maximum soluble concentration.

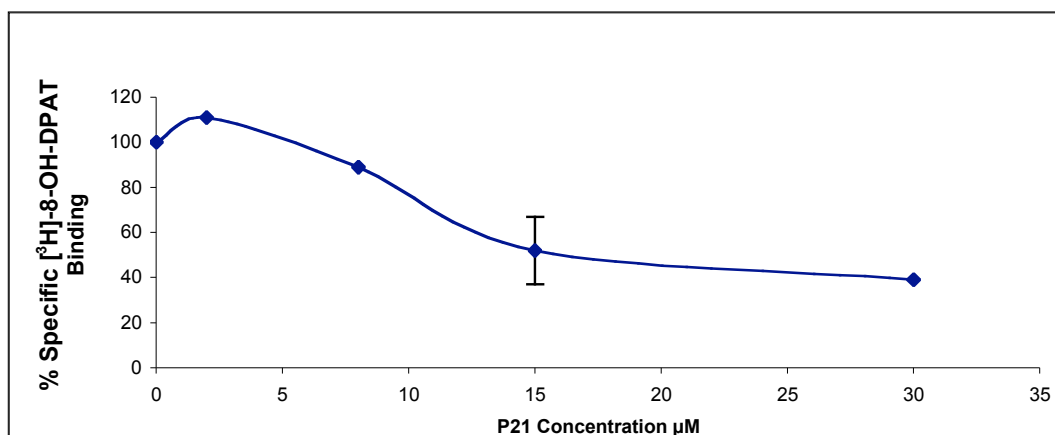


**Figure 6:** P21 Concentration Dependent Displacement of Bound 8-OH-DPAT  
This curve represents the change in specific binding of [<sup>3</sup>H]-8-OH-DPAT, a 5HT1aR agonist, to the receptor in the presence of various concentrations of the ic2 peptide mimic P21. The curve shows that as the concentration of P21 is increased the amount of agonist bound to the receptor decreases.

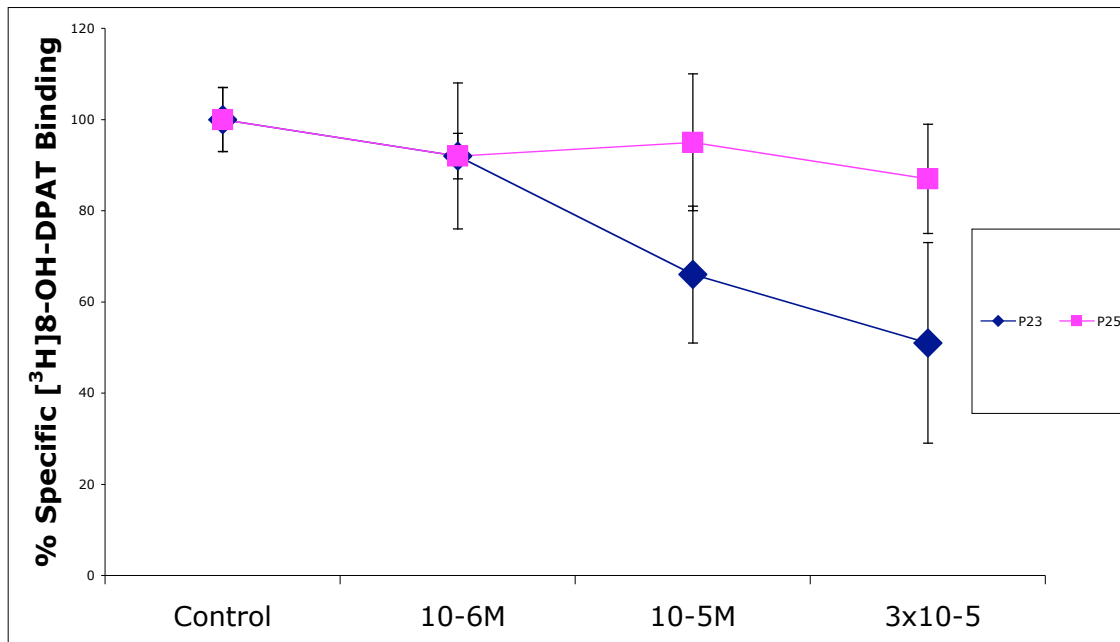


**Figure 7:** Concentration Dependent Changes in 8-OH-DPAT Binding for P23 and P25  
 This graph shows the differential abilities of 5HT1aR ic2 peptide mimics P23 (lower line, diamond shape) and P25 (upper line, square shape) to alter the specific binding of [<sup>3</sup>H]-8-OH-DPAT as the peptide concentration increases.

Peptide	%Agonist Binding	IC50 (uM)
P11 (7 uM)	50	7±1
P21 (15 uM)	52	15±4
P22 (16 uM)	50	16±2
P23 (30 uM)	51	30±22

Peptide	% Agonist Binding	SEM
P24 (10 uM)	94	9
P25 (30 uM)	87	12
P26 (30 uM)	75	19
P27 (30 uM)	90	5

**Table 2:** ic2 Peptide Mimic Effect on 8-OH-DPAT Binding

Cumulative agonist binding inhibition values are shown for all 5HT1aR ic2 peptide mimics. All values are percent of control, except the IC50 values, which are concentration (uM). The upper portion of the table is the peptides, including P11 from previous work by Thiagaraj et al., 2007. These peptides decreased the specific high affinity binding of 5HT1aR agonist [<sup>3</sup>H]-8-OH-DPAT by 50%. The lower portion of the table, are the ic2 peptides further toward the loop's carboxy terminus. These peptides were less effective at decreasing specific high affinity binding of [<sup>3</sup>H]-8-OH-DPAT.

5HT1aR Intracellular Loop 2 Thermodynamic Binding Results; HYPOTHESIS: The binding of ligand to receptor is an entropically driven reaction.

The specific binding of the radioligand [<sup>3</sup>H]-8-OH-DPAT to 5HT1aR can be measured at a range of temperatures, which allows for the calculation of various thermodynamic binding parameters. The specific binding of [<sup>3</sup>H]-8-OH-DPAT was calculated from binding assays which had reached equilibrium at the following times and temperatures: 60 minutes at 0°C, 45 minutes at 15°C, 30 minutes at 25°C, 30 minutes at 30°C, and 30 minutes at 35°C. A dissociation constant, K<sub>d</sub>, was calculated for each temperature (Table 3). The K<sub>d</sub> is the concentration of [<sup>3</sup>H]-8-OH-DPAT at which 50% of the receptor ligand-binding sites are occupied. The observed trend for the K<sub>d</sub> of [<sup>3</sup>H]-8-OH-DPAT was that temperature and K<sub>d</sub> are inversely related; as temperature increases, the dissociation constant decreases. This is shown for P23 in a modified Lineweaver-Burke plot showing the difference in the specific binding of [<sup>3</sup>H]-8-OH-DPAT at 15 °C (lower line) and 30 °C (upper line) (Figure 8). The K<sub>d</sub> is the inverse of the x-intercept of the regression line. The inverse of the y-intercept is the amount of drug specifically bound to the receptor, which shows that more [<sup>3</sup>H]-8-OH-DPAT is bound to the receptor at 30 °C.

The data for the changes in K<sub>d</sub> for [<sup>3</sup>H]-8-OH-DPAT alone was previously determined and are generally smaller than when the ic<sub>2</sub> peptides are introduced into the binding assay. The variability in the K<sub>d</sub>s for P22-P24 is explained by the decrease in high affinity ligand binding caused by the peptides. With the receptor shifted to its low affinity ligand binding conformation the concentration of ligand needed to reach the 50% bound and unbound is increased. Interestingly the results for P23 show that the peptide is

not that different from the ligand alone, especially at increased temperatures. This mirrors the previous data, which showed that the P23 region of ic2 affected the receptor's signal transduction pathway in a manner similar to agonist. It will also be shown that P23 affected the thermodynamics of the system like the agonist, also yielding positive entropy, supporting the hypothesis.

Temperature	0 °C (273 K)	15 °C (288 K)	25 °C (298 K)	30 °C (303 K)	35 °C (308 K)
Compound	Kd (nM)				
<b>[<sup>3</sup>H]-8-OH-DPAT (Alone)</b>	3.42 (0.42)	2.66 (0.12)	2.19 (0.45)	1.29 (0.17)	1.86 (0.12)
<b>P11 (8 uM)</b>	99.80 (16.57)	7.79 (0.27)	5.60 (0.60)	3.76 (0.37)	2.78 (0.32)
<b>P22</b>	60.8 (5.2)	29.53 (2.5)	5.21 (0.36)	2.50 (0.14)	ND
<b>P23</b>	15.42 (1.02)	4.52 (0.61)	2.01 (0.53)	1.85 (0.24)	ND
<b>P24</b>	68.6 (23.4)	5.83 (0.88)	3.78 (0.37)	2.52 (0.38)	ND

**Table 3:** ic2 Peptide Mimic Effect on Kd of 8-OH-DPAT

This table is a summary of the dissociation constants (Kd) calculated for the ligand [<sup>3</sup>H]-8-OH-DPAT in the absence and the presence of H5HT1aR ic2 peptide mimics at different temperatures. Minimums of two independent experiments were done at each temperature for each peptide. The Kd is the concentration of [<sup>3</sup>H]-8-OH-DPAT at which 50% of the receptor ligand-binding sites are occupied. Values in the table are Kd for agonist, values in parenthesis are standard error of the means (SEM). ND = not done.

Statistics:

Across row comparisons, 0-35C, left to right; only significant differences are listed; all other non-significant comparisons are not listed (unless otherwise noted):

**8-OH-DPAT:** p < 0.05 for 0/30, 15/30

**P11:** p < 0.05 for 0/15, 0/25, 0/30, 0/35, 15/30

**P22:** p < 0.05 for all comparisons.

**P23:** p < 0.05 for 0/15, 0/25, and 0/30.

**P24:** none of the comparisons were statistically significant. Part of this result is because of a large error bar for 0 degrees.

Down Column Comparisons, top to bottom, only significant differences listed, unless otherwise noted:

**0°C:** p < 0.05 for DPAT/P11, DPAT/P22, DPAT/P23, P11/P23, and P22/P23.

**15°C:** p < 0.05 for DPAT/P11, DPAT/P22, P11/P22, P11/P23, P22/P23, and P22/P24.

**25°C:** p < 0.05 for DPAT/P11, DPAT/P22, P11/P23, and P22/P23.

**30°C:** p < 0.05 for DPAT/P11, DPAT/P22, and P11/P23.

**35°C:** The only comparison, DPAT vs. P11 is not statistically significant.

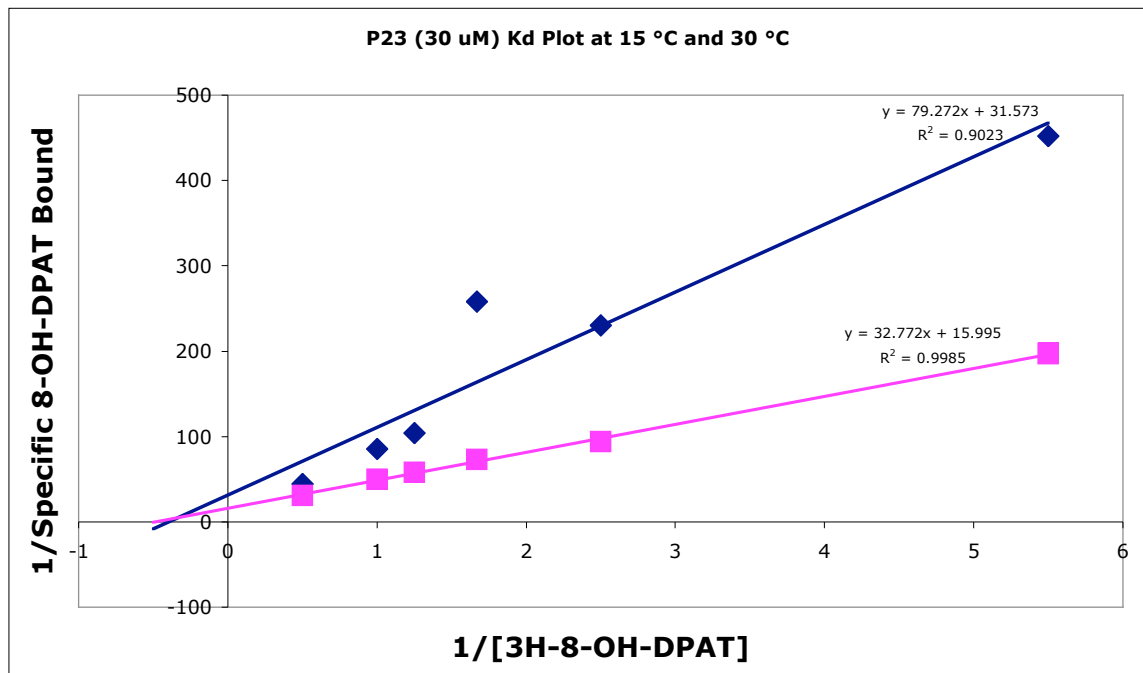


**Figure 8: P23 Kd Plot at 15 °C and 30 °C**

A modified Lineweaver Burke plot showing the difference in the specific binding of [<sup>3</sup>H]-8-OH-DPAT at 15 °C (upper line, diamond shape) and 30 °C (lower line, square shape). The K<sub>d</sub> is the inverse of the x-intercept. The inverse of the y-intercept is the amount of drug specifically bound to the receptor. 15 °C  $y = 79.272x + 31.573$   $r = 0.9023$ ; 30 °C  $y = 32.772x + 15.995$   $r = 0.9985$

The determination of the K<sub>d</sub> of [<sup>3</sup>H]-8-OH-DPAT over a range of temperatures allows for the calculation of the standard thermodynamic parameters Gibb's free energy ( $\Delta G^\circ$ ), enthalpy ( $\Delta H^\circ$ ), and entropy ( $\Delta S^\circ$ ). Gibbs Free Energy is the energy required for a chemical reaction to proceed (change in energy based upon ligand binding in these experiments), a negative number means the reaction proceeds spontaneously.

The enthalpy is a sum of all energy in a reaction (or binding event), which is indicative of whether the reaction requires an input of energy to proceed or if it releases energy. A negative number means the reaction is exothermic (releases energy) and is thus more energetically favorable. The entropy is calculated from Gibb's free energy and the



enthalpy; it is a measure of the disorder of the system. For a system to overcome disorder it takes an input of energy. In highly organized biological systems, energy is required to maintain the order for the system to function properly. A positive number is favorable entropy.

Gibb's standard free energy ( $\Delta G^\circ$ ) was calculated for [ $^3\text{H}$ ]-8-OH-DPAT alone, and in the presence of the ic2 peptides P22, P23, and P24 (Table 4). All of these values were negative, which is energetically favorable meaning that the binding event will occur spontaneously. The calculated value of  $\Delta G^\circ$  is not significantly altered by the addition of the ic2 peptides. This means that the peptides are not changing the ligand binding reactions energetics. Thus the difference in amount of ligand bound to receptor observed is not due to the peptides increasing the energy required for the ligand to bind to the receptor, it can still occur spontaneously. This supports the hypothesis that the peptides are acting at the receptor-G protein interface and not at the ligand binding site.

The enthalpy ( $\Delta H^\circ$ ) is calculated from the slope of the regression line in the Van't Hoff plot (Figure 9, Table 4). The slope of the lines in the Van't Hoff plot is variable for ligand with the addition of the ic2 peptides, with the [ $^3\text{H}$ ]-8-OH-DPAT alone (lowest line in the plot on the y axis, progressing upward are the lines for P23, P22, and P24) having the flattest slope. This yields a positive (unfavorable) enthalpy; however, compared to the slopes of the lines for which P22, P23, and P24 have been introduced to the binding assay, it is less unfavorable without their presence. Thus the ligand requires more energy from the system to bind the receptor in the presence of the peptides.

The entropy ( $\Delta S^\circ$ ) was calculated for [ $^3\text{H}$ ]-8-OH-DPAT alone and in the presence of the ic2 peptides (Table 4). The peptides increased the entropy of the [ $^3\text{H}$ ]-8-OH-

DPAT binding system compared to the ligand alone. This indicates the peptides increase the entropic favorability of [<sup>3</sup>H]-8-OH-DPAT receptor binding. The net effect of this is the ligand binding to the receptor is driven by entropy, and able to overcome the effect of the unfavorable enthalpy. This means that the peptides increased the order of the ligand binding system making it more favorable for the ligand binding to occur.

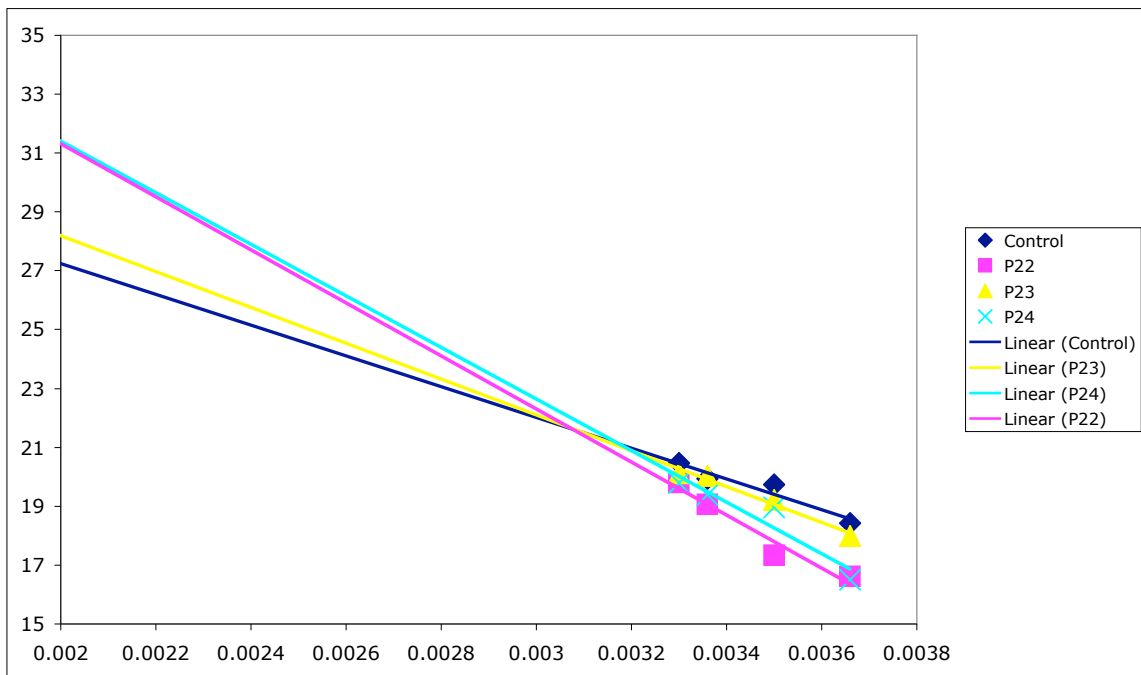


**Figure 9:** Van't Hoff plot for P22, P23, and P24. Negative slopes indicate the positive enthalpies ( $\Delta H^\circ$ ) calculated for each peptide, thus making the receptor G-protein coupling energetically unfavorable. [<sup>3</sup>H]-8-OH-DPAT alone (lowest line in the plot on the y axis), P23 line is next above followed by P22 line, and P24 has the highest y-intercept

Van't Hoff regression equations:

Control:  $y = -0.052x + 37.691; r = 0.96$

P22:  $y = -0.090x + 49.35; r = 0.98$

P23:  $y = -0.077x + 46.01; r = 0.99$

P24:  $y = -0.088x + 48.93; r = 0.95$

Compound	$\Delta G^\circ$ (kJ/mole)	$\Delta H^\circ$ (kJ/mole)	$\Delta S^\circ$ (J/mole)
[ <sup>3</sup> H]-8-OH-DPAT (Alone)	-49 (10)	43 (4)	311 (47)
P22	-47 (3)	124 (13)	547 (49)
P23	-49 (13)	64 (6)	380 (68)
P24	-48 (5)	86 (13)	452 (57)

Table 4: ic2 Peptide Mimic Effect on Gibbs Free Energy, Enthalpy, and Entropy of 8-OH-DPAT

Thermodynamic parameters were determined in a minimum of two independent experiments. Gibb's standard free energy ( $\Delta G^\circ$ ) was calculated from [<sup>3</sup>H]-8-OH-DPAT Kd at the standard temperature 25 °C (298 K). The enthalpy ( $\Delta H^\circ$ ) was determined from the slope of Van't Hoff plots. The entropy ( $\Delta S^\circ$ ) was then calculated from the Gibb's Free energy equation using the experimental values determined for free energies and enthalpies.

Statistics:

Entropy: None of the values are significantly different from control or from each other.

Enthalpy: P22 vs. control,  $p < 0.05$ . None of the other values differ significantly.

Incorporation of  $\gamma$ -[<sup>35</sup>S]-GTP into G protein; HYPOTHESIS: The N-terminal region of ic2 is mostly involved in coupling to rather than activation of the G protein.

The basis for the hypothesis is the preliminary work with peptide P11 for ic2. This peptide was shown to interfere with the receptor-G protein coupling, but had no G protein activation properties. Thus a study for all of the ic2 peptides' effect on G protein activation was undertaken to support the hypothesis. The stimulation of the G protein to exchange GDP for GTP is an important step in the signal transduction cascade initiated by 5HT1aR activation. The measurement of the hydrolysis of GTP to GDP can be done, but is challenging. Therefore, an analogous binding assay procedure was developed using a thioester analogue of GTP. The thioester analogue  $\gamma$ -[<sup>35</sup>S]-GTP is about ten times more resistant to hydrolysis by  $G_{i\alpha}$  (GTP 6 pmol/min/mg protein vs.  $\gamma$ -[<sup>35</sup>S]-GTP <0.6 pmol/min/mg protein) (Wieland et al., 1994). The introduction of the ic2 peptide mimics had the following affect on  $\gamma$ -[<sup>35</sup>S]-GTP into  $G_{i\alpha}$  (Table 5, Figure 10). The control level of basal GTP incorporation in the absence of 5HT or peptide is set as 100%. The addition of 5HT increased the incorporation of  $\gamma$ -[<sup>35</sup>S]-GTP to 168±12%(vs. control, p<0.05). The addition of the peptides P11, P22, P24, P25, P26, and P27 stimulated incorporation from 100-148% of control, all less than the ligand 5HT. P21 stimulated incorporation to 158±11% of control. P23 was the only peptide which showed a stimulation of incorporation better than 5HT (188±10% of control).

Treatment	Percent $\gamma$ -[ <sup>35</sup> S]-GTP Incorporation	Standard Error of the Mean
Control	100	7
5HT (10 <sup>-7</sup> M)	168	12
P11 (10 uM)	100	3
P21 (30 uM)	158	11
P22 (30 uM)	128	9
P23 (30 uM)	188	10
P24 (30 uM)	146	17
P25 (30 uM)	126	10
P26 (30 uM)	111	9
P27 (30 uM)	130	7

**Table 5:** ic2 Peptide Mimic Effect on  $\gamma$ -[<sup>35</sup>S]-GTP into G<sub>ic</sub>

Cumulative values for all 5HT1aR ic2 peptide mimics are shown for affect on the incorporation of  $\gamma$ -[<sup>35</sup>S]-GTP into G<sub>ic</sub>. All values are percent of control. P23 stimulated GTP incorporation is notably greater than the ligand 5HT (188% vs. 168% of control).

Statistics:

In the comparison of either 5HT or each peptide vs. control all are significant at the p < 0.05 level, except: P11, P25, and P26.

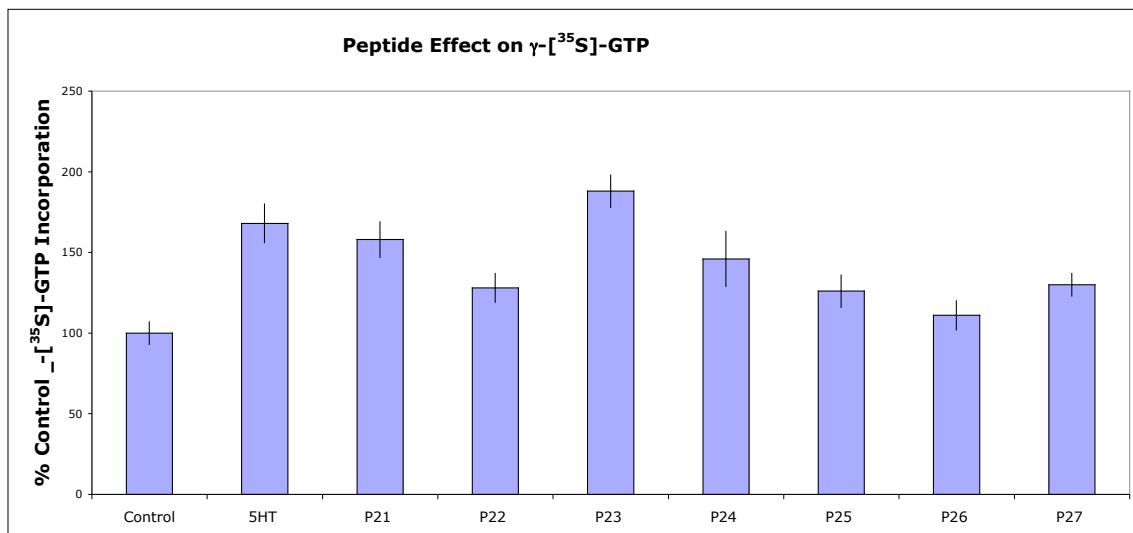


**Figure 10:** ic2 Peptide Effect on  $\gamma$ -[<sup>35</sup>S]-GTP incorporated into G<sub>i</sub>

A measure of G protein activation. Control is the basal amount of  $\gamma$ -[<sup>35</sup>S]-GTP incorporated into G<sub>i</sub> in CHO cells expressing the human 5HT1aR, set as 100%. The Y-axis is the percent of specifically bound  $\gamma$ -[<sup>35</sup>S]-GTP. All other treatments are percents of the control value. P23 stimulated GTP incorporation is notably greater than the ligand 5HT (188% vs. 168% of control). All peptides are 30 uM concentration, 5HT 10<sup>-7</sup> M concentration.

cAMP Production by Adenylyl Cyclase; HYPOTHESIS: The N-terminal region of ic2 is primarily involved in coupling to, rather than activation of, the G protein and its second messenger cAMP.

G protein activation can be measured directly by measuring incorporation of GTP. However, incorporation of GTP does not mean that the G protein is fully active. To be fully active the G protein has to bind GTP and dissociate from the receptor to affect adenylyl cyclase's production of cAMP. This step in the 5HT<sub>1a</sub>R signal transduction pathway following the activation of G<sub>i</sub> is the inhibition of cAMP production by AC. The experiments designed measured the effect of ic2 peptides on the intracellular levels of cAMP following the stimulation of AC with FSK in the presence of the phosphodiesterase inhibitor IBMX (an inhibitor of cAMP metabolism). FSK stimulates AC to produce cAMP, making the determination of cAMP concentration easier. The control value 100% represents treatment of the CHO cells with FSK, in the absence of 5HT and ic2 peptides (Figure 11, Table 6). The addition of FSK and 5HT to the cells led to the decrease of cAMP via activation of G<sub>i</sub> to 21±4% of control. This demonstrates that the 5HT<sub>1a</sub>R signal transduction pathway is intact because activation of G protein decreases intracellular cAMP concentration. The addition of the ic2 peptides to the FSK stimulated cells had variable affect on cAMP concentration. The peptides P21, P26, and P27, at 30 uM, (122±8%, 100±5.3%, 132±5.9%) were not able to decrease cAMP concentration versus control. The combination of peptides P21, P26, and P27 (22±2%, 15.3±8.5%, 10.8±8.4%) with 5HT had no effect of the action of the 5HT mediated decrease cAMP in the FSK treated cells.

The peptides P22 and P25, at 30 uM, were slightly active at decreasing cAMP concentration in FSK treated cells ( $71\pm 2\%$ ,  $64\pm 3\%$ ). The combination of P22 and P25 with 5HT showed an additive effect at decreasing cAMP concentration ( $4\pm 1\%$ ,  $12\pm 6\%$ ) in FSK treated cells, which was better than 5HT alone. The peptides P23 and P24 were the most active at decreasing cAMP concentrations in FSK treated cells ( $42\pm 4\%$ ,  $45\pm 7\%$ ). The combination of P23 and P24 with 5HT also showed an additive effect at decreasing cAMP concentration ( $15\pm 3\%$ ,  $12\pm 7\%$ ) in FSK treated cells, which was also better than 5HT alone.

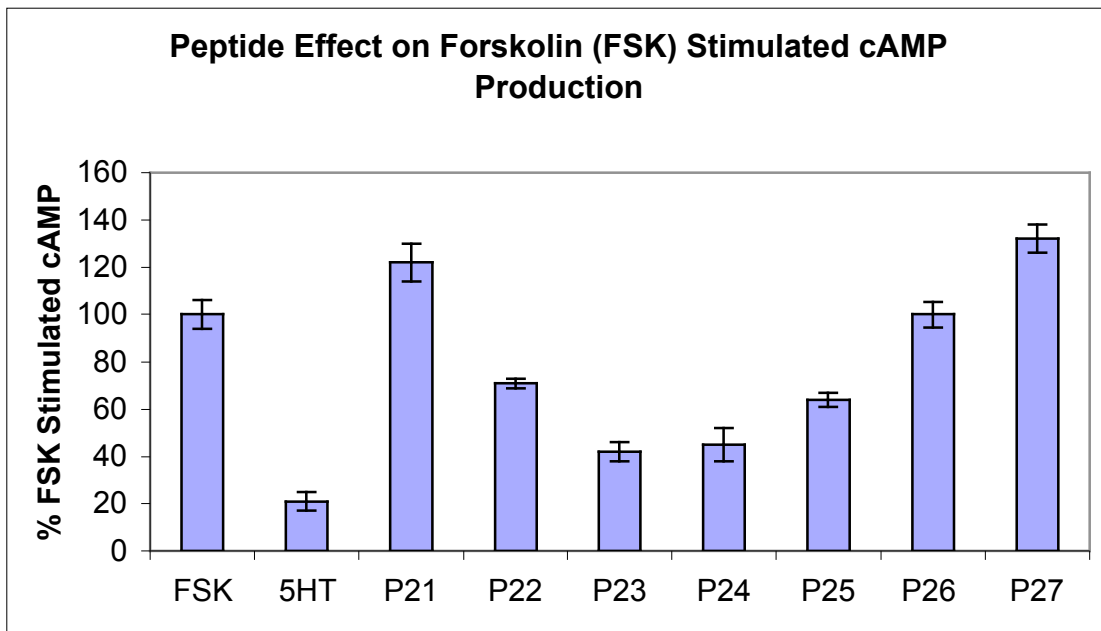


**Figure 11:** ic2 Peptide Effect on Forskolin Stimulated cAMP Production  
 A measure of activated G protein regulation of adenylyl cyclase. Forskolin (FSK) stimulated cAMP production by adenylyl cyclase (AC) in CHO cells expressing the human 5HT1aR. FSK is the control, which is set to 100%. All other treatments are expressed as a percent of the control value. All treatments include isobutylmethylxanthine (IBMX) an inhibitor of the metabolism of cAMP by phosphodiesterase.

Treatment	cAMP % of Control	SEM
FSK	100	6
5HT	21	4
P21	122	8
P21/5HT	22	2
P22	71	2
P22/5HT	4	1
P23	42	4
P23/5HT	15	3
P24	45	7
P24/5HT	12	7
P25	64	3
P25/5HT	12	6
5HT/P26	15.3	8.5
P26	100	5.3
5HT/P27	10.8	8.4
P27	132	5.9

Table 6: ic2 Peptide Mimic Effect on cAMP Concentration

Cumulative values for all 5HT1aR ic2 peptide mimics are shown for effect on forskolin (FSK) stimulated cAMP production.

These experiments represent the downstream effect of G protein activation. All values are percent of control FSK.

Statistics:

In the comparison of either 5HT alone or the various peptides alone vs. FSK control, all are significant at the  $p < 0.05$  level except: P26.

In the comparison of each peptide in combination with 5HT vs. 5HT alone, none are significant at the  $p < 0.05$  level except: P22/5HT.



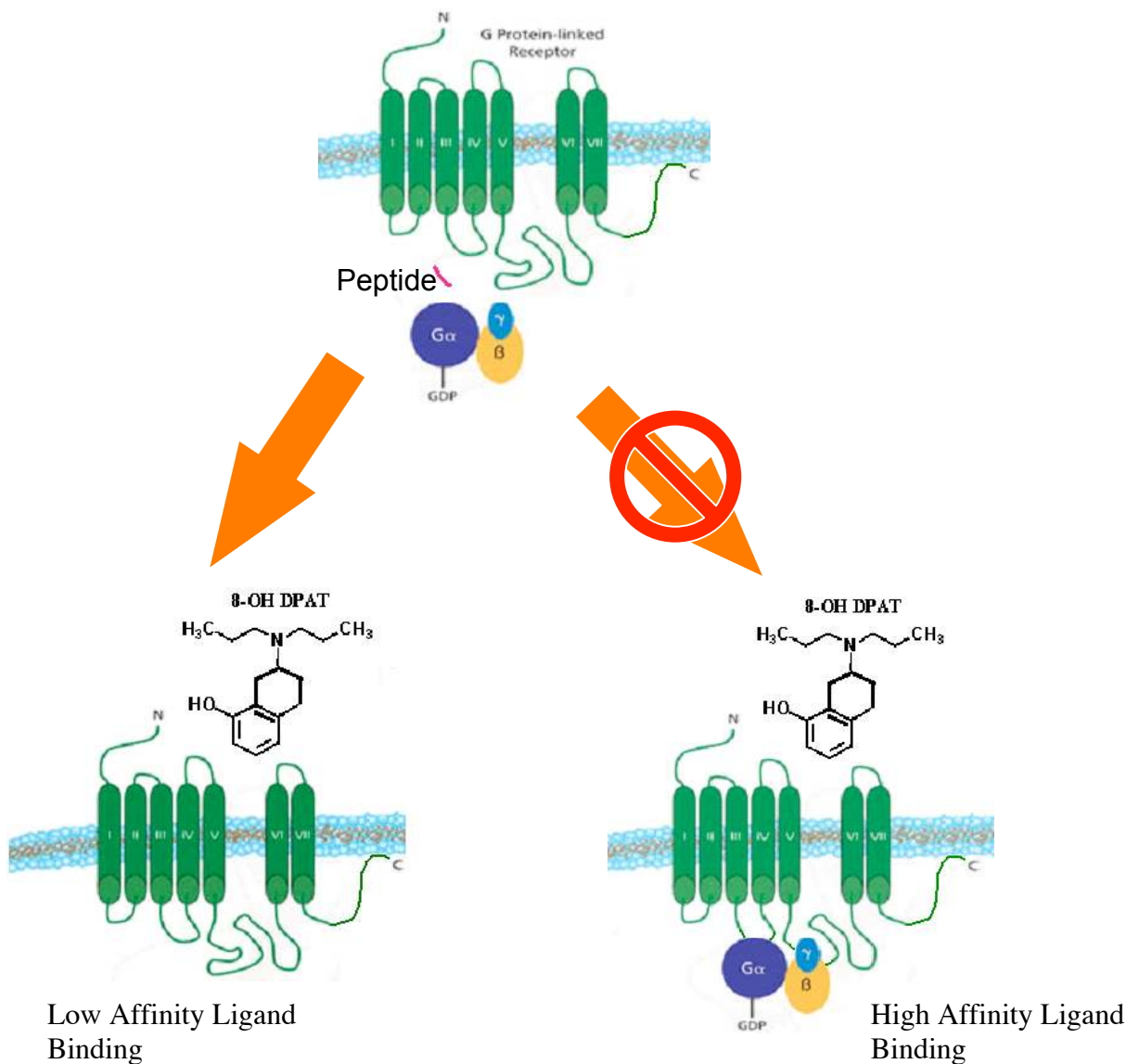


**Figure 12: Low Affinity Versus High Affinity Ligand Binding**  
 Intracellular loop peptide mimics interference with specific ligand binding. The introduction of the small peptide probes into the binding assay uncouples the receptor and Gi. The uncoupled receptor shifts the receptor to its low affinity ligand binding state. This was measured in the [<sup>3</sup>H]-8-OH-DPAT vs. 5HT1aR binding assays. The low ligand binding affinity K<sub>d</sub> for 8-OH-DPAT at 5HT1aR is 22 nM (Fargin et al., 1988). The experimental value of K<sub>d</sub> from our experiments were high affinity K<sub>d</sub> range from about 0.6 to 1.3 nM. The difference between K<sub>d</sub>s being 20 nM for their low affinity K<sub>d</sub> and about 1 nM for our high affinity K<sub>d</sub>, then we are looking at a 20 fold difference, an easily measurable difference.

## Discussion

Binding and Thermodynamics: The general outcome of peptide action in the agonist inhibition format (Table 2) is summarized schematically in Figure 12. Peptides P21-27 have differential capacity to uncouple the receptor-G protein complex, and the accompanying thermodynamic results with peptides in the middle of this group (P22-24) may add insight on these differential processes (Tables 3 & 4). Work previously done has established the role that enthalpy and entropy play in receptor ligand binding in the beta-adrenergic receptor, dopamine receptor, opioid receptor, adenosine receptor (Heitman et al., 2006), rat 5HT1aR, and human 5HT1aR receptor systems. In the  $\beta$ -adrenergic receptor system studies by Weiland et al. (1982), it was found that  $\beta$ -adrenergic agonists yield more favorable enthalpic changes and unfavorable entropy changes. In comparison,  $\beta$ -adrenergic antagonists were found to have less favorable enthalpic changes and more favorable entropies. The dopaminergic receptor system studies by Zahniser et al. (1983) found that the displacement of bound antagonists and agonists is entropically driven, and changes in temperature have little effect on agonist displacement. The opioid receptor system studies by Hitzemann et al. (1982) show that agonist binding is associated with favorable entropies and unfavorable enthalpies, while opioid antagonist binding is associated with favorable enthalpies and entropies. The central idea to be taken from these experiments is that each GPCR studied has unique thermodynamic parameters that govern its functionality.

The experiments with [<sup>3</sup>H]-8-OH-DPAT alone for the rat 5HT1aR done by Dalpiaz et al., 1995 found a negatively sloped Van't Hoff plot while our data for H5HT1aR has a flatter slope but still negative trend. The standard free energies for the

rat and human 5HT1aR are similar (-51.3 versus -49 kJ/mole). The shallower slope of the H5HT1aR Van't Hoff plot compared to the rat receptor yields a more favorable enthalpy of 43 versus 58 kJ/mole. This trend is reversed in respect to entropy. The rat 5HT1aR has more favorable entropy vs. the human receptor 366 vs. 311 J/kmole. These findings possibly indicate that [<sup>3</sup>H]-8-OH-DPAT ligand binding is less entropically driven in the human than rat 5HT1aR (Hall et al., submitted 2008).

Thiagaraj et al. 2005 compared the thermodynamics of ligand binding to H5HT1aR for the agonists dipropyltryptamine (DPT) and [<sup>3</sup>H]-8-OH-DPAT. DPT, the larger of the two agonists, has a smaller negative standard free energy -45 kJ/mole, and larger enthalpy 107 kJ/mole and entropy 510 J/mole (8-OH-DPAT thermodynamic parameters:  $\Delta G^\circ = -49$ ,  $\Delta H^\circ = 43$ ,  $\Delta S^\circ = 311$ ). Thus, the binding of DPT to H5HT1aR seems to be more driven by entropy compared to the binding of [<sup>3</sup>H]-8-OH-DPAT. This difference is possibly thermodynamic evidence showing that the more energetically favorable binding of [<sup>3</sup>H]-8-OH-DPAT makes it a full-agonist (sub-nanomolar K<sub>d</sub>) when compared to DPT (micromolar IC<sub>50</sub>), which is a partial agonist.

These experiments differ from the current study because they used agents which directly compete at the same site at which the agonist binds. In our experiments the 5HT1aR intracellular loop peptide mimic is hypothesized to be acting at the receptor-G protein interface, which affects the receptor's ligand binding affinity state. This resulting change in affinity affects the thermodynamics of receptor binding to varying degrees (8-OH-DPAT @5HT1aR low affinity K<sub>d</sub> = 20 nM, high affinity K<sub>d</sub> = 1 nM).

The current thermodynamic study focuses on the ic2 peptides P22, P23, and P24. These peptides were chosen because they showed the greatest activating effect on the

5HT1aR signal transduction system. The study measured the changes in the  $K_d$  of [ $^3\text{H}$ ]-8-OH-DPAT in the presence of these peptides at temperatures of 0°C, 15°C, 25°C, and 30°C. The introduction of the all peptides caused an increase in the  $K_d$  for [ $^3\text{H}$ ]-8-OH-DPAT as the temperature of the binding system decreased. The magnitude of effect of the different peptides on [ $^3\text{H}$ ]-8-OH-DPAT specific binding was not the same. Generally speaking, P22 and P24 had a similar effect both on  $K_d$ , enthalpy, and entropy. This seems to mirror the effectiveness of the peptides at activation of the signal transduction cascade. The general trend observed is that P23 contains the core region of ic2, which is responsible for G protein activation. As the peptides, especially to the N-terminal side of P23, move away from this core region, they show diminished G protein activation properties and more involvement in G protein coupling (Table 2, Figures 10 & 11). The results for P11 (G protein coupling but no activation activity), an ic2 peptide from a previous study, would likely be similar to those for the ic2 carboxy terminus peptide P27 if a thermodynamic study is completed for P27.

Effect of Peptides on G Protein Activation and Signal Transduction: These data collected in our experiments with P23 support that this peptide mimic has the most agonistic like properties of all the ic2 peptide mimics tested. These data measured G protein activation (based upon amount of  $\gamma$ -[ $^{35}\text{S}$ ]-GTP incorporated into  $G_{i\alpha}$ ) and negative regulatory affect on AC (based upon the decrease in FSK stimulated cAMP production). When the thermodynamic data for  $K_d$ , standard free energy, enthalpy, and entropy for P23 is compared to that for the agonist, [ $^3\text{H}$ ]-8-OH-DPAT some similarity is evident. P23 has the least additional effect of all the peptides on increasing the  $K_d$  of [ $^3\text{H}$ ]-8-OH-DPAT as temperature decreases. None of the peptides which were tested yielded a significant

change in the standard free energy from that of the agonist [<sup>3</sup>H]-8-OH-DPAT ( $p > 0.05$ ). This means that none of the peptides affected the spontaneity of the ligand binding event. All of the peptides showed unfavorable increases in enthalpy compared to the agonist [<sup>3</sup>H]-8-OH-DPAT. This means that in order for that agonist to bind to the receptor a net input of energy was required in the presence of the peptides. All of the peptides showed favorable increases in entropy compared to the agonist [<sup>3</sup>H]-8-OH-DPAT. This means that the organization of the binding system increased in the presence of the peptides, accompanied by increased disorder elsewhere in the system.

The increases in enthalpy and entropy for the peptides mirrored the results from the  $K_d$  with P23 being the most similar in properties to [<sup>3</sup>H]-8-OH-DPAT. The lines in the Van't Hoff plot for [<sup>3</sup>H]-8-OH-DPAT and P23 are also the closest in slope compared to other peptides tested. Our interpretations of these results are that P23 acts most like the agonist. Possibly due to P23 having the least additional affect of all the peptides on the conformation of the receptor and G proteins, necessary for the activation of the signal transduction cascade. These changes are very similar to those induced in the complex by the bound agonist.

Data collected in these experiments with regard to the signal transduction cascade of 5HT<sub>1a</sub>R have implicated a role for ic<sub>2</sub> in receptor coupling and G protein activation. The amino terminus end of the loop involving the sequence IALDRYWAITDPIDYV and including peptides P11-P23 is important for coupling to the G-protein. Evidence for this includes the highly conserved DRY sequence and the IC<sub>50</sub> activity for the peptides, which ranges from 7-30  $\mu$ M. The decay of G protein coupling and activation activity was observed as the peptides progress towards the carboxy terminus of ic<sub>2</sub>. However, as the

amino acids seem to wane in importance for receptor coupling they increase in importance for G protein activation with its peak at the P23 amino acid stretch WAITDPIDYV. This is clearly shown by the bell shaped progression of the data bars for the incorporation  $\gamma$ -[<sup>35</sup>S]-GTP into G<sub>iα</sub>(Figure 10). This can be superimposed over the inverted bell shaped depression in the data bars for the intracellular levels of FSK stimulated cAMP production (Figure 11). The carboxy terminal end of ic2 consisting of the amino acids RTPRPR may be important as simply as space occupiers in the receptor protein chain. This stretch of amino acids in the carboxy terminal end of ic2 serves as a space filler, holding the amino terminal of ic2 in a favorable orientation for coupling to the G protein. Also interesting about the carboxy terminal end of ic2, is the presence of the 2 proline residues separated by only 1 amino acid. These proline residues in close proximity to each other introduce a kink in the receptor structure constraining its range of motion. Overall, these experiments demonstrate the clear role for H5HT1aR's ic2 in coupling receptor to G protein, and toward the loop's middle, G protein activation.

## 5HT<sub>1A</sub>R INTRACELLULAR LOOP 3 SIGNAL TRANSDUCTION; HYPOTHESIS: SEGMENTS OF LOOP 3 ARE DIFFERENTIALLY INVOLVED IN COUPLING AND ACTIVATION OF G<sub>i</sub>.

### 5HT<sub>1A</sub>R Intracellular Loop 3 Introduction

The third intracellular loop (ic3) of the human 5-HT<sub>1A</sub> receptor (Turner et al., 2004) is the largest of the receptor's four intracellular loops. This loop is 135 amino acids in size. It has been shown for other members of the GPCR family ( $\beta$ -adrenergic,  $\sigma$ -opioid, 5HT<sub>2aR</sub>) that this loop is important for receptor coupling to the G protein (Munch et al., 1991; Palm et al., 1995; Merkouris et al., 1996; Oksenberg et al., 1995). Data representing the role of ic3 in the functionality of GPCR has also been reported in the literature (Bikker et al, 1998; Dohlman et al., 1991). One report of deletion mutations in GPCR is for the ic3 region of the thyroid stimulating hormone receptor (TSHR). These mutations were reported to cause constitutive activity in the receptor protein. Further refinement of this study identified that the deletion of D564 residue was sufficient to cause constitutive receptor activity (Schulz et al., 1999). Constitutive activity of this receptor leads to hyperthyroidism because it stimulates the thyroid to produce and release more thyroid hormone.

Previous work in our laboratory using small peptide probes that mimic the amino acid sequence of the amino terminal end of ic3 of the 5-HT<sub>1A</sub> receptor have yielded the following results. The peptide P1 is a 15 amino acid synthetic peptide (Table 7), which mimics the first 15 amino acids in the ic3 region of the receptor. The introduction of the P1 peptide into a ligand binding experiment demonstrated that it was able to decrease the specific binding of [<sup>3</sup>H]-8-OH-DPAT (Table 8). We speculated that the peptide is uncoupling the receptor from the G protein, which shifts the receptor to its low affinity

ligand binding state. It was also demonstrated that the introduction of the peptide affects the signal transduction cascade by stimulating the incorporation of  $\gamma$ -[<sup>35</sup>S]-GTP into G<sub>i</sub> and decreasing the amount of cAMP generated by the stimulation of adenylyl cyclase with FSK (Table 8). The data from these studies indicate that the RFRIR stretch of amino acids are important for the coupling of the receptor to G<sub>i</sub> while the ARFRIRKTVKK stretch of amino acids is important for the activation of G<sub>i</sub> (Thiagaraj et al., 2002; 2007). To continue these initial studies and further elucidate the function of ic3 in G protein coupling and activation, two more peptides, P12 and P13, were tested in ligand binding assays,  $\gamma$ -[<sup>35</sup>S]-GTP incorporation assays, and cAMP assays. These peptides are 10 amino acids in length; each is shifted two amino acids towards the receptor's carboxy terminus (Table 7).

Compound	Sequence
P1	IFRAARFRIRKTVKK
P12	KTVKKVEKTG
P13	VKKVEKTGAD
[ <sup>3</sup> H]-8-OH-DPAT	[ <sup>3</sup> H]8-OH-2-di-n-propylaminotetralin

**Table 7:** ic3 Peptide Mimics

Primary sequences of 5HT<sub>1A</sub>R ic3 loop peptides; and one non-peptide agonist. N-terminal for each peptide is to the left. P1 is from a previous study done by Thiagaraj et al., 2007. P12 and P13 are the ic3 peptide mimics used in our studies. [<sup>3</sup>H]-8-OH-DPAT is a 5HT<sub>1A</sub>R agonist used in these studies.



Peptide	Agonist (%) Inhibition	[35S]- $\gamma$ -S-GTP Incorporation % Above Control	% Inhibition of FSK-Stimulated cAMP
P1*	50 (3uM)	30 (1uM)	10 (10uM)
P12	28 (30uM)	24 (30 uM)	0 (30uM)
P13	50 (15 uM)	12 (30 uM)	-24 (30 uM)

**Table 8: ic3 Peptide Mimic Signal Transduction Data**  
Summary of data generated for all ic3 experiments with P12 and P13. P1 is included as a reference, from Thiagaraj et al., 2007.

### 5HT1aR ic3 Peptide Effect on Ligand Binding

The high affinity binding of a ligand to a receptor is dependent upon the receptors being in their high affinity ligand binding state (receptor coupled to G protein). The effect of an experimental variable on the binding can be represented as percent of control (100%) or by specifying the amount of inhibition relative to control. The introduction of ic3 peptide mimic P12 at 30  $\mu$ M into the ligand binding experiment, yielded a 28% inhibition in the amount of agonist specifically bound to the receptor G protein complex (Figure 13). P13 at 15  $\mu$ M yielded a 50% inhibition of specific binding, which was similar to P1, but required a higher concentration of peptide. In summary, both peptides uncouple receptor and G protein as evidenced by a decrease in the amount of specifically bound [<sup>3</sup>H]8-OH-DPAT, although P13 is more active. These data implicate this region of H5HT1aR ic3 as important for coupling receptor to G protein. The evidence for this conclusion is the decrease in high affinity ligand binding observed. We believe this is due to peptide interference at the receptor-G protein interface.

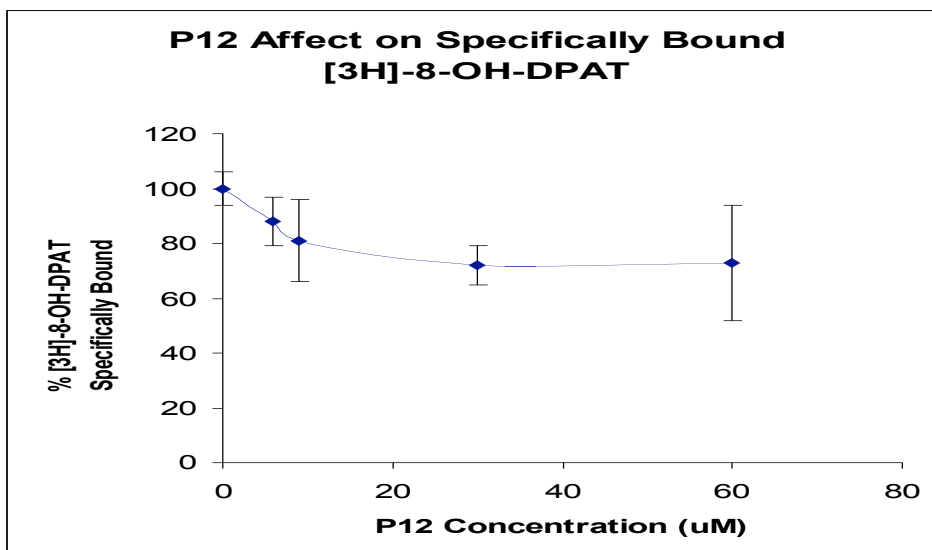


**Figure 13:** P12 Concentration Dependent Displacement of Specifically Bound 8-OH-DPAT Displacement curve for ic3 peptide P12 and [<sup>3</sup>H]8-OH-DPAT at H5HT1aR. As the concentration of P12 increased, the amount of specifically bound [<sup>3</sup>H]8-OH-DPAT decreased; the maximum with P12 (30 uM) is 28% inhibition of agonist binding. All data points represented are n=8; error bars represent the SEM.

#### Incorporation of $\gamma$ -[<sup>35</sup>S]-GTP into G protein

The binding data for the two ic3 peptides P12 and P13 suggest that the peptide is uncoupling the receptor from its G protein. To investigate if the peptide binding leads to activation of the G protein, experiments were designed to measure the incorporation of  $\gamma$ -[<sup>35</sup>S]-GTP, a more stable thioester analogue of GTP, into G<sub>i</sub>. Its incorporation is a well established measure of G-protein activity. Interestingly, both peptides (30  $\mu$ M) were able to stimulate the incorporation of  $\gamma$ -[<sup>35</sup>S]-GTP into G<sub>i</sub> at a significantly greater rate than in control experiments (P12 124 $\pm$ 6, P13 112 $\pm$ 6 vs. control 100, p<0.01) (Figures 14 and 15). Neither peptide was able to stimulate as much incorporation of  $\gamma$ -[<sup>35</sup>S]-GTP as 5HT alone; however, when combined (5HT/P12 261 $\pm$ 9, 5HT/P13 204 $\pm$ 15, p<0.01) with 5HT, they had an additive effect, which was significantly greater than 5HT alone.

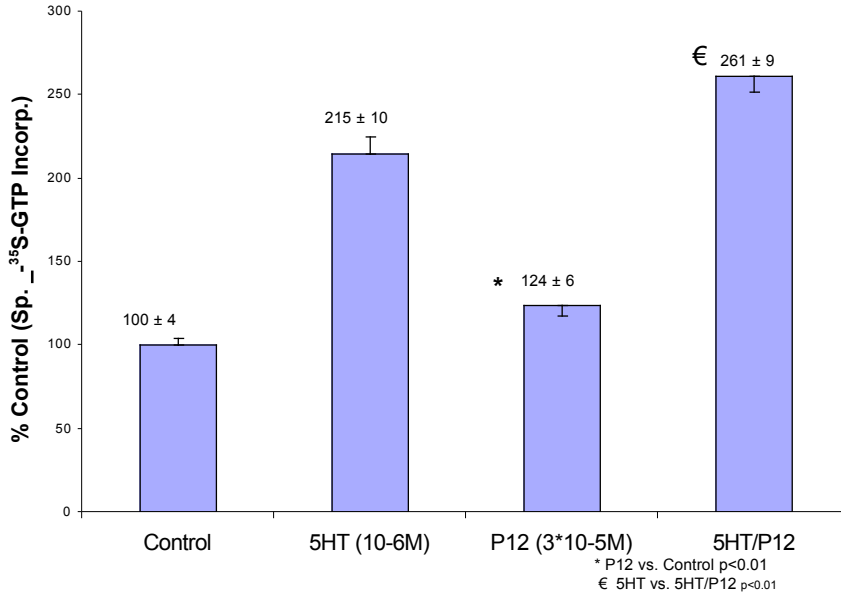


**Figure 14:** P12 Stimulated Incorporation of  $\gamma$ - $^{35}\text{S}$ -GTP

A measure of G protein activation. Control is the basal amount of  $\gamma$ - $^{35}\text{S}$ -GTP incorporated into  $G_i$  in CHO cells expressing the human 5HT1aR set as 100%. The Y axis is the percent of specifically bound  $\gamma$ - $^{35}\text{S}$ -GTP. All other treatments are percents of the control value. \*p<0.01 P12 vs. Control; € p<0.01 5HT vs. 5HT/P12

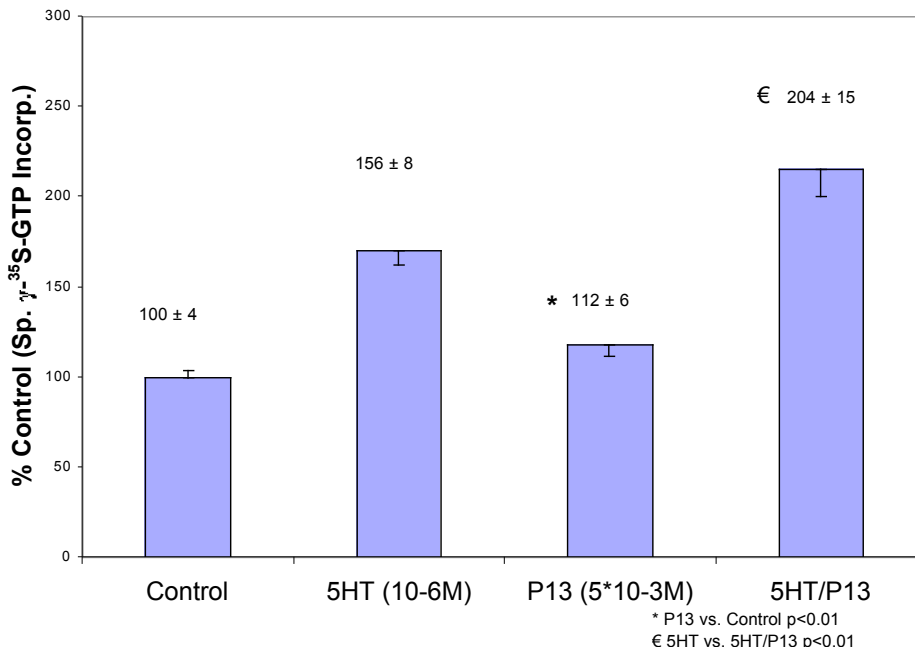


**Figure 15:** P13 Stimulated Incorporation of  $\gamma$ - $^{35}\text{S}$ -GTP

A measure of G protein activation. Control is the basal amount of  $\gamma$ - $^{35}\text{S}$ -GTP incorporated into  $G_i$  in CHO cells expressing the human 5HT1aR set as 100%. The Y axis is the percent of specifically bound  $\gamma$ - $^{35}\text{S}$ -GTP. All other treatments are percents of the control value. \* P13 vs. Control p<0.01; € 5HT vs. 5HT/P13 p<0.01

## cAMP Production by Adenylyl Cyclase

The next step in the 5HT<sub>1a</sub>R signal transduction pathway following the activation of G<sub>i</sub> is the inhibition of cAMP production by AC. These experiments measured the effect of P12 and P13 on the intracellular levels of cAMP following the stimulation of AC with FSK in the presence of the phosphodiesterase inhibitor IBMX (Figure 16). Treatment with P12 did not affect the concentration of cAMP. In contrast, P13 stimulated the production of cAMP greater than the control FSK. Treatment with 5HT decreased cAMP concentrations to only 24±1 % of control as expected. The peptides combined with 5HT (5HT/P12 41±1, 5HT/P13 60±4, p<0.05) had an inhibitory effect on the ability of 5HT to activate G<sub>i</sub>, which led to a decrease in its inhibitory effects on cAMP production.

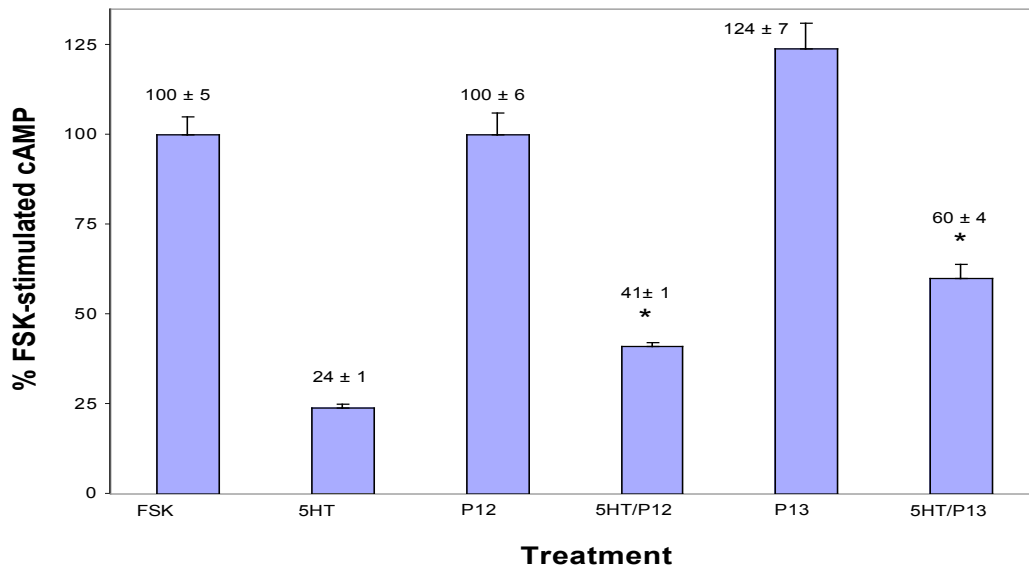


**Figure 16:** P12 and P13 Effect of Forskolin Stimulated cAMP Production  
Forskolin (FSK) stimulated cAMP production by adenylyl cyclase (AC) in CHO cells expressing the human 5HT<sub>1a</sub>R. These experiments were a measure of second messenger regulation by G protein. FSK is the control, which is set to 100%. All other treatments are expressed as a percent of the control value. All treatments include isobutylmethyl-xanthine (IBMX) an inhibitor of the metabolism of cAMP. 5HT vs. 5HT/P12 and 5HT vs. 5HT/P13 \*p<0.05

### 5HT1aR ic3 Discussion

The ic3 region of the 5HT1aR covered in these studies is quite small compared to the overall size of the loop. However, the differential activities of the peptides at different steps of the signal transduction cascade (Table 8) give some clues about the function of the segment of the receptor that the small peptides P12 and P13 are antagonizing. The decrease in the amount of [<sup>3</sup>H]8-OH-DPAT specifically bound to the 5HT1aR is important because it indicates a change in the receptor's affinity for the ligand. The mechanism proposed for this is that introduction of the small peptide mimics of the amino end of ic3 are interfering with the coupling of the 5HT1aR with G<sub>i</sub>. The decrease in coupling efficiency causes fewer receptors to be in their high affinity ligand binding state thus, fewer [<sup>3</sup>H]8-OH-DPAT molecules are able to bind to the receptor.

The activity of the G protein as measured by the incorporation of GTP into G<sub>iα</sub> is an important indication of the activation of the signal transduction cascade. The increase in γ-[<sup>35</sup>S]-GTP incorporation following the introduction of the peptides P12 and P13 into the experimental system indicates that the amino acid residues in this ic3 region are important not only for receptor coupling, but also for activation of the exchange of GDP for GTP in G<sub>iα</sub>. It is important, however, to note that neither of the peptides is as efficient as 5HT at stimulating the exchange. Interestingly though, when the peptides are combined with 5HT, they have an additive effect on the incorporation of γ-[<sup>35</sup>S]-GTP. This suggests that they are working independently: 5HT through the receptor G<sub>i</sub> complex, and the peptides acting directly at uncoupled G<sub>i</sub>. There is also an indication that the ability of ic3 to directly activate G<sub>i</sub> is due to the amino acid run of

ARFRIRKTVKK with the activity of the peptide mimics decreasing as they include less of this sequence (P1>P12>P13) (Table 7).

The inhibition of AC by  $G_i$  is an important negative regulator of intracellular signal transduction. The peptides tested, P12 and P13, differed in their ability to regulate this step in the cascade. P12 was unable to decrease the FSK stimulated levels of cAMP. This is in contrast to the action of 5HT which was able to significantly decrease the FSK stimulated levels of cAMP via activation of  $G_i$ . The combination of 5HT and the peptides decreased the affect of 5HT on lowering intracellular cAMP concentration. P13 had the opposite effect; it increased cAMP concentrations! This suggests that the two new amino acids (AD) from ic3 are the beginning of a new region of the loop, which has negative regulatory properties on  $G_i$  blunting its normal ability to regulate AC. It is interesting to speculate regarding the differences in data from the  $\gamma$ -[<sup>35</sup>S]-GTP incorporation assays and cAMP assays. With the relatively small changes produced by these two peptides, one possibility is experimental error that has not been accounted for. Another possibility is that the peptides are acting at some site or sites other than the proposed receptor-G protein interface or that the process at the interface is more complicated than anticipated or both.

The most tantalizing possibility is that the newly explored region represented by P12 and P13 is the beginning of a region of ic3 involved in coupling of receptor to G protein and is still capable of participating in activation of  $G_i$ . Additionally, however, the activation of  $G_i$  in this case involves additional conformational changes that inhibit rather than activate  $G_i$ . This would produce the opposite effect on cAMP concentration than anticipated, and would be equivalent to the downstream actions of an inverse agonist at

the ligand binding site. Since 5HT1aR is capable of constitutive activity (Martel et al., 2007), inverse agonism is possible, and it will be fascinating to see if the P12/P13 region is involved in this speculative activity once the crystal structure for the receptor has been determined.

## DISCUSSION: 5HT<sub>1A</sub>R IC2 AND IC3 SIGNAL TRANSDUCTION

The peptide mimic study for the intracellular loops (ic) 2 & 3 of the 5HT<sub>1A</sub>R was begun with the hypothesis: *Segments of loop 2 are differentially involved in coupling and activation of G<sub>i</sub>.* From previous work in the lab, we determined that use of sequential ten amino acid truncates of ic2 and ic3 would suggest differentiation of the function for corresponding sections of the receptor protein (Thiagaraj et al., 2007). The functions referred to in the hypothesis are the coupling of the G protein to the receptor and upon agonist binding to the receptor's ligand binding-site, activation of the coupled G protein.

A related second hypothesis expanded analysis into the thermodynamic realm: *Peptides from intracellular loop 2, active in experiments conducted in aim 1, will increase the system's entropy, altering the interaction between agonist and receptor.* The data presented in this section is for peptides (P22-24), which showed the most activity in the 5HT<sub>1A</sub> receptor signal transduction system in the first specific aim (GTP incorporation and cAMP production).

The last hypothesis broadened analysis by moving from ic2 to ic3: *Segments of loop 3 are differentially involved in coupling and activation of G<sub>i</sub>.* The use of ten amino acid truncates of ic3 would allow the differentiation of the function of the corresponding section of the receptor protein. The functions referred to in the hypothesis are the coupling of the G protein to the receptor and upon agonist binding to the ligand binding-site, activation of the coupled G protein. Work on this final hypothesis actually started before the ic2 loop studies because previous work in the lab had emphasized ic3 (Hayataka et al., 1998; Ortiz et al., 2000). However, from a strategic standpoint, we



decided to focus on ic2 in the current investigation. There is a greater than five fold difference in size of the two loops, and we concluded that systematic investigation of ic3, exceeded the temporal scope of this project. Nevertheless, 2 peptides were tested in this study, and we feel the results obtained contribute to the previously studied peptides from ic3.

There are some aspects of the previous work that help provide context for the current work. Conversely, some of the new results provide perspective to the previous work that was not possible before. Aspects of peptide specificity are vital to estimating the generality of the results reported here. There are two aspects of specificity of key importance: the site or sites of action for the peptides; and the peptides' ability to gain access to those sites of action. Somewhat less crucial to the current thesis, but meaningful overall, has to do with generality of these results across species as the source of receptor in the current series of investigations has been exclusively human.

A synopsis of these specificity parameters follows: During the original work, started over ten years ago, there was considerable effort devoted to developing multiple types of controls. A peptide of similar size (bombesin), but different sequence from parent peptide P1 (from ic3's N-terminus), was inactive in all of our measures. Another peptide (P10) from H5HT1aR's C-terminus that we hypothesized to be active, was not (Thiagaraj et al., 2002). These results gave confidence that not just any peptide we put into the system was active. Further, truncates and substituted derivatives of P1 gave differential activities in our various measures of coupling and activation. For example, a small peptide (P6) from ic3's N-terminus was inactive in all measures; another small peptide with residues from the mid-section of P1 was active in uncoupling, but was

inactive in signal transduction; P2, a substituted derivative of P1 was less active in uncoupling but more active in signal transduction than P1. These types of results gave us further confidence that activity was sequence-dependent (matching the sequence of ic3) and not the random result of testing just any peptide.

Initially, we were quite concerned about a peptide's ability to gain intracellular access to the putative sites of action at the receptor-G protein interface. Accordingly, early studies with the ic3 parent P1 and its relatives (P2-9) and the ic2 parent P11 were done with three different types of receptor preparations: whole cell, membrane, and solubilized (Hayataka et al., 1998; Ortiz et al., 2000; Thiagaraj et al., 2002; Thiagaraj et al., 2007). This approach is very time consuming and the solubilized format is extremely difficult because of receptor lability. Although some differences were noted, generally the membrane preparations were highly representative of all results in the agonist inhibition assays. Thus, in the current study, membrane preparations were used exclusively in the agonist inhibition format.

The question always arises, as well it should: Do the peptides cross the cellular membrane? We have not directly addressed this question, but synthetic and naturally occurring peptides from wasp venom that are similar to the H5HT1aR peptides have been shown to gain intracellular access via yet poorly understood mechanisms (Mousli et al., 1990). The current studies still use the whole cell approach in the cAMP assays; so differential intracellular penetration could still be a problem. The current work provides a reasonable, but not completely equivalent, comparator for signal transduction by conducting GTP incorporation into the G proteins using membrane preparations.

We postulate peptide sites of action as being intracellular either at the G protein-receptor interface or at the surface of the receptor or G protein, but not at, for example, the ligand binding-site. Early work in the lab looked into this issue by conducting binding experiments in which both agonist and peptide concentrations were variables (viewed in double reciprocal, Lineweaver-Burk-like graphs similar to those provided in the thermodynamic section of this dissertation). Examples from these studies include a somewhat longer version of P1, P8, that shows a non-competitive mechanism and P11, that gives an uncompetitive mechanism (Thiagaraj et al., 2007). These conclusions gave credence to the postulate that the test peptides are either, not competing for, nor mimicking agonist at the ligand-binding site, in comparison to an agent like DPT that is a ligand-binding site directed partial agonist (Thiagaraj et al., 2005).

Finally, what implications for 5HT<sub>1a</sub>R from other species do these human peptides have? A small amount of previous work in the lab addresses this matter by using rat brain receptor, which has been sequenced (Albert et al., 1990; Lembo et al., 1997), and rabbit brain receptor (Weber et al., 1997), in which our laboratory has partially characterized the un-sequenced receptor. P1 and P2 (ic<sub>3</sub> peptides) gave similar results to human receptor in agonist inhibition (Hayataka et al., 1998; Ortiz et al., 2000), an expected result as the rat and human receptors are highly homologous and all three receptors have almost identical biochemical pharmacology. Although highly interesting, use of these peptides against other 5HT<sub>R</sub>'s and other related GPCR's such as the beta adrenergic receptor have not been done. Overall, these previous studies provide evidence that the peptides under study are reasonably specific, but not perfect, tools that also have some generality in the sense of comparative biology.

## Changes in Receptor Binding Affinity: Focus on the Ligand Binding-Site

The introduction of the ic2 and ic3 peptide mimics had variable effect on the specific binding of an agonist. Agonist binding to a GPCR is complicated. It requires that all of the various pieces of the puzzle be in the proper orientation at the same time. The agonist in this case, 8-OH-DPAT, binds with the most robust intermolecular interactions when the 5HT1a receptor is coupled to G<sub>i</sub>. The coupling of the two proteins changes their conformations, leading to superior agonist binding; this is referred to as the receptor's high affinity agonist binding state (Maguire et al., 1977; Peroutka et al., 1979). The hypothesized role for the small peptide mimics in this system is to disrupt the receptor-G protein coupling (Hayataka et al., 1998). The disrupted coupling of the proteins causes a decrease in the amount of agonist that can bind to the receptor because the receptor conformation has been shifted to its low affinity agonist binding state.

While the scope of this dissertation has largely been bordered by the receptor-G protein interface, a few observations relative to the ligand binding-site itself should be useful in context of the larger receptor-G protein system. A large literature has developed with respect to both ligand binding-site determinants in GPCR generally (see for example, to start this literature: Dohlman et al., 1991), 5HTR (Hoyer et al., 1994; Barnes and Sharp, 1999), and the 5HT1aR, specifically (Raymond et al., 1999; Robichaud and Largent, 2000).

These developments have centered around understanding of the GPCR prototype, rhodopsin, via its crystal structure (Palczewski et al., 2000). Of great hindrance to the GPCR field has been the lack of crystallographic information for any of the other hundreds of receptors in the superfamily (Baldwin 1993, 1994; Sprang 2007). One of the

major goals of the current peptide project was to help, by contributing biochemical and pharmacological information that, in conjunction with many other techniques used by other investigators, piece together insights into receptor structure and function in light of the crystallographic deficit.

Additionally, studies summarized in the first two appendices of this dissertation and in previously documented work (Thiagaraj et al., 2005; Russo et al., 2005) are directly relevant to H5HTR's ligand binding-site. It is tremendously exciting that during the writing of this dissertation, the first crystal structure for a GPCR other than rhodopsin, 5HT1aR's close relative, the beta 2 adrenergic receptor ( $\beta$ AR), has been reported (Cherezov et al., 2007; Rasmussen et al., 2007; Rosenbaum et al., 2007). Ramifications of this revolutionary development (Day et al., 2007; Kobilka, 2007; Kobilka and Deupi, 2007) will be briefly discussed below.

#### Changes in Specific Agonist Binding: Focus on the G Protein Interface

The most efficient uncouplers from the ic2 region were P21-P23 (also P11), which decrease the amount of specifically bound 8-OH-DPAT to 50% of control. These data demonstrate that the N-terminal region of ic2 is important for coupling the receptor to the G protein (ic2 amino acid sequence IALDRYWAITDPIDYV). The other ic2 peptides P24-P27 from the carboxy terminus, in contrast, have far less effect on uncoupling the receptor from the G protein, decreasing the binding of 8-OH-DPAT to 75-94% of control. These data suggest the possibility that this segment of ic2 is only partially in contact with the G protein when it is coupled to the receptor and the segment's efficacy in the coupling process was minimal.

The data collected for the amino terminal region of ic3 for P12 and P13 cause a decrease in specifically bound 8-OH-DPAT to 73% and 50% of control, respectively. These data suggest that this region of ic3 is important for receptor coupling to the G protein. P12 consists of the final five amino acids of ic3 parent P1 and then proceeds five more residues toward the loop's center. P13 is shifted into the loop two more residues toward the loops carboxy terminus. While the data support this region's role in receptor-G protein coupling, the peptides' relative ability to uncouple declines relative to previously studied peptides whose structures represent segments closer to ic3's N-terminus. P12 and 13 are also beyond (toward the C-terminus) the key RFRI region of P1 previously identified as key to that part of ic3 responsible for G protein activation (Ortiz et al., 2000).

Varrault et al. (1994) demonstrated that the C-terminal section of i3 is involved in G protein coupling and regulation. So, if our work can be interpreted to mean that peak coupling and activating properties are associated with ic3's N-terminal residues and Varrault's work can be interpreted to mean that peak coupling and activating properties are associated with ic3's C-terminal residues, then what is the role for the vast internal region of the loop in 5HT1aR? Variability of GPCR ic3's size in rhodopsin versus 5HT1aR and BAR's, which have larger ic3 loops (at least twice the size of rhodopsin's ic3). It would be meaningful (although arduous) to eventually extend this peptide approach into the mid-loop region of ic3, and as a crystal structure becomes available for 5HT1aR, the comparisons of 5HT1aR loop function with BAR and rhodopsin will be fascinating.

### G Protein Activation Measured by Incorporation of $\gamma$ -[<sup>35</sup>S]-GTP

Activation of  $G_{i\alpha}$  is an important step in regulating the intracellular second messenger system. The ic2 peptides had variable affect on stimulating the incorporation of  $\gamma$ -[<sup>35</sup>S]-GTP into  $G_{i\alpha}$ . The peptides P11, P22, P24, P25, P26, and P27 stimulated incorporation from 100-148% of control, all less than the ligand 5HT. P21 stimulated incorporation to 158±11% of control, slightly less than 5HT. P23 was the only peptide which showed a stimulation of incorporation better than 5HT (188±10% of control). These data suggest a bimodal area of ic2, which very efficiently transmits changes in receptor conformation to the G protein to catalyze the exchange of GDP for GTP in  $G_{i\alpha}$ . However, the activity peak with P23 implicates this part of ic2 as being very important for activation of  $G_{i\alpha}$ . The ic3 peptides P12 and P13 were weak stimulators of incorporation of  $\gamma$ -[<sup>35</sup>S]-GTP into  $G_{i\alpha}$ .

Neither of the peptides (P12 and P13) was as potent as 5HT at activation of  $G_{i\alpha}$ . Many peptides tested in combination with 5HT yielded an additive effect on stimulating the incorporation of  $\gamma$ -[<sup>35</sup>S]-GTP into  $G_{i\alpha}$ , and were better than 5HT or the peptides alone. This suggests that they are augmenting signal transduction through complementary mechanisms to activate  $G_{i\alpha}$ . One very real possibility here is that multiple regions are responsible for G protein activation, and the individual peptides mimic only part of this structure, thereby producing a diminished effect relative to 5HT.

### Negative Regulation of Adenylyl Cyclase (AC)

The activation of  $G_{i\alpha}$  by 5HT<sub>1a</sub>R causes a decrease in the intracellular cAMP concentrations by inhibiting AC. Data for the ic2 and ic3 peptides showed variable effect on  $G_{i\alpha}$  activation. The peak of this activation was observed in ic2 at P23, a matching

depression in cAMP levels intracellularly was also observed. Interestingly P21, which demonstrated a trend towards activation of  $G_{i\alpha}$ , did not inhibit adenylyl cyclase. In fact P21 increased the intracellular cAMP concentration, the opposite of what was expected. These data from the ic3 peptides were also interesting because P12 had no effect on cAMP concentration. P13's signal transduction activity bears special mention. Since the peptide increases, rather than decreases cAMP concentration, it is tempting to speculate that the residues represented by P13 (and possibly P21) may be involved in signal transduction associated with inverse agonists (Gbahou et al., 2003; Urban et al., 2007).

The unique activity of previously studied P9 is also interesting in this regard (Thiagaraj et al., 2007). P9 increases rather than decreases cAMP concentration. This is a trend, not a significant effect, however. In respect to the GTP data, however, the unusual effect is significant. That is, P9 decreases, rather than increases, GTP incorporation, another effect reminiscent of inverse agonism. Turner et al. (2004) have identified a critical calmodulin regulatory site in the TM5/i3 loop region of 5HT1aR (RKTVK). This site is a five residue stretch in the current study within P9's sequence (RFIRIKTVKK). It is conceivable that the removal of the first five residues of P1 to give P9 produces a peptide that targets this regulatory site with some specificity.

Recently, 5HT1aR has been shown to possess constitutive activity (Martel et al., 2007). Constitutive activity of the 5HT1aR causes adenylyl cyclase to decrease the production of cAMP down to a basal level. The  $\beta$ AR has also been observed to possess constitutive activity, but rhodopsin has not. One of the key features of the crystals for  $\beta$ AR is the use of the inverse agonist carazolol in solving the structure, an event that could not occur if  $\beta$ AR did not have constitutive activity. An inverse agonist is a



substance which upon binding to a receptor terminates all receptor transduced signal, below even its resting basal level. Inverse agonism has not been explored in a concerted sense in 5HT1aR. Would a thorough examination of the P9 region plus a trip deeper into ic3 (as suggested by P13) and into ic2 (P21) begin to shed light on inverse agonism? This could be a very exhilarating exploration as speculation exists that inverse agonism may be much more common than previously thought (Gbahou et al., 2003; Urban et al., 2007).

#### Summary of Signal Transduction Activity

The peptides studied in this project from ic2 and ic3 of H5HT1aR were shown to modulate the signal transduction system based upon influencing high affinity agonist binding, G protein activation, and negative regulation of the target second messenger. The peptides showed an inhibitory effect on the specific binding of 8-OH-DPAT decreasing it to below 50% of control in the best cases, suggesting the uncoupling of  $G_i$  from the receptor changing its conformation to the low affinity agonist binding state. This effect was greatest at the amino terminal ends of ic2 and ic3. The trend in the data for activation of  $G_i$  and the subsequent inhibition of cAMP production by AC peaks at P23 of ic2 (that is, about mid-loop). The data on either side of this maximum shows decreased incorporation of  $\gamma$ -[ $^{35}\text{S}$ ]-GTP into  $G_{i\alpha}$  and diminishing cAMP changes, indicating less activity in the  $G_{i\alpha}$  signaling pathway.

We believe that a comparison between ic2 and ic3 with regard to structure and activity will be similar between them. The mid loop regions of the intracellular loops will possess similar properties for activation of the signal transduction cascade. This is most likely due to their exposure following agonist binding and the resulting change in structural conformation of the receptor protein. Meanwhile, the coupling of the receptor

to the G protein is most prominent at the loops' amino terminals. This is because portions of the receptor are exposed to and interact with the G protein when the receptor is in its high affinity ligand binding conformation.

### Thermodynamics of ic2 Peptides

The specific binding of the radioligand [<sup>3</sup>H]-8-OH-DPAT to 5HT<sub>1a</sub>R can be measured at a range of temperatures, which allows for the calculation of various thermodynamic binding parameters (Hitzemann, 1998). Thermodynamics are important measures of the functionality of GPCRs. The changes in energy input and output yield information about the underlying mechanisms of ligand binding and intramolecular interactions, which are necessary for proper receptor function. The dissociation constant, K<sub>d</sub>, is the concentration of [<sup>3</sup>H]-8-OH-DPAT at which the ligand-binding site of the receptor is 50% occupied (McGonigle and Molinoff, 1989). The K<sub>d</sub>, determined at each temperature forms the basis for all of these calculations. The K<sub>d</sub> calculation was also determined in the presence of the ic2 peptides in parallel sets of experiments.

Gibb's Free Energy ( $\Delta G^\circ$ ) is the energy required for a chemical reaction to proceed (change in energy based upon agonist binding in these experiments), a negative number means that the reactions proceed spontaneously. This parameter utilizes the K<sub>d</sub> at a single temperature (25°) in an Arrhenius-like equation for calculation of  $\Delta G^\circ$ . Specifically, Gibb's standard free energy ( $\Delta G^\circ$ ) was calculated for 8-OH-DPAT alone (control) and in the presence of the ic2 peptides P22, P23, and P24. All of these values are negative, meaning that the binding event will occur spontaneously. The calculated value of  $\Delta G^\circ$  is not significantly altered by the addition of the ic2 peptides. Thus, the

peptides did not change the overall energetics of the system much. This is evident because the peptides did not completely abolish agonist binding. If this occurred, the  $\Delta G^\circ$  value calculated would be positive, which means that agonist binding would not occur spontaneously.

The observed trend for the  $K_d$  determinations for [ $^3\text{H}$ ]-8-OH-DPAT at the 5HT $1a$ R over the range of temperatures was that temperature and  $K_d$  are inversely related in this system; as temperature increases, the dissociation constant decreases. Stated another way, as the temperature increases the concentration of agonist required to occupy 50% of the agonist binding sites decreases. This experimental approach allows for the calculation of the thermodynamic parameter enthalpy ( $\Delta H^\circ$ ) in a Van't Hoff determination. The standard enthalpy ( $\Delta H^\circ$ ) is calculated from the slope of the regression line based upon the natural logarithm of inverse  $K_d$  vs. inverse absolute temperature.

Since enthalpy is loosely equitable to heat of reaction (or the net of bonding changes, small and large), a negative number means the reaction is exothermic (releases energy) thus being energetically favorable. The calculated  $\Delta H^\circ$  for 8-OH-DPAT yielded a positive (unfavorable) enthalpy in all cases. However, the data for the changes in  $K_d$  as a function of temperature for [ $^3\text{H}$ ]-8-OH-DPAT alone (controls) are generally smaller than when the ic2 peptides P22, P23, and P24 are introduced into the binding assay. Thus, agonist binding is barely temperature-dependent and becomes more temperature dependent when the peptides are present. Stated another way, the agonist can bind to the receptor at any temperature with little difference, however; the ic2 and ic3 peptide mimics make agonist-receptor binding more temperature dependent.

The standard entropy ( $\Delta S^\circ$ ) (calculated from the standard Gibb's free energy and the standard enthalpy in a Gibb's equation determination) is a measure of the disorder of the system. The more highly ordered a system is, the more energy required to maintain that order. A positive number is favorable entropy. The  $\Delta S^\circ$  was calculated for 8-OH-DPAT alone and in the presence of the ic2 peptides. The peptides increased the entropy of the 8-OH-DPAT binding system compared to the agonist alone. This indicates the peptides increase the entropic favorability of [<sup>3</sup>H]-8-OH-DPAT receptor binding (increased order of the agonist-receptor binding system, but overall increased disorder). This favorable event compensates for the unfavorable enthalpic changes the peptides produced, keeping the overall energetics (free energy) relatively stable. P22 and P24 had a similar effect on K<sub>d</sub>, enthalpy, and entropy. This seems to mirror the effectiveness of the peptides at activation of the signal transduction cascade. The general trend observed is that P23 contains the core region of ic2 (PIDYV), which is responsible for G protein activation. As the peptides on either side of P23 move away from this core region, they show fewer G protein activation properties and more involvement in G protein coupling.

Viewed in a broader perspective, a few points seem to stand out in the context of general thermodynamic theory for receptor interactions. First, the paradigm used to analyze receptor thermodynamics is crucial to the conclusions reached (for example, in this study, agonist is bound to the ligand-binding site, whereas in some investigations antagonist is bound). Second, the binding sites for different receptor systems are unique energetically. So, energetic differences between systems have led to the theory of thermodynamic discrimination for ligand-receptor binding (Heitman et al., 2006). That is, although there may not be entropic versus enthalpic differences overall in comparative

pharmacology between receptor systems, in a given receptor system various binding events (binding of different ligands) may be so discriminated.

Thus, for example to illustrate system uniqueness, in  $\beta$ AR, which is a closely related system to 5HT1aR, favorable enthalpic decreases accompanied agonist binding (Weiland et al., 1980). At the nicotinic neuronal receptor (which is ionotropic and not related to 5HT1aR or GPCR), agonist binding is driven by both enthalpy and entropy (Borea et al., 2004). The entropy side of this result is like our observations. Dopamine receptors (DAR), relatives of 5HT1aR, but more distant than  $\beta$ AR, give agonist binding events that are not temperature driven, a result similar to what we have observed with the agonist [3H]8-OH-DPAT in the H5HT1aR system (Zahniser and Molinoff, 1983; Kilpatrick et al., 1986), and similar to rat 5HT1aR (Dalpiaz et al., 1995; 1996)

Most of our current study does not fit nicely into the direct ligand-binding site characterization paradigm as we postulate that the peptides are only indirectly influencing agonist binding through affinity changes accompanying receptor-G protein uncoupling. Nevertheless, the current findings can play a role in contributing to basic molecular understanding of 5HT1aR's and the application of this information to new drug development, and to the place that 5HT1aR has in the broader context of biological receptors. This should be especially so in that we are not aware that this type of thermodynamic information has been previously available for peptide probes of receptor-G protein interactions.

It is important to also interpret the results of the thermodynamic studies from the vantage point of the original design of the peptides as probes of the receptor-G protein interface. The observation that the peptides have little effect on agonist free energy but

differentially changed enthalpy and entropy has direct bearing on the peptides' ability to produce displacement of agonist from the ligand-binding site via indirectly produced alterations of affinity. In every case, introduction of peptide decreases agonist binding (differentially between peptides), and in each measured case (peptides P8, 9, 11, 22-24), a less favorable enthalpic change compared to control accompanies agonist binding (Hall et al, 2008).

Significantly, in each measured case, entropy increases relative to control, an event likely to involve alterations in lipid/aqueous order, changes likely to also influence the receptor's ability to perturb the G protein (a differential effect that also accompanies peptide intervention). Long-standing, dynamic theory has been advanced to understand general allosteric mechanisms in biological regulation (Changeux and Edelstein, 2005), and it will be fascinating to see if these thermodynamic observations can be fit into this rapidly advancing field when crystal structure information becomes available for 5HT1aR.

### Conclusions

The peptide mimic study for the intracellular loops (ic) 2 & 3 of the 5HT1aR was designed to examine which segments were involved in coupling and activation of  $G_i$ . The amino terminal ends of ic2 and ic3 are important for coupling the receptor and G protein. The activation of the G protein peaks at P23 (WAITDPIDYV) in ic2 (Figure 35). The activity is decreased as the peptides move in either direction away from this core sequence. The curious results of increased cAMP concentrations caused by some peptides suggests that the two new amino acids (AD) from P13 are the beginning of a new region of ic3, which has negative regulatory properties on  $G_i$ .

The introduction of the ic2 peptides perturbed the thermodynamic norm in the agonist binding system. A summary of the peptides effects are as follows. When the binding data for Kd and the thermodynamic parameters of standard free energy, enthalpy, and entropy for P23 are compared to that for the agonist 8-OH-DPAT alone, some similarity is evident. The lines in the Van't Hoff plot (Figure 9) for 8-OH-DPAT and P23 are the closest in slope compared to other peptides tested (that is, P23 has the least additional effect of all peptides on increasing the Kd of 8-OH-DPAT as temperature decreases). None of the peptides, which were tested, yielded a significant change in the standard free energy from that of the agonist 8-OH-DPAT. All of the peptides showed unfavorable increases in enthalpy compared to the agonist 8-OH-DPAT. All of the peptides showed favorable increases in entropy compared to the agonist 8-OH-DPAT alone (control), which adds credence to the original hypothesis.

Therefore, it seems from these results that P23 mimics the receptor state most like that produced by agonist. This may be because P23 has the least additional effect of all the peptides on the conformation of the receptor-G protein complex necessary for the activation of the signal transduction cascade. The results reported here were initially generated to provide biochemical input into 5HT1aR structure determination, and certainly we have speculated in that regard. As 5HT1aR x-ray structure is solved, these peptide results and other indirect biochemical probes of structure may or may not completely stand up.

We believe that the favorable changes in entropy observed in the thermodynamic experiments for agonist binding are possibly due to the peptides exclusion of water from the receptor-G protein interface. The peptide then exerts a stabilizing effect on the

molecular interactions between the receptor and G protein. The disruption of water molecules cage around the receptor may allow for more degrees of freedom for the movement of the proteins allowing them to interact a more energetically favorable manner.

Even if the final judgement of these peptide probes is mixed in this sense, the information produced may be useful as independent pharmacological observations. That is, future studies in this area and pragmatic implications of the work may be most relevant in a framework where the multiple, differential activities of the peptides can be exploited by medicinal chemists to build unique pharmacological agents targeting previously un-utilized sites at the receptor-G protein interfacial region.

Results for ic2 and ic3 presented in this report are interesting in perspective of the x-ray crystal structure for human beta 2 adrenergic receptor ( $\beta_2$ AR) that has just been published (Cherezov et al., 2007; Rasmussen et al., 2007, Rosenbaum et al., 2007). The long-awaited crystal structure for some GPCR other than rhodopsin should open the flood gates for consolidation of understanding (Kobilka, 2007; Kobilka and Deupi, 2007) of structure-function relationships within the receptor superfamily. It is perhaps fitting to think about the relatively open, less structured  $\beta$ AR (and likely 5HT1aR) compared to rhodopsin as this dissertation closes (Cherezov et al., 2007).

Unstructured segments of these receptors are a problem in creating proper crystals. One of the most unstructured regions in  $\beta_2$ AR is the third intracellular loop, which is much larger in  $\beta_2$ AR than rhodopsin (even larger still in 5HT1aR). One of the current  $\beta_2$ AR studies basically involved cutting out the third intracellular loop and inserting an enzyme (T4 lysozyme) known to produce nicely stacked crystals (Day et al.,



2007). Alternatively, in the companion study a rigid antibody (Mab5) was bound to the third intracellular loop. In both cases, the highly disordered carboxy-terminus of the receptor was removed. While methodological, these considerations point beyond technique to differences between  $\beta_2$ AR (and presumably 5HT1aR) and rhodopsin. The less structured, more open, nature of  $\beta_2$ AR points to greater conformational and functional complexity.

The G 21 clone of the H5HT1aR used in our experiments has 43% homology with Human  $\beta_2$ AR in the TM domains (Kobilka et al., 1987, Fargin et al., 1988). The greatest homology is in TM6 where 19 of 20 amino acids are identical (an astounding 95% homology). Intracellular loop 2 is well-conserved between the two receptors, but ic3 and the C-terminus are not. This paper also has a print out of the residue by residue comparison of the 5HT1aR vs.  $\beta_2$ AR (Fargin et al., 1988).

Regarding the comparison between H5HT1aR and  $\beta_2$ AR relative to effector activation or signal magnitude, Fargin et al. (1989) transiently transfected the H5HT1aR clone and the BAR2 clone into two types of cultured cells. Using 5HT concentrations similar to what we used, and appropriate isoproterenol ( $\beta_2$ AR agonist) concentrations, they were able to achieve about equal magnitude effects for cAMP production, but in opposite directions ( $\beta_2$ AR is a positive regulator of adenylyl cyclase). I interpret this to mean that the two receptors have about the same magnitude effect on signal transduction but opposite in sign intracellular effect at equivalent doses for the appropriate receptors.

Our results, in conjunction with those of Varrault et al., 1994, suggest that various regions of 5HT1aR's ic2 loop are necessary to support coupling to G protein, but only the mid-loop to C-terminal segment goes on to activate G protein. The critical role of the

DRY sequence (at the very N-terminus of ic2) of the 5HT1aR (Kushwaha et al., 2006) in stabilizing within loop and between loop interactions leading to receptor G protein coupling is consistent with our conclusions. Further, these conclusions are supported by the recent  $\beta_2$ AR x-ray crystallographic data, and, indeed, seems to hold for the entire superfamily in this almost universally conserved sequence. There is a very relevant curiosity about  $\beta_2$ AR, compared to rhodopsin involving the so called ion lock, of which the DRY region of TM3/ic2 is involved. In the presence of inverse agonist carazolol, the lock is broken in  $\beta_2$ AR. Overall, the  $\beta_2$ AR structure suggests less involvement of ic2 with G protein activation; this observation coupled with the inverse agonism of  $\beta_2$ AR are likely important for 5HT1aR (which also shows inverse agonism) and the conclusions of this dissertation. It certainly seems reasonable at this juncture to hypothesize that 5HT1aR's structure is more open like BAR, compared to rhodopsin.

Thus, ic2's N-terminus for several GPCRs is involved in receptor-G protein coupling, and there is variability in whether the N-terminal ic2 loop supports G protein activation. In early work with rhodopsin (Lembo et al., 1997; Bikker et al., 1998), evidence supported the involvement of ic2 in activation of G protein. In the alpha 2A adrenergic receptor (Edwards and Limbird, 1999), ic2 does not activate the G protein, a conclusion parallel to that reached in our investigations of 5HT1aR; both of these receptors are coupled to Gi. It is certainly possible that functional attributes of ic2 have evolved differentially across the super family of 7TMDR, especially regarding activation, which can occur only after the necessary condition of coupling has been met.

With regard to ic3,  $\beta_2$ AR utilizes the N- as well as the C-terminal regions to couple to G protein; nevertheless, results clearly suggest that BAR's ic3 C-terminus is ideally designed to stimulate Gs without help (Munch et al, 1991). The recent crystallographic structure for BAR finds an intact "toggle switch," originally seen in

rhodopsin. It seems a small leap of inference to suggest that 5HT1aR has an intact toggle since both  $\beta_2$ AR and rhodopsin have it.

This trigger region affirms the significant role that ic3 has in G protein activation. The ic3-C-terminus of alpha 2 adrenergic receptors plays a role in binding to Go's betagamma region. Our results with the H5HT1aR conclude that ic3's N-terminal region activates G protein, as does the C-terminal of ic3 (Varrault et al. 1994). Together, these results may indicate that the entire ic3 loop is broadly involved across the receptor family, but sub-segments of ic3 may be more or less important to individual types of receptors as well as to the target signal transduction system (Turner et al., 2004).

Therefore, sub-segments of both ic2 and ic3 may have become more or less important, especially regarding G protein activation and regulation, to individual types of receptors as they have adapted to meet local needs. BAR's relatively "open" crystal structure compared to rhodopsin enables the cytoplasmic ends of TM segments and attached ic loops to interact with a water cluster, ultimately leading to differential G protein activation from a variety of conformations.

It is interesting to speculate that the entropic changes produced by peptide introduction in our experiments may have something to do with this dynamic structural/G protein activation relationship. BAR's openness leads to structural flexibility and instability, creating challenges for crystallographers. As the authors of the x-ray work speculate (Kobilka, 2007; Kobilka and Deupi, 2007), final resolution of GPCR structures beyond the stable rhodopsin may require crystals of the coupled receptor-G protein complex. The many laboratories who have contributed biochemical approaches to understanding 5HT1aR eagerly await such developments.

## REFERENCES:

- Aghajanian, G. K., and H. J. Hailgler. 1975. Hallucinogenic indoleamines: Preferential action upon presynaptic serotonin receptors. *Psychopharmacology communications* 1, no. 6:619-629.
- Albert, P. R., et al. 1990. Cloning, functional expression, and mRNA tissue distribution of the rat 5-Hydroxytryptamine<sub>1A</sub> receptor gene. *Journal of Biological Chemistry* 265, 5825-5832.
- Arora, K. K., H. O. Chung, and K. J. Catt. 1999. Influence of a species-specific extracellular amino acid on expression and function of the human gonadotropin-releasing hormone receptor. *Molecular endocrinology (Baltimore, Md.)* 13, no. 6:890-896.
- Azmitia, E. C. 2007. Serotonin and brain: evolution, neuroplasticity, and homeostasis. *International review of neurobiology* 77, 31-56.
- Baldwin, J. M. 1994. Structure and function of receptors coupled to G proteins. *Current Opinions in Cellular Biology* 6, 180-190.
- Baldwin, J. M. 1993. The probable arrangement of the helices of G protein-coupled receptors. *EMBO J.* 12 (4), 1693-1703.
- Barnes, N. M., and T. Sharp. 1999. A review of central 5-HT receptors and their functions. *Neuropharmacology* 38, no. 8:1083-1152.
- Bikker, J. A., S. Trumpp-Kallmeyer, and C. Humblet. 1998. G-protein coupled receptors: models, mutagenesis, and drug design. *Journal of Medicinal Chemistry* 41, 2911-2927.
- Bradford, M. M. 1976. A rapid sensitive method for the quantitation of microgram quantities of protein utilizing the principle of protein-dye binding. *Analytical Biochemistry* 72, 248-254.
- Carli, M., R. Luschi, and R. Samanin. 1995. (S)-WAY 100135, a 5-HT<sub>1A</sub> receptor antagonist, prevents the impairment of spatial learning caused by intrahippocampal scopolamine. *European journal of pharmacology* 283, no. 1-3:133-139.

- Carlini, E. A., and J. M. Cunha. 1981. Hypnotic and antiepileptic effects of cannabidiol. *Journal of clinical pharmacology* 21, no. 8-9 Suppl:417S-427S.
- Changeux, J. P., and S. J. Edelman. 2005. Allosteric mechanisms of signal transduction. *Science* 308, 1424-1428.
- Cherezov, V., et al. 2007. High-resolution crystal structure of an engineered human beta2-adrenergic G protein-coupled receptor. *Science (New York, N.Y.)* 318, no. 5854:1258-1265.
- Clarke, H. F., et al. 2004. Cognitive inflexibility after prefrontal serotonin depletion. *Science (New York, N.Y.)* 304, no. 5672:878-880.
- Cowen, P. J. 2000. Psychopharmacology of 5-HT1a receptors. *Nuclear Medicine and Biology* 27, 437-439.
- Dalpiatz, A., P. A. Borea, S. Gessi, and G. Gilli. 1996. Binding Thermodynamics of 5-HT1A Receptor Ligands. *European Journal of Pharmacology* 312, 107-114.
- Dalpiatz, A., S. Gessi, P. A. Borea, and G. Gilli. 1995. Binding thermodynamics of serotonin to rat-brain 5-HT1A, 5HT2A and 5-HT3 receptors. *Life Sciences* 57, no. 12:PL141-6.
- Day, P. W., et al. 2007. A monoclonal antibody for G protein-coupled receptor crystallography. *Nature methods* 4, no. 11:927-929.
- De Clerck, F. 1990. The role of serotonin in thrombogenesis. *Clinical physiology and biochemistry* 8 Suppl 3, 40-49.
- de las Heras, B., B. Rodriguez, L. Bosca, and A. M. Villar. 2003. Terpenoids: sources, structure elucidation and therapeutic potential in inflammation. *Current topics in medicinal chemistry* 3, no. 2:171-185.
- Deecher, D. C., et al. 1993. Detection of 5-hydroxytryptamine2 receptors by radioligand binding, northern blot analysis, and Ca<sup>2+</sup> responses in rat primary astrocyte cultures. *Journal of neuroscience research* 35, no. 3:246-256.
- Deliganis, A. V., P. A. Pierce, and S. J. Peroutka. 1991. Differential interactions of dimethyltryptamine (DMT) with 5-HT1a and 5-HT2a receptors. *Biochemical Pharmacology* 41, no. 11:1739-1744.

- Dohlman, H. G., J. Thorner, M. G. Caron, and R. J. Lefkowitz. 1991. Model systems for the study of seven-transmembrane-segment receptors. *Annual Review of Biochemistry* 60, 653-688.
- Dolphin, A. C. 2003. G protein modulation of voltage-gated calcium channels. *Pharmacological reviews* 55, no. 4:607-627.
- Fargin, A., et al. 1988. The genomic clone G-21 which resembles a beta-adrenergic receptor sequence encodes the 5-HT1a receptor. *Nature* 335, 358-360.
- Fargin, A., et al. 1989. Effector coupling mechanisms of the cloned 5HT1a receptor. *Journal of Biological Chemistry* 264, no. 14:848-852.
- Feeney, K., M. Cain, and A. K. Nowak. 2007. Chemotherapy induced nausea and vomiting--prevention and treatment. *Australian Family Physician* 36, no. 9:702-706.
- Garnovskaya, M. N., et al. 1997. 5-HT1A receptor activates Na<sup>+</sup>/H<sup>+</sup> exchange in CHO-K1 cells through G $\alpha$ 2 and G $\alpha$ 3. *The Journal of biological chemistry* 272, no. 12:7770-7776.
- Gbahou, F., et al. 2003. Protean agonism at histamine H3 receptors in vitro and in vivo. *Proceedings of the National Academy of Sciences of the United States of America* 100, no. 19:11086-11091.
- Gilman, A. G. 1987. G proteins: transducers of receptor-generated signals. *Annual Review of Biochemistry* 56, 615-649.
- Guan, X. M., S. J. Peroutka, and B. K. Kobilka. 1992. Identification of a single amino acid residue responsible for the binding of a class of beta-adrenergic receptor antagonists to 5-hydroxytryptamine1A receptors. *Molecular pharmacology* 41, no. 4:695-698.
- Hall, B., et al. 2008. Thermodynamics of Peptide and Non-Peptide Interactions With the Human 5HT1a Receptor. *Biochemistry and Cell Biology*.
- Hampson, A. J., M. Grimaldi, J. Axelrod, and D. Wink. 1998. Cannabidiol and (-)Delta9-tetrahydrocannabinol are neuroprotective antioxidants. *Proceedings of the National Academy of Sciences of the United States of America* 95, no. 14:8268-8273.

- Heitman, L. H., et al. 2006. Allosteric modulation, thermodynamics and binding to wild-type and mutant (T277A) adenosine A1 receptors of LUF5831, a novel nonadenosine-like agonist. *British journal of pharmacology* 147, no. 5:533-541.
- Hitzemann, R. 1988. Thermodynamic aspects of drug-receptor interactions. *Trends in pharmacological sciences* 9, no. 11:408-411.
- Hitzemann, R., M. Murphy, and J. Curell. 1985. Opiate receptor thermodynamics: agonist and antagonist binding. *European journal of pharmacology* 108, no. 2:171-177.
- Hoyer, D. E., et al. 1994. International Union of Pharmacology classification of receptors for 5-hydroxytryptamine (serotonin). *Pharmacological Reviews* 46, 157-203.
- Jayakumar, A. R., K. V. Rao, ChR Murthy, and M. D. Norenberg. 2006. Glutamine in the mechanism of ammonia-induced astrocyte swelling. *Neurochemistry international* 48, no. 6-7:623-628.
- Jiang, W., et al. 2005. Cannabinoids promote embryonic and adult hippocampus neurogenesis and produce anxiolytic- and antidepressant-like effects. *The Journal of clinical investigation* 115, no. 11:3104-3116.
- Julius, D., et al. 1990. The 5HT<sub>2</sub> receptor defines a family of structurally distinct but functionally conserved serotonin receptors. *Proceedings of the National Academy of Sciences USA* 87, 928-932.
- Kobilka, B. K., et al. 1987. An intronless gene encoding a potential member of the family of receptors coupled to guanine nucleotide regulatory proteins. *Nature* 329, no. 75-79.
- Kobilka, B. K. 2007. G protein coupled receptor structure and activation. *Biochimica et biophysica acta* 1768, no. 4:794-807.
- Kobilka, B. K., and X. Deupi. 2007. Conformational complexity of G-protein-coupled receptors. *Trends in pharmacological sciences* 28, no. 8:397-406.
- Kuipers, W., et al. 1997. Study of the interaction between aryloxypropanolamines and Asn386 in helix VII of the human 5-hydroxytryptamine<sub>1A</sub> receptor. *Molecular pharmacology* 51, no. 5:889-896.

- Kushwaha, N., et al. 2006. Molecular determinants in the second intracellular loop of the 5-hydroxytryptamine-1A receptor for G-Protein Coupling. *Molecular Pharmacology* 69, 1518-1526.
- Lanfumeey, L., and M. Hamon. 2000. Central 5-HT(1A) receptors: regional distribution and functional characteristics. *Nuclear medicine and biology* 27, no. 5:429-435.
- Lembo, P. M., M. H. Ghahremani, S. J. Morris, and P. R. Albert. 1997. A conserved threonine residue in the second intracellular loop of the 5-hydroxytryptamine 1A receptor directs signaling specificity. *Molecular Pharmacology* 52, 164-171.
- Leonard, B. E. 1996. Serotonin receptors and their function in sleep, anxiety disorders and depression. *Psychotherapy and psychosomatics* 65, no. 2:66-75.
- Maguire, M. E., P. M. VanArsdale, and A. G. Gilman. 1976. An agonist-specific effect of guanine nucleotides on binding to the beta adrenergic receptor. *Molecular Pharmacology* 12, 335-339.
- Mann, J. J. 2005. The medical management of depression. *The New England journal of medicine* 353, no. 17:1819-1834.
- Martel, J. C., et al. 2007. Native rat hippocampal 5-HT<sub>1A</sub> receptors show constitutive activity. *Molecular pharmacology* 71, no. 3:638-643.
- McCarthy, B. G., and S. J. Peroutka. 1989. Comparative neuropharmacology of dihydroergotamine and sumatriptan (GR 43175). *Headache* 29, no. 7:420-422.
- McGonigle, P., and Molinoff, P. B. 1989. Quantitative aspects of drug-receptor interactions. In *Basic Neurochemistry: Molecular, Cellular, and Medical Aspects*, edited by G. J. Siegel. New York: Raven Press.
- Merkouris, M., et al. 1996. Identification of the critical domains of the sigma-opioid receptor involved in G protein coupling using site-specific synthetic peptides. *Molecular Pharmacology* 50, 985-993.
- Mousa, H. A., and Z. Alfirevic. 2007. Treatment for primary postpartum haemorrhage. *Cochrane database of systematic reviews (Online)* (1), no. 1:CD003249.
- Mousli, M., et al. 1990. G protein activation: a receptor-independent mode of action for cationic amphiphilic neuropeptides and venom peptides. *Trends in Pharmacological Sciences* 11, 358-362.



- Munch, G., C. Dees, M. Hekman, and D. Palm. 1991. Multisite contacts involved in coupling of the beta-adrenergic receptor with the stimulatory guanine-nucleotide-binding protein. *European Journal of Biochemistry* 198, 357-364.
- Oksenberg, D., S. Havlik, S. J. Peroutka, and A. Ashkenazi. 1995. The third intracellular loop of the 5-hydroxy-tryptamine<sub>2A</sub> receptor determines effector coupling specificity. *Journal of Neurochemistry* 64, 1440-1447.
- Omori, K., and J. Kotera. 2007. Overview of PDEs and their regulation. *Circulation research* 100, no. 3:309-327.
- Palczewski, K., et al. 2000. Crystal structure of rhodopsin: A G protein-coupled receptor. *Science* 289, no. 739-745:.
- Palm, D., G. Munch, and D. Malek. 1995. Mapping G protein coupling domains by site-specific peptides. *Methods in Neuroscience* 25, 302-321.
- Peroutka, S. J., R. M. Lebovitz, and S. H. Snyder. 1979. Serotonin receptor binding sites affected differentially by guanine nucleotides. *Molecular Pharmacology* 16, 700-708.
- Peroutka, S. J. 1994. Molecular biology of serotonin (5-HT) receptors. *Synapse (New York, N.Y.)* 18, no. 3:241-260.
- Pietrobon, D., and J. Striessnig. 2003. Neurobiology of migraine. *Nature reviews. Neuroscience* 4, no. 5:386-398.
- Price, G. W., et al. 1996. Species differences in 5-HT autoreceptors. *Behavioural brain research* 73, no. 1-2:79-82.
- Rai, D., et al. 2003. Adaptogenic effect of *Bacopa monniera* (Brahmi). *Pharmacology, biochemistry, and behavior* 75, no. 4:823-830.
- Rama Rao, K. V., M. Chen, J. M. Simard, and M. D. Norenberg. 2003. Suppression of ammonia-induced astrocyte swelling by cyclosporin A. *Journal of neuroscience research* 74, no. 6:891-897.
- Ramos, A. J., et al. 2004. The 5HT<sub>1a</sub> receptor agonist, 8-OH-DPAT, protects neurons and reduces astroglial reaction after ischemic damage caused by cortical devascularization. *Brain Research* 1030, 201-220.

- Rasmussen, S. G., et al. 2007. Crystal structure of the human beta(2) adrenergic G-protein-coupled receptor. *Nature*.
- Raymond, J. R., Y. V. Mukhin, T. W. Gettys, and M. N. Garnovskaya. 1999. The recombinant 5-HT1a receptor: G protein coupling and signaling pathways. *British Journal of Pharmacology* 127, 1751-1764.
- Raymond, J. R., F. J. Albers, and J. P. Middleton. 1992. Functional expression of human 5-HT1A receptors and differential coupling to second messengers in CHO cells. *Naunyn-Schmiedeberg's archives of pharmacology* 346, no. 2:127-137.
- Robichaud, A. J., and B. L. Largent. 2000. Recent advances in selective serotonin receptor modulation. *Annual Reports in Medicinal Chemistry* 35, no. 11-20:
- Roodenrys, S., et al. 2002. Chronic effects of Brahmi (*Bacopa monnieri*) on human memory. *Neuropsychopharmacology: official publication of the American College of Neuropsychopharmacology* 27, no. 2:279-281.
- Rosenbaum, D. M., et al. 2007. GPCR engineering yields high-resolution structural insights into beta2-adrenergic receptor function. *Science (New York, N.Y.)* 318, no. 5854:1266-1273.
- Russo, A., and F. Borrelli. 2005. *Bacopa monniera*, a reputed nootropic plant: an overview. *Phytomedicine: International Journal of Phytotherapy and Phytomedicine* 12, no. 4:305-317.
- Russo, E. B., A. Burnett, B. Hall, and K. K. Parker. 2005. Agonistic properties of cannabidiol at 5-HT1a receptors. *Neurochemical research* 30, no. 8:1037-1043.
- Sanders-Bush E, and Mayer SE. 2001. 5-Hydroxytryptamine (Serotonin): Receptor Agonists and Antagonists. In *Goodman & Gilman's The Pharmacological Basis of Therapeutics*, edited by Hardman JG, Limbird LE and Gilman AGMcGraw-Hill.
- Schnellmann, R. G., S. J. Waters, and D. L. Nelson. 1984. <sup>3</sup>H]5-Hydroxytryptamine binding sites: species and tissue variation. *Journal of neurochemistry* 42, no. 1:65-70.
- Schoneberg, T., et al. 2004. Mutant G-protein-coupled receptors as a cause of human diseases. *Pharmacology & therapeutics* 104, no. 3:173-206.

- Schulz, A., et al. 1999. Role of the third intracellular loop for the activation of gonadotropin receptors. *Molecular endocrinology (Baltimore, Md.)* 13, no. 2:181-190.
- Simard, M., and M. Nedergaard. 2004. The neurobiology of glia in the context of water and ion homeostasis. *Neuroscience* 129, no. 4:877-896.
- Simonds, W. F. 1999. G protein regulation of adenylate cyclase. *Trends in pharmacological sciences* 20, no. 2:66-73.
- Sinha, S. C., and S. R. Sprang. 2006. Structures, mechanism, regulation and evolution of class III nucleotidyl cyclases. *Reviews of physiology, biochemistry and pharmacology* 157, 105-140.
- Spiegel, A. M., and L. S. Weinstein. 2004. Inherited diseases involving g proteins and g protein-coupled receptors. *Annual Review of Medicine* 55, 27-39.
- Sprang, S. R. 2007. Structural biology: a receptor unlocked. *Nature* 450, no. 7168:355-356.
- Sprouse, J. S., and G. K. Aghajanian. 1986. (-)-Propranolol blocks the inhibition of serotonergic dorsal raphe cell firing by 5-HT<sub>1A</sub> selective agonists. *European journal of pharmacology* 128, no. 3:295-298.
- Stryer, L., and H. R. Bourne. 1986. G proteins: a family of signal transducers. *Annual Review of Cell Biology* 2, 391-419.
- Taylor, J. M., et al. 1994. Binding of an alpha 2 adrenergic receptor third intracellular loop peptide to G beta and the amino terminus of G alpha. *The Journal of biological chemistry* 269, no. 44:27618-27624.
- Taylor, M. J., N. Freemantle, J. R. Geddes, and Z. Bhagwagar. 2006. Early onset of selective serotonin reuptake inhibitor antidepressant action: systematic review and meta-analysis. *Archives of General Psychiatry* 63, no. 11:1217-1223.
- Thiagaraj, H. V., et al. 2007. Regulation of G proteins by human 5-HT<sub>1a</sub> receptor TM3/i2 and TM5/i3 loop peptides. *Neurochemistry international* 50, no. 1:109-118.
- Thiagaraj, H. V., et al. 2005. Binding properties of dipropyltryptamine at the human 5-HT<sub>1a</sub> receptor. *Pharmacology* 74, no. 4:193-199.

- Turner, J. H., A. K. Gelasco, and J. R. Raymond. 2004. Calmodulin interacts with the third intracellular loop of the serotonin 5-hydroxytryptamine<sub>1A</sub> receptor at two distinct sites: putative role in receptor phosphorylation by protein kinase C. *Journal of Biological Chemistry* 279, no. 17:17027-17037.
- Urban, J. D., et al. 2007. Functional selectivity and classical concepts of quantitative pharmacology. *The Journal of pharmacology and experimental therapeutics* 320, no. 1:1-13.
- Varrault, A., et al. 1994. 5-hydroxytryptamine<sub>1a</sub> receptor synthetic peptides: Mechanisms of adenylyl cyclase inhibition. *Journal of Biological Chemistry* 269, 16720-16725.
- Webster, J., and H. F. Koch. 1996. Aspects of tolerability of centrally acting antihypertensive drugs. *Journal of cardiovascular pharmacology* 27 Suppl 3, S49-54.
- Weiland, G. A., K. P. Minneman, and P. B. Molinoff. 1980. Thermodynamics of agonist and antagonist interactions with mammalian beta-adrenergic receptors. *Molecular pharmacology* 18, no. 3:341-347.
- Wieland, T., and K. H. Jacobs. 1994. Measurement of receptor-stimulated guanosine S'-O-(gamma-thiophosphate) binding by G protein. *Methods in Enzymology* 217, 3-27.
- Zahniser, N. R., and P. B. Molinoff. 1983. Thermodynamic differences between agonist and antagonist interactions with binding sites for [<sup>3</sup>H]spiroperidol in rat striatum. *Molecular pharmacology* 23, no. 2:303-309.
- Zuardi, A. W., S. L. Morais, F. S. Guimaraes, and R. Mechoulam. 1995. Antipsychotic effect of cannabidiol. *The Journal of clinical psychiatry* 56, no. 10:485-486.

## APPENDICES

- A. CANNABINOIDS
- B. BACOPA
- C. CELL VOLUME

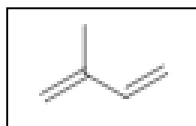
## APPENDIX A: CANNABINOIDS

### Cannabis Introduction

The related natural products cannabis (*Cannabis sativa*) and hemp have many biological components which have not been studied, with the exception of  $\Delta^9$ -tetrahydrocannabinol (THC) and to a lesser extent cannabidiol (CBD). However, each of these contain many other chemicals which have the potential to be bioactive. The biological system which is the most perturbed by the introduction of these chemicals by the ingestion of the natural products is the endogenous cannabinoid system. In humans there are 2 known cannabinoid receptors CBD1 and CBD2 which are activated by the endogenous ligand anandamide. These receptors are both G protein ( $G_{i/o}$ ) coupled receptors which affect adenylyl cyclase (negatively) and mitogen-activated protein kinase (positively).

Hemp oil an essential oil, made from the leaves of cannabis, is a cocktail of many oleagenous compounds called terpenes. Terpenes are secondary metabolites made up of 5 carbon isoprene units. These terpene compounds have been shown to possess significant anti-inflammatory properties both in *in vivo* animal and *ex vivo* cell culture (de las Heras et al., 2003) studies. Hemp oil does not contain any cannabinoids.

Figure 17: Isoprene  
The isoprene is the basic structural unit from which plants synthesize terpenoids compounds.



These natural products, cannabis and hemp, also contain compounds known as cannabinoids. There are at least 66 cannabinoids that have been identified. THC is the most widely known of these and is believed to be responsible for the psychoactive effects of cannabis. However, another lesser studied compound, cannabidiol (CBD) is also present and is not known to be psychoactive. CBD has shown potential for treating anxiety disorders, seizure disorders, anti-psychotic (psychosis), and as a neuroprotective agent (Zuardi et al., 1997; Carlini et al., 1981; Hampson et al., 1998; Jiang et al., 2005). The serotonergic neurotransmitter system is affected by the hallucinogens such as psilocybin and LSD (Aghajanian et al., 1975; Deliganis et al., 1991; Peroutka et al., 1979). Therefore a preliminary investigation was undertaken to see if the psychoactive effects of these constituents of cannabis and its relative hemp are mediated by the serotonin receptors 5HT<sub>1a</sub>R and 5HT<sub>2a</sub>R.

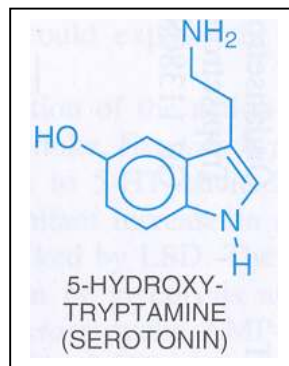
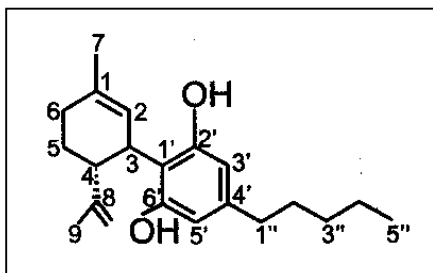


**Figure 18:** Cannabidiol and Serotonin  
Structure of (-)-Cannabidiol (CBD) and serotonin (5HT, 5-Hydroxy-Tryptamine)

The 5-HT<sub>1A</sub> receptor is found in the neural tissue of the central nervous system at highest concentrations in the hippocampus, septum, frontal cortex, and dorsal raphe nucleus. The receptor is negatively coupled to adenylyl cyclase, via G<sub>oi</sub> which causes a decrease in the amount of intracellular cAMP (Raymond et al., 1999).

In addition to agonist binding studies for 5HT1aR, these studies were also done in the 5HT2aR. The 5HT2a receptor is found in the cortex, caudate nucleus, nucleus accumbens, hippocampus, and olfactory tubercle. It was identified as a serotonin receptor subtype by its higher affinity for the ligand [<sup>3</sup>H]-spiperone, although its affinity for 5HT is lower. The receptor is positively coupled to phospholipase C (PLC) system via the g protein G<sub>αq</sub>. The activation of PLC drives the hydrolysis of membrane lipids to form diacylglycerol (DAG) and inositol triphosphate (IP3). The increased concentration of IP3 causes the release of intracellular calcium (Ca<sup>++</sup>) from stores in the endoplasmic reticulum. The increased concentration of DAG along with calcium activates protein kinase C (PKC). The binding affinity assays for the constituents of cannabis and hemp oil utilize the 5HT2aR antagonist [<sup>3</sup>H]-ketanserin (Barnes et al., 1999). These studies examine if constituents of interest are able to displace an antagonist, rather than an agonist as in the 5HT1aR studies.

### Methods

Cell Culture: Chinese hamster ovarian (CHO) cells expressing the human 5HT1aR were cultured in Ham's F-12 medium fortified with 10% fetal calf serum and 200 µg/ml geneticin in 75 or 175 cm<sup>2</sup> flasks. Cultures were maintained at 37 °C in a humidified atmosphere of 5% CO<sub>2</sub>. Cells were subcultured or assayed upon confluency (5–8 days). CHO cells with cloned human 5HT1aR were kindly provided by Dr. John Raymond (Medical University of South Carolina). NIH 3T3 cells expressing the rat 5-HT2aR were cultured under similar conditions in DMEM fortified with 10% calf serum and 200 µg/ml geneticin. These transfected cells were generously provided (Julius et al., 1990).by Dr.



David Julius (UCSF). Both cell lines have been tested for mycoplasma with a PCR kit (ATCC), and are free of contamination.

Receptor Preparation: Cells were harvested by the removal of culture medium followed by the addition of a 0.25% trypsin solution. Upon the removal of the cell monolayer, an equal volume of ice-cold culture medium was added to the cell-trypsin solution. The resulting cell suspension was centrifuged at low speed (3000 rpm) in ice-cold medium for 10 minutes. The pellet was re-suspended in ice-cold Earle's balanced salt solution followed by centrifugation (3000 rpm) for 10 minutes. The cell pellet was re-suspended in 10 ml of ice-cold binding buffer (50 mmol/l Tris, 4 mmol/l CaCl<sub>2</sub>, 10 µmol/l pargyline, pH 7.4), homogenized with Teflon-glass homogenizer, and centrifuged at 450,000 g at 4 ° C. to produce a crude membrane preparation, the pellet was re-suspended in 30 ml of ice-cold binding buffer, and homogenized, first with Teflon-glass then with a Polytron (setting 4) for 5 seconds. The receptor preparation was stored on ice and assayed within the next 1.5 hour.

#### Assay of Receptor Activity

Binding of the agonist [<sup>3</sup>H]8-OH-DPAT ([<sup>3</sup>H]8-hydroxy-2-(di-*n*-propylaminotetralin)) to 5HT<sub>1a</sub>R, or [<sup>3</sup>H]-ketanserin for 5HT<sub>2a</sub>R followed well-characterized *in vitro* protocols (Russo et al., 2005). Radioligands were purchased from New England Nuclear (Boston, Mass., USA). The experimental 1 ml reaction mixtures, in triplicate, were incubated for 30 minutes in a 30 °C water shaker bath. The composition of the 1 ml reaction mixture was:

Experimental controls: 700 µl of receptor preparation; 100 µl of either binding buffer (for total ligand binding) or 10 µM 5HT (final concentration for non-specific ligand

binding), 100  $\mu$ l of the tritiated agent (final concentration of 0.5 nmol/l [ $^3$ H]8-OH-DPAT, 0.2 nM [ $^3$ H]-ketanserin), and 100  $\mu$ l of binding buffer in the case of controls.

5 ml of ice-cold Tris buffer, dried, and counted in 5 ml of Ecoscint (National Diagnostics) liquid scintillation fluid in a Beckman LS 6500 instrument. Homogenates were assayed for protein to maintain a nominal value of 50  $\mu$ g protein per filter over weekly assays. Total and non-specific binding tubes were run in triplicate.

### Hemp oil versus [ $^3$ H]-Ketanserin

Preliminary receptor binding experiments with dilutions of hemp oil were performed with membrane preparations from cells transfected with the 5HT<sub>2a</sub>R. This resulted in the binding curve below (Figure 19). The curve shows that hemp oil at a dilution of 1/100 (2 on the graph) is able to decrease the amount of specifically bound [ $^3$ H]-Ketanserin to about 20% (as a percent of control). As the hemp oil concentration is decreased there is a corresponding decrease in the amount of displacement of [ $^3$ H]-Ketanserin specifically bound to the receptor.

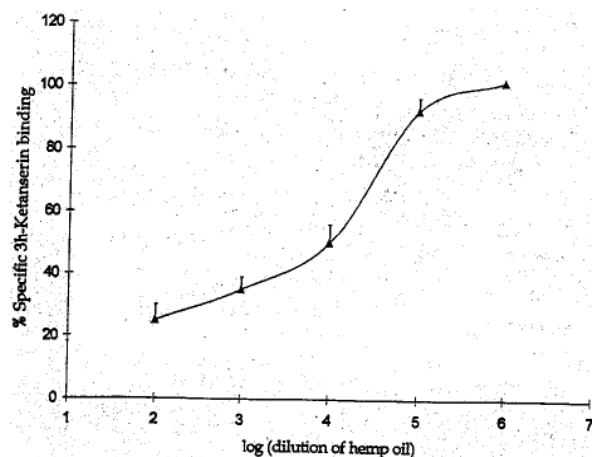


**Figure 19:** Ketanserin Displacement by Hemp Oil at 5HT<sub>2a</sub> Receptor  
Hemp oil vs. 5HT<sub>2a</sub>R. The 5HT<sub>2a</sub>R antagonist [ $^3$ H]-Ketanserin is displaced by components of hemp oil in membrane preparations of 5HT<sub>2a</sub>R. All points are percent of control (control=100%, no displacement). The x-axis is the  $-\log$  dilution of hemp oil. 3=1/1000, 5=1/100,000.

### Individual Components of hemp oil versus [<sup>3</sup>H]-Ketanserin

In an attempt to identify the individual terpene components of hemp oil which may be responsible for the decrease in specifically bound [<sup>3</sup>H]-Ketanserin, individual components of the oil were introduced to binding experiments using membrane preparations from cells transfected with the 5HT<sub>2</sub>A (Figure 20). The terpenes chosen were: β-caryophyllene, 1,8-cineole, *d*-limonene, linalool, α-pinene, and α-terpinol. The terpenes β-caryophyllene, linalool, and α-pinene were not able to decrease the binding of [<sup>3</sup>H]-Ketanserin as compared to control. Small decreases in specific [<sup>3</sup>H]-Ketanserin binding to 5HT<sub>2</sub>A were seen with the terpenes 1,8-cineole (7%), *d*-limonene (10%), and α-terpinol (18%).

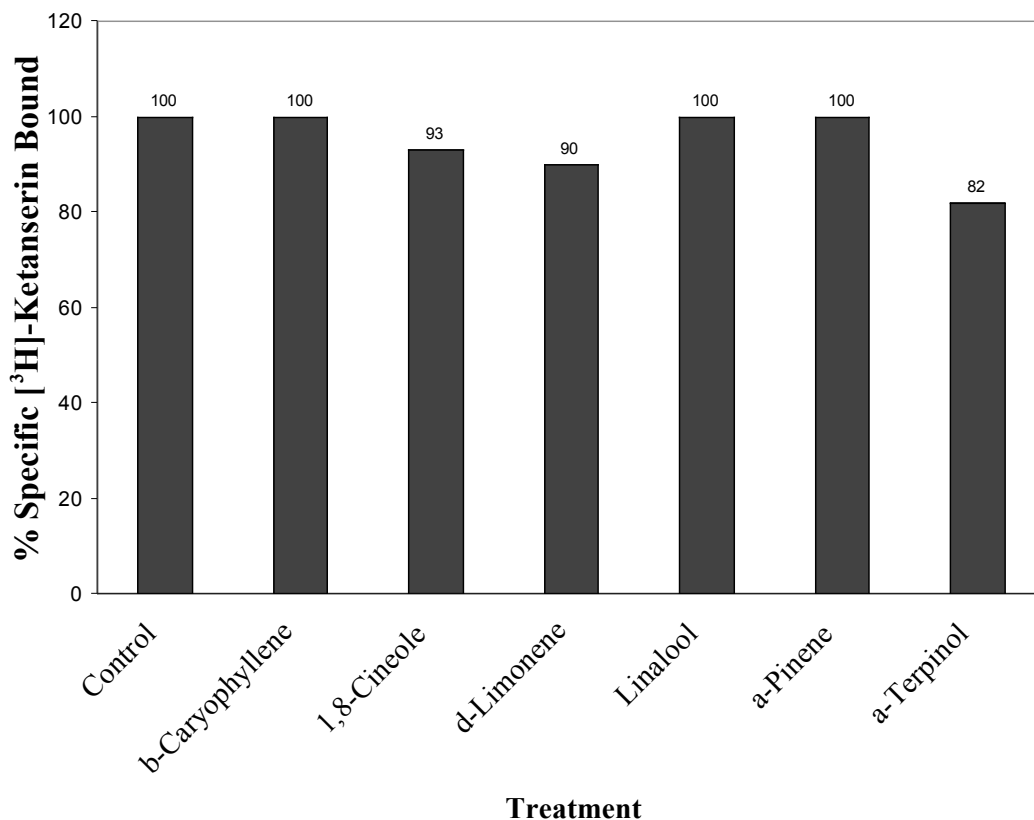


**Figure 20:** Terpene Components of Hemp Oil Effect on Ketanserin Binding Ligand binding competition experiments in membrane preparations of rat fibroblast cells expressing 5HT<sub>2</sub>A. Individual terpene components of hemp oil vs. 5HT<sub>2</sub>A. The 5HT<sub>2</sub>A antagonist [<sup>3</sup>H]-Ketanserin (0.2nM) is displaced by the 1,8-cineole, *d*-limonene, and α-terpinol components of hemp oil.

The terpenoid carvone was introduced into the binding assay with membrane preparations from cells expressing 5HT2aR (Figure 21). Carvone at a concentration of 0.7 mM decreased the specific binding of [<sup>3</sup>H]-Ketanserin by 13% compared to control. The combination of carvone with the terpene, terpineol decreased the effectiveness of carvone alone only decreasing the specific binding of [<sup>3</sup>H]-Ketanserin by 5% compared to control. Similarly, the combination of carvone with terpineol and limonene decreased the effectiveness of carvone alone decreasing the specific binding of [<sup>3</sup>H]-Ketanserin by 3% compared to control.

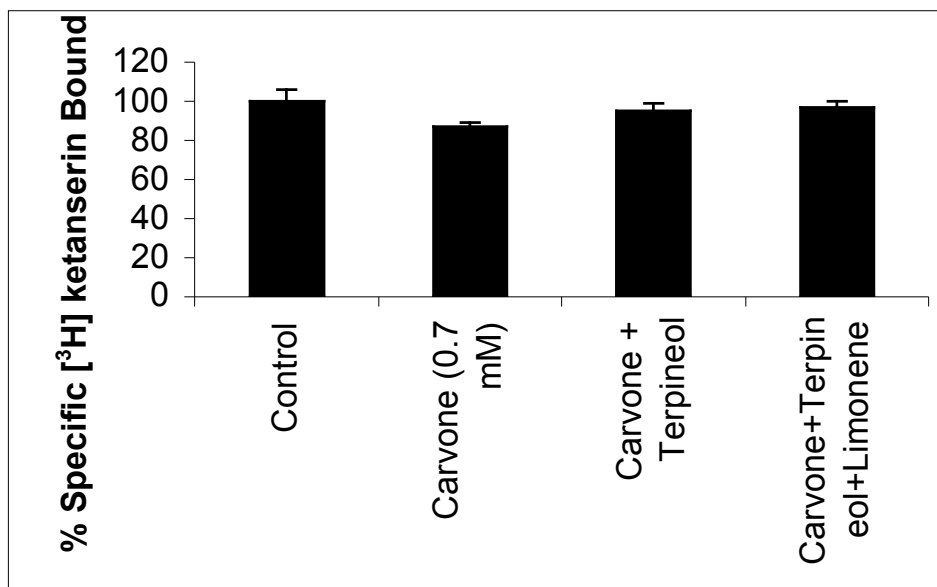


**Figure 21: Terpene Effect on Ketanserin Binding**

Ligand binding competition experiments in membrane preparations of rat fibroblast cells expressing 5HT2aR. Carvone (0.7mM), Carvone+terpineol, carvone+terpineol+limonene vs. 5HT2aR. The 5HT2aR antagonist [<sup>3</sup>H]-Ketanserin (0.2 nM) is displaced by the Carvone.

The dilution of the crude hemp oil mixture was able to displace specifically bound ketanserin from 5HT<sub>2a</sub>. Our attempt to identify the individual components of hemp oil responsible for this was only partially successful. We identified these components of hemp oil which were weak displacers of ketanserin; 1,8-cineole (7%), *d*-limonene (10%),  $\alpha$ -terpinol (18%), and carvone (13%) (decreased specific binding). However our attempt to identify the combinations of agents responsible for hemp oil's activity only revealed that the agents we chose were not synergistic in combination, but blunted the effect of carvone alone.

#### Cannabidiol (CBD) and $\Delta^9$ -tetrahydrocannabinol (THC) versus [<sup>3</sup>H]-Ketanserin

The activity of CBD and THC at the 5HT<sub>2a</sub>R was assessed by their ability to displace specifically bound [<sup>3</sup>H]-Ketanserin (Figure 22). THC was able to decrease the amount of specifically bound [<sup>3</sup>H]-Ketanserin by 11% at a concentration of 32  $\mu$ M. CBD was able to decrease the amount of specifically bound [<sup>3</sup>H]-Ketanserin by 52% at 32  $\mu$ M, and 24% at a concentration of 16  $\mu$ M. Methanol, which was included because it was used in the initial dilutions of CBD and THC, had a very small effect on specific binding.

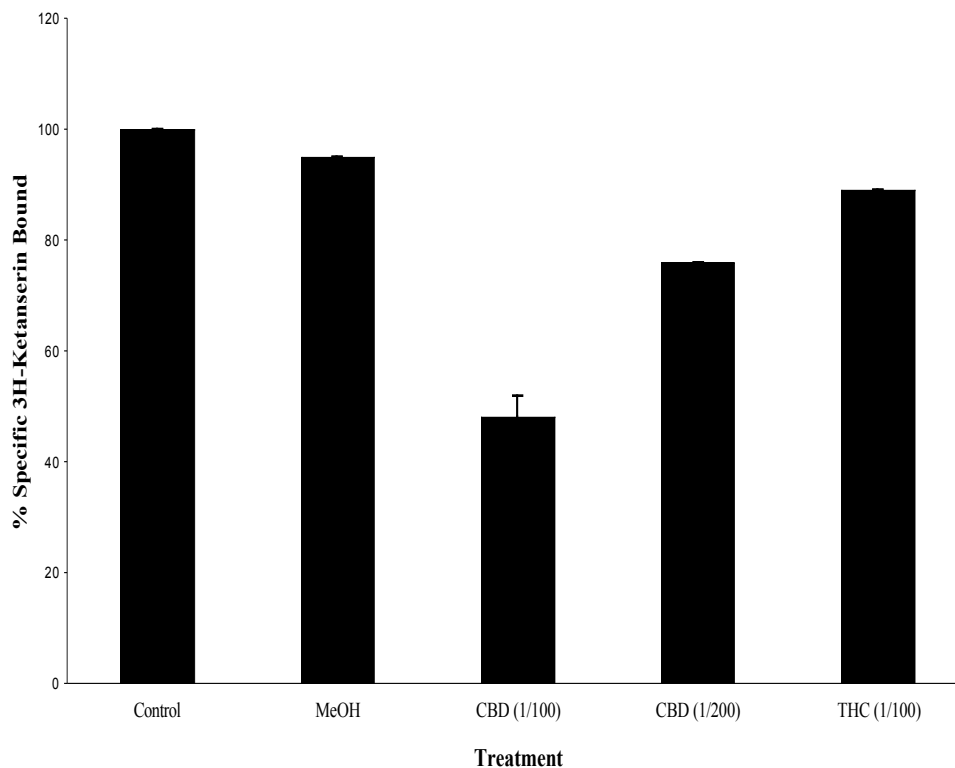


**Figure 22:** Cannabidiol and THC Displacement of Bound Ketanserin  
 Displacement of specifically bound [<sup>3</sup>H]-Ketanserin (0.2 nM) at rat 5HT<sub>2a</sub>R by CBD (1/100 = 32 uM; 1/200 = 16 uM) and THC (1/100 = 32 uM). MeOH (methanol = 1%) was included as it was the initial diluent for CBD and THC. All values are percent of control. N's greater than 4 in samples assayed in triplicate in multiple experiments (n=12).

#### Cannabidiol (CBD) and Δ<sup>9</sup>-tetrahydrocannabinol (THC) versus [<sup>3</sup>H]8-OH-DPAT

The activity of CBD and THC in the 5HT<sub>1a</sub>R was assessed by their ability to displace the ligand [<sup>3</sup>H]8-OH-DPAT (Figure 23). THC was not able to decrease the specifically bound [<sup>3</sup>H]8-OH-DPAT when compared to control. Conversely CBD was able to decrease the specifically bound [<sup>3</sup>H]8-OH-DPAT 90% at a concentration of 32 uM, 73% at a concentration of 16 uM, and 11% at a concentration of 8 uM. Because CBD had a measured effect on decreasing bound 8-OH-DPAT, it could be acting at the

ligand binding site. Therefore, it is warranted to investigate if CBD is also acting as an agonist at 5HT1aR by examining G protein activation and second messenger regulation.

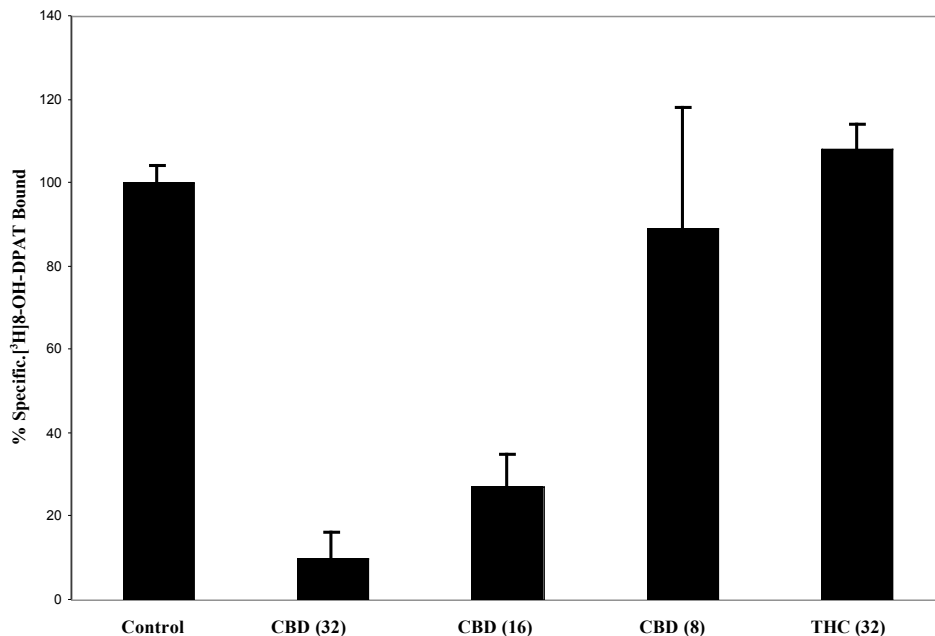


**Figure 23: Cannabidiol and THC Effect on 8-OH-DPAT Binding**  
Displacement of specifically bound [<sup>3</sup>H]8-OH-DPAT at 5HT1aR by CBD (1/100 = 32  $\mu$ M; 1/200 = 16  $\mu$ M; 1/400 = 8  $\mu$ M) and THC (1/100 = 32  $\mu$ M). N's 4-6, except 1/200 and 1/400 (1) in three separate experiments conducted in triplicate. All values are percent of control.  
 $p < 0.05$  for Control vs. CBD (32) and Control vs. CBD (16)

#### Cannabidiol (CBD) Stimulated [<sup>35</sup>S]- $\gamma$ -GTP Incorporation Into G<sub>ci</sub>

Due to the lack of data to support the actions of THC as an agonist for 5HT1aR it was not included in the [<sup>35</sup>S]- $\gamma$ -GTP incorporation assays. CBD, which showed considerable displacement of [<sup>3</sup>H]8-OH-DPAT in the binding assays, also activated G<sub>ci</sub> (Figure 24). The native ligand 5HT stimulated the incorporation of [<sup>35</sup>S]- $\gamma$ -GTP into G<sub>ci</sub> at 10  $\mu$ M to 157% of control. CBD stimulated the incorporation of [<sup>35</sup>S]- $\gamma$ -GTP into G<sub>ci</sub> at 16  $\mu$ M to 167% of control (\* $p < 0.05$ , relative to control). The combination of 5HT and

CBD showed an additive effect on the incorporation of [<sup>35</sup>S]-γ-GTP into G<sub>oi</sub> to 223% of control (\*\*p<0.01, relative to control). These data indicate that CBD may be binding at the ligand binding site of 5HT1aR and eliciting G protein activation thus, acting like an agonist. To confirm that the G protein is being activated by CBD it is necessary to measure its regulatory activity on adenylyl cyclase and its production of the second messenger cAMP.

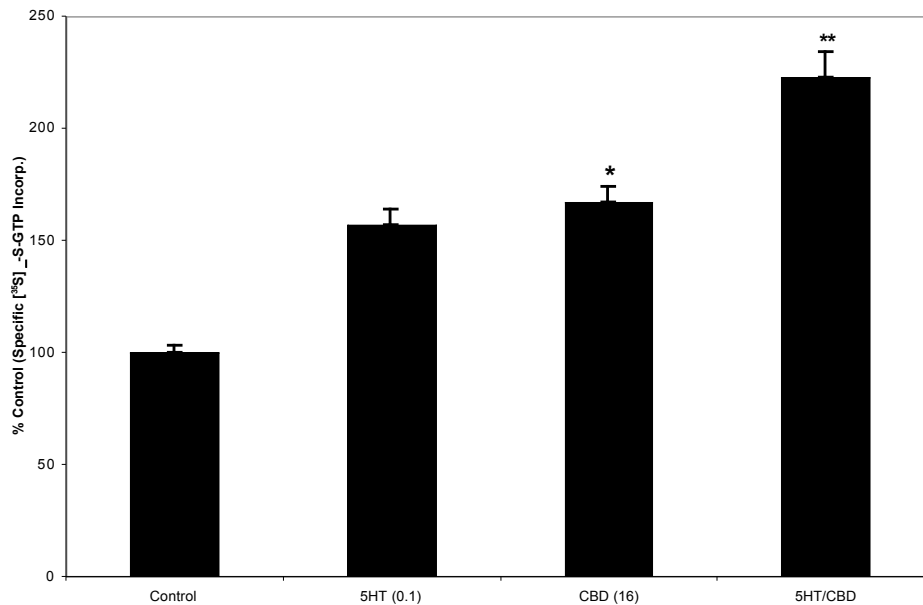


**Figure 24:** Cannabidiol Effect on Incorporation of [<sup>35</sup>S]-γ-GTP into G<sub>oi</sub>. These experiments were a measure of G protein activation. 5HT (10 uM) and CBD (16 uM) stimulated incorporation of [<sup>35</sup>S]-γ-GTP into G<sub>oi</sub> in cells expressing 5HT1aR membrane preparations. CBD \*p<0.05, relative to control; 5HT/CBD \*\*p<0.01, relative to control

#### Cannabidiol (CBD) Stimulated cAMP Production by Adenylyl Cyclase

Due to the lack of data to support the actions of THC as an agonist for 5HT1aR it was not included in the cAMP assays. CBD was shown to act as an agonist at 5HT1aR by the incorporation of [<sup>35</sup>S]-γ-GTP into G<sub>oi</sub>. The next step in the signal transduction cascade is to determine if activated G<sub>oi</sub> is decreasing intracellular cAMP concentrations by affecting adenylyl cyclase (Figure 25). The control in this experiment was the amount



of FSK stimulated cAMP production. The native ligand 5HT was able to decrease intracellular cAMP concentration to 28% of control. The combination of 5HT and NAN (a 5HT<sub>1a</sub>R antagonist) decreased the effectiveness of 5HT alone to decrease FSK stimulated cAMP production to 60% of control. CBD decreased FSK stimulated cAMP production to 38% of control. The combination of 5HT and CBD had an additive effect on the decrease in FSK stimulated cAMP production to 20% of control. The combination of CBD with NAN also blunted its effect on FSK stimulated cAMP production to 76% of control.

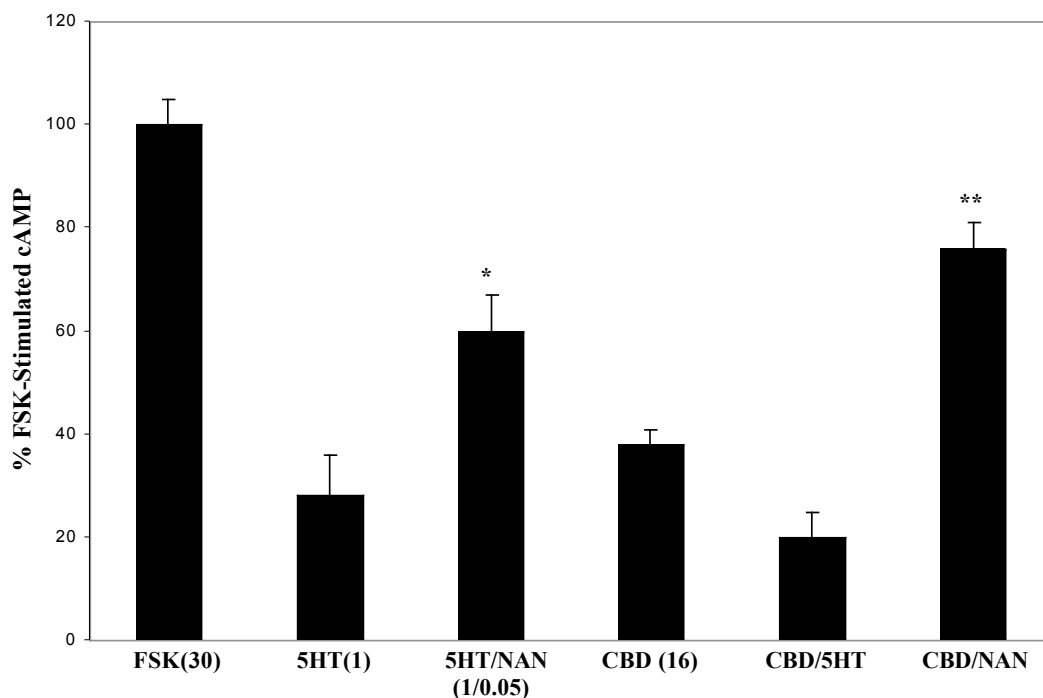


**Figure 25: Cannabidiol Effect on Intracellular cAMP Concentration**

A measure of signal transduction properties of the agonist 5HT (1  $\mu$ M), the antagonist NAN-190(50 nM), and the cannabinoid CBD (16  $\mu$ M) at H5HT<sub>1a</sub>R. These experiments were a measure of G protein regulation of its second messenger. Inhibition of Forskolin (FSK)-Stimulated cAMP by Cannabidiol (CBD), Serotonin (5-HT), and the inhibitor NAN-190 (NAN) in Whole Cells Transfected With the Human 5-HT<sub>1a</sub> Receptor. All conditions contain FSK at 30  $\mu$ M and the phosphodiesterase inhibitor isobutylmethylxanthine (IBMX) at 100  $\mu$ M. Other concentrations in micromolar are: 5-HT (1); CBD (16); and NAN (0.05). Results are expressed as percentage of FSK control as mean  $\pm$  S.E.M. with n's = 3-6. \* p<0.05, relative to 5-HT; \*\* p<0.01, relative to CBD. Further experimental details are found in Experimental Procedure.

## Cannabinoid Discussion

The examination of the individual agents contained in essential oil of hemp for activity at the 5HT<sub>2a</sub>R has yielded information which may explain some of the diverse effects of this natural product. The hemp oil cocktail itself showed much greater activity at displacing [<sup>3</sup>H]-Ketanserin at the 5HT<sub>2a</sub>R, than any of its individual components tested. This indicates that more of the components of hemp oil should be investigated as the source of the ketanserin displacement. Small decreases in specifically bound [<sup>3</sup>H]-Ketanserin were observed in the 5HT<sub>2a</sub>R receptor binding experiments with the terpenoids 1,8-cineole (7%), *d*-limonene (10%),  $\alpha$ -terpinol (18%), and carvone (13%). It is not known if these compounds possess any agonistic properties in this receptor system. However, because of their ability to slightly decrease the specific binding of the antagonist ketanserin, these compounds may be modulating serotonergic neurotransmission rather than acting as true agonists. The combination of the terpenoids and carvone not having an additive effect on decreasing the specific binding of [<sup>3</sup>H]-ketanserin more than the agents alone may indicate that they are competing for receptor binding having an antagonistic effect on the binding of carvone.

The data for CBD and THC in the 5HT<sub>2a</sub>R and 5HT<sub>1a</sub>R has been previously published in our lab (Russo et al., 2005). CBD was shown to decrease the specific binding of [<sup>3</sup>H]-ketanserin and [<sup>3</sup>H]8-OH-DPAT, compared to control, although it is more active in the 5HT<sub>1a</sub>R system. CBD clearly has agonistic properties at the 5HT<sub>1a</sub>R as judged by its ability to stimulate the incorporation of [<sup>35</sup>S]- $\gamma$ -GTP into G<sub>oi</sub>, and decrease FSK stimulated intracellular concentrations of cAMP via the negative regulation of AC. The observation that the specific 5HT<sub>1a</sub>R binding site antagonist NAN is capable of

blocking the agonistic effect of CBD is potentially significant. Since NAN blocks both the action of established agonist 5HT and putative agonist CBD, these results support the contention that CBD is acting at the receptor's ligand binding site.

THC was shown to be very weakly active at displacement of [<sup>3</sup>H]-ketanserin at the 5HT<sub>2a</sub>R, and had no measurable affect on the binding of [<sup>3</sup>H]8-OH-DPAT at 5HT<sub>1a</sub>R. Overall, the results with CBD provide evidence that cannabinoids have activity *in vitro* beyond the expected interactions with cannabinoid receptors. If these results are verified *in vivo*, we can speculate that future drug development studies may be impacted. CBD itself, or modified versions might be utilized to treat maladies of serotonergic dysfunction (depression, obsessive compulsive disorder, migraine headache) or be used as adjunct treatment agents to boost the efficacy of current treatments.

## APPENDIX B: BACOPA

### *Bacopa monniera* Introduction.

The natural product *Bacopa monniera* (BA) has a long history of herbal use in the Indian Ayurvedic Medical System (Figure 26). More recently, the herbal use in western medicine has been grounded in scientifically validated properties relevant to human health. The focus of use in animal studies and human clinical trials has been the beneficial properties in enhancing cognitive functions, especially memory processes, and in the adaptogenic qualities of bacopa (Russo and Borrelli, 2005; Rai et al., 2003). These properties have been particularly well studied with respect to cholinergic systems relevant to cognition and neurodegenerative disease (Roodenrys et al., 2002). The components of BA which are believed to be the active in biological systems are the triterpene saponins bacopasides A & B.

Other neurotransmitter systems of interest, such as the serotonergic may be relevant to bacopa's pharmacology. Reports of relevance of the role of serotonin in modulation of cognition involve the use of (S)-WAY 100135, a 5-HT<sub>1A</sub>R antagonist, to counteract the impairment of spatial learning in rats due to intra-hippocampal administration of the cholinergic antagonist scopolamine (Carli et al., 1995). Serotonin depletion in the prefrontal cortex was also shown to cause cognitive inflexibility in primates (Clarke et al., 2004). Thus, an investigation of the specific serotonergic properties of BA is warranted. These studies utilized extracts of bacopa, supplied by Geni Herbs (Nobelsville, IN), to examine if it has any activity at the human 5HT<sub>1A</sub>R and the rat 5HT<sub>2A</sub>R.

### Bacopa Dilution for Experiments

Bacopa fractions were re-dissolved in 0.4 mL of absolute ethanol. This was then diluted 1/10 in distilled water. Further dilutions were in distilled water 1/10 for a total dilution of 1/100. This approach was based upon preliminary experiments [3H]

Ketanserin binding at the rat 5HT<sub>2a</sub>R (Figure 27).



Fig. 26: *Bacopa monniera* (Brahmi)

Bacopa Extract Affect on the specific binding of [<sup>3</sup>H]8-OH-DPAT at 5HT1aR and [<sup>3</sup>H]-Ketanserin at rat 5HT2aR.

Ligand binding experiments were completed for five dilutions of an extract of *Bacopa monniera*. All of the BA dilutions tested were able to displace [<sup>3</sup>H]8-OH-DPAT from its binding site at the 5HT1aR (Figure 28). The best results were observed with the smallest dilutions (1/100 and 1/4000), which decreased the specific binding of [<sup>3</sup>H]8-OH-DPAT to 37±5% and 33±9% as a percent of control respectively. Thus about a 60% reduction in agonist binding was achieved at these concentrations. The 3 higher dilutions showed some displacement activity however, the agonist displacement observed was less and more variable at these concentrations.

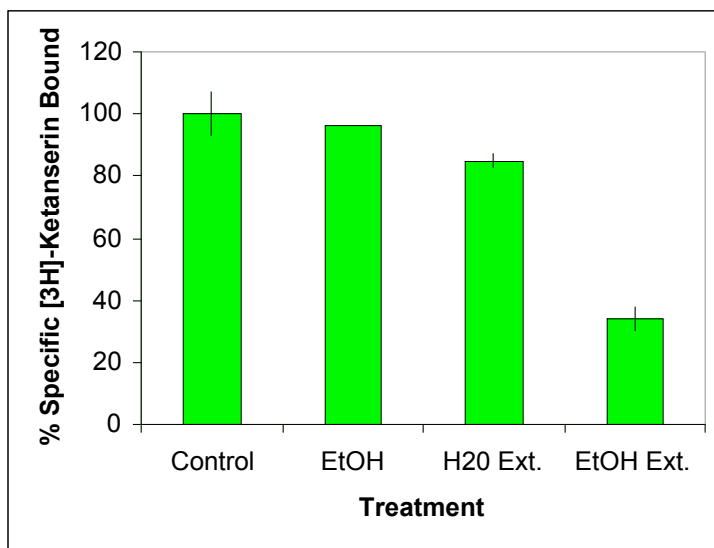
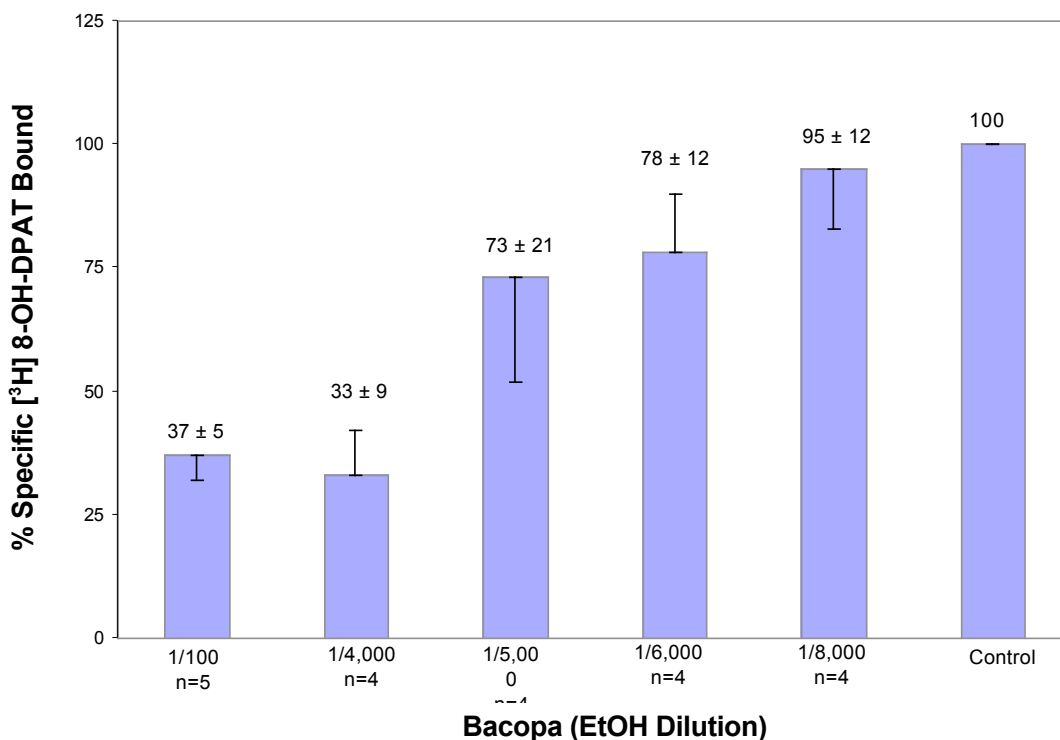
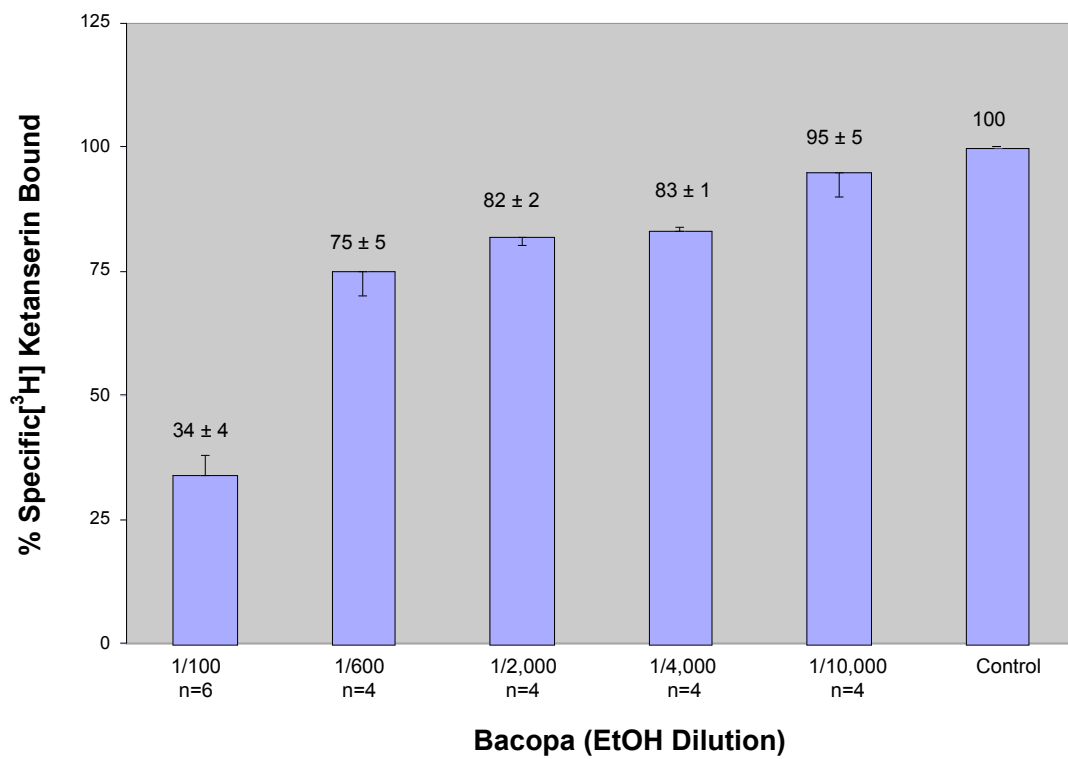


Fig. 27. A comparison of bacopa extracted in water versus ethanol. Specific binding of [<sup>3</sup>H]-Ketanserin in membranes containing the rat 5HT2a receptor was measured. Extracts were diluted 1/100 prior to assay. Ethanol alone did not influence binding. Values are mean +/- S.E.M. with n's = 4-6.

A parallel set of experiments to those summarized in Figure 28 with H5HT1aR were conducted with [3H]-Ketanserin in rat 5HT2aR (Figure 29). At the 1/100 dilution, BA's ability to displace ligand is about the same at 5HT2aR (about 66%) as at H5HT1aR (about 63%). At 1/600 dilution, BA displaces only about 25% of [3H]-Ketanserin (Figure 29). This compares with a 1/4000 dilution of BA at the H5HT1aR where about 67% of [3H]8-OH-DPAT is displaced (Figure 28). A 1/4000 dilution of BA displaces only 17% of [3H]-Ketanserin at rat 5HT2aR (Figure 29). The overall conclusion is that while BA is active at both receptors, it has greater binding potential at H5HT1aR compared to rat 5HT2aR.



**Figure 28:** Effect of Bacopa Extracts on Specific Binding of 8-OH-DPAT Binding of bacopa at human 5HT1aR. Five dilutions of the extract in ethanol were tested for ability to displace specifically bound [3H]8-OH-DPAT. All values are percent of control ± SEM; n's 4-5.  $p < 0.05$  for Control vs. BA (1/4000) and Control vs. BA (1/100)



**Figure 29:** Effect of Bacopa extracts on Specific Binding of Ketanserin Binding at rat 5HT2aR. Five dilutions of the extract in ethanol were tested for their ability to displace specifically bound [3H]-Ketanserin. All values are percent control +/- SEM; n's 4-5.



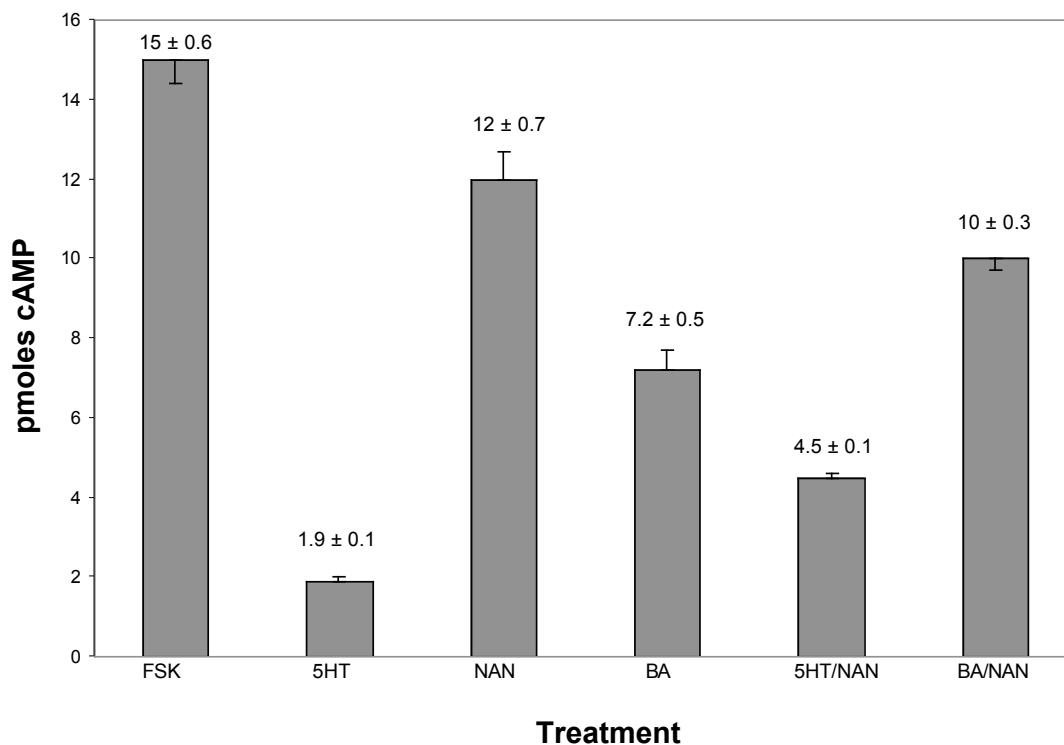


**Figure 30: Bacopa Effect on Intracellular cAMP Concentration**

cAMP experiments were a secondary measure of G protein activation. Bacopa (BA; 1/200) was tested for its ability to effect cAMP levels in vitro all conditions include FSK and IBMX. Bacopa significantly decreased intracellular cAMP levels after pre-treatment with forskolin (FSK). NAN is a 5HT<sub>1a</sub>R antagonist. All values are pmol cAMP ± SEM, n's 3-9.

\* p<0.01 5HT vs. 5HT/NAN

\*\* p<0.01 BA vs. BA/NAN

### Bacopa Extract Affect on Intracellular cAMP Concentration

Bacopa was shown to displace agonist at 5HT<sub>1a</sub>R. The incorporation of [<sup>35</sup>S]-γ-GTP into G<sub>ci</sub> was not measured in these experiments for this bacopa extract. However, its agonistic activity was demonstrated in cAMP experiments, with bacopa activated G<sub>ci</sub> decreasing intracellular cAMP concentrations by affecting adenylyl cyclase. The control in this experiment is the amount of FSK stimulated cAMP production by adenylyl cyclase (AC) (Figure 28). The native ligand 5HT was able to decrease intracellular

cAMP concentration to  $1.9 \pm 0.1$  pmol compared to  $15 \pm 0.6$  pmol for control. NAN alone demonstrated a decrease in cAMP concentration to  $12 \pm 0.7$  pmol. The combination of 5HT and NAN (a 5HT<sub>1a</sub>R antagonist) decreased the effectiveness of 5HT alone to decrease FSK stimulated cAMP production to  $4.5 \pm 0.1$  pmol. BA decreased FSK stimulated cAMP production to  $7.2 \pm 0.5$  pmol. The combination of BA with NAN also blunted its effect on FSK stimulated cAMP production to  $10 \pm 0.3$  pmol. The reductions in cAMP concentration were statistically significant for 5HT vs. 5HT/NAN ( $p < 0.01$ ) and BA vs. BA/NAN ( $p < 0.01$ ). These data along with the binding displacement data for 8-OH-DPAT demonstrate a role for constituents present in bacopa as 5HT<sub>1a</sub>R agonists. Signal transduction activity of BA was not measured at rat 5HT<sub>2a</sub>R.

#### *Bacopa monniera* Discussion

The extracts of the natural product *Bacopa monniera* tested in these experiments for signal transduction activity in the human 5HT<sub>1a</sub>R have shown that constituents of bacopa have agonistic properties in this neurotransmitter system. The majority of the extracts tested significantly displaced specifically bound agonist [<sup>3</sup>H]8-OH-DPAT. The most active extract displaced about 60% of the ligand. The agonistic properties of bacopa were demonstrated by the activation of the 5HT<sub>1a</sub>R coupling protein G<sub>i</sub> by testing the signal transduction system via its target second messenger, causing a significant decrease in the FSK stimulated intracellular concentration of cAMP. This is an indication that the bacopa activated G<sub>ai</sub> is negatively regulating adenylyl cyclase and decreasing its production of cAMP. Thus, it has been demonstrated that components present in the extracts of the natural product *Bacopa monniera* are able to bind to the

5HT1aR, activate  $G_{\alpha i}$ , and affect the second messenger system in a similar manner to 5HT.

These extracts do not demonstrate equipotent activity to the ligand 5HT. However, further purification and identification of the individual components in the fractions may elucidate the source of bacopa's serotonergic activity. Currently, such studies are being conducted. It will also be of interest to further pursue characterization at the 5HT2aR to clarify whether BA is agonistic or antagonistic. These studies have yet to be conducted. Interest in bacopa, both in terms of its effects in the nervous system and other tissues as well as its clinical efficacy is increasing world wide. Additional studies, both in the serotonergic system and with other neurotransmitters and in the applied realm are well worth pursuing.

## APPENDIX C: CELL VOLUME

Serotonin (5HT) has many actions on neuronal function in its role as a neurotransmitter. However, its actions go far beyond neurophysiology, branching into very basic cellular processes such as osmotic homeostasis (Azmitia et al., 2001; Simard et al., 2004). Additionally, 5HT's actions are not limited to neurons; many other cell types are involved, including mast cells, cells of the gastrointestinal tract, and significantly for the nervous system, glial cells (Ramos et al., 2004). Of the seven known classes of 5HTR, only one, the 5HT<sub>3R</sub>'s are membrane ion channels. The remainder of the 5HT receptor family are G protein-coupled (GPC), seven transmembrane domain (7TMD) receptors. G protein-coupled 7TMD receptors are the target for many neurotransmitter, hormone, and autacoid ligands whose structures, binding properties, and signal transduction characteristics are under active investigation.

A prominent member of the GPC 5HTR's is the 5HT<sub>1aR</sub>, which has been associated not only with vital neurological and psychological processes (depression, obsessive compulsive disorder), but also with astroglial physiology (Ramos et al., 2004) and a Na<sup>+</sup>/H<sup>+</sup> exchanger (Garnovskaya et al., 1997). We have previously conducted a series of studies with 5HT<sub>1aR</sub>, including investigations at the receptor/G protein interface and with small binding ligands, such as cannabidiol (Russo et al., 2005) and DPT (Thiagaraj et al., 2005). The work presented here represents preliminary studies conducted with primary astroglia from rats (Jayakumar et al., 2006), a monkey kidney (MCK) cell line, transfected CHO cells expressing 5HT<sub>1aR</sub>, rat fibroblasts (3T3) expressing 5HT<sub>2aR</sub>, and wild type CHO cells. These studies used the 5HT ligands quipazine, buspirone, 8-OH-DPAT, ketanserin, ondansetron, and carbamidotryptamine...

Astrocytes perform many vital activities in the central nervous system: glutathione synthesis, neurotransmitter uptake and metabolism, allowing neurons to continue functioning properly. Toxins such as ammonia, which can cause cell swelling, can compromise the proper function of astrocytes (Simard et al., 2003). Finding a therapeutic agent to reduce that swelling could be useful in treating hepatic encephalopathy. These preliminary studies focus on the relationship between 5HT and astroglial function with some comparisons to other cell types.

### Methods

Cell Culture: Chinese Hamster Ovary (CHO) cells expressing the H5HT1aR (S27- ATCC designation) were cultured in Ham's F-12 medium (GIBCO) fortified with 10% fetal bovine serum (FBS) and 200 ug/ml geneticin. Cultures were maintained at 37°C in a humidified atmosphere of 5% CO<sub>2</sub>. Cells were sub-cultured or assayed upon confluency (5-8 days). Cell lines have been tested for mycoplasma with a PCR kit (ATCC), and are free of contamination. Cloned H5HT1aR was kindly provided by Dr. John Raymond. NIH 3T3 (ATCC designation) cells expressing the rat 5HT2aR were cultured under similar conditions in DMEM fortified with 10% calf serum (CS) and 200 ug/ml geneticin. These transfected cells (Julius et al., 1990) were kindly provided by Dr. David Julius (UCSF). Non-transfected cell lines were obtained from the American Type Culture Collection (ATCC); Wild type (WT) CHO cells (CHO-K1; CCL 61); and Rhesus monkey kidney cells (MKC) (LLC-MK2; CCL 7). These cells were cultured in the following media: WT CHO, S 27 medium minus geneticin; MKC, DMEM + 10% cosmic CS.

Primary rat astrocytes were prepared as described by Rama Rao et al. (2003). Cells were dissociated from the cerebral cortex of neonatal rats in serum-fortified DMEM. After two weeks, the cultures of 95% (+) astrocytes were differentiated with dibutyryl cAMP. Cells were typically used for functional and receptor binding activity after about one total month in culture.

Treatment Protocols for Functional (Cell Volume) Experiments: In the case of primary astroglial cultures, old medium was removed, and fresh medium containing test drugs (e.g. buspirone (500 nM); NAN-190 (50 nM); quipazine (500 nM)), was added. 18 hours later, the cells were assayed by the OMG cell volume method (see below). In the case of serial cultures, cells were harvested in 0.25% trypsin (in phosphate-buffered saline), counted and plated in 6-well plates and cultured to near confluency. At this point, old culture medium was removed, and new medium containing drugs was added as described above.

O-Methyl-Glucose (OMG) Assay (Functional Cell Volume Assay): Following the 18 hours incubation with drugs, [3H]-O-methyl-glucose (OMG) was added to a final concentration of 200 nM, and the cultures were returned to the incubator. 24 hours later, old culture medium was collected and saved for determination of extra-cellular OMG concentration. Cells were then rinsed three times in the following ice-cold buffer: 10 mM Tris; 290 mM sucrose; 0.5 mM calcium nitrate; 10 mM phloretin.

0.5 ml of 1 N NaOH was added to each well, to lyse the cells, and the cultures were incubated at 37°C for 2 hours. Cells were scraped, removed, and aliquots were saved for protein determination and OMG assay. Protein determinations used a colorimetric Coomassie blue assay (Bradford, 1976). 0.25 mL of the cellular homogenate

were mixed with 0.1 ml of formic acid to neutralize the NaOH and counted in Ecoscint scintillation fluid (National Diagnostics, Atlanta) for determination of intracellular OMG. 0.1 mL of the culture medium was also added to Ecoscint and counted by liquid scintillation for determination of extra-cellular OMG. OMG results are expressed as the ratio of intracellular to extra-cellular concentrations. For most assays, conditions were run in triplicate or quadruplicate.

### 5HT Agents and Cell Volume

These experiments were undertaken to explore the following question: Can 5HT agonists and antagonists alter cultured rat astrocyte physiology as measured by a functional cell volume determination. Cell volume was measured using the [<sup>3</sup>H]-OMG method described above. Glucose uptake reflects cell volume as it is not only necessary as a source of energy but also acts as an osmotic agent to keep extracellular and intracellular spaces iso-osmolar. Following an 18-hour treatment with quizapine the extracellular and intracellular amounts of [<sup>3</sup>H]-methyl-glucose were determined. The ligand quipazine, is not highly specific, affecting both 5HT<sub>2a</sub>R and 5HT<sub>3</sub>R. 500 nM quipazine (Figure 31) resulted in a significant reduction in cell volume in rat primary astrocyte cultures versus control, 85.9±2.6% vs. 100±3.1% (p< 0.02). In parallel experiments in rat astrocyte cultures, the 5HT<sub>1a</sub>R partial agonist, buspirone, also modestly reduced cell volume; the 5HT<sub>1a</sub> antagonist, NAN-190 blocked this effect (data not shown). Functional assays with 5HT<sub>2a</sub>R agents in these exploratory experiments were inconclusive. These functional pharmacology experiments gave provisional evidence that cultures of rat astrocytes contain multiple sub-types of 5HT receptors.

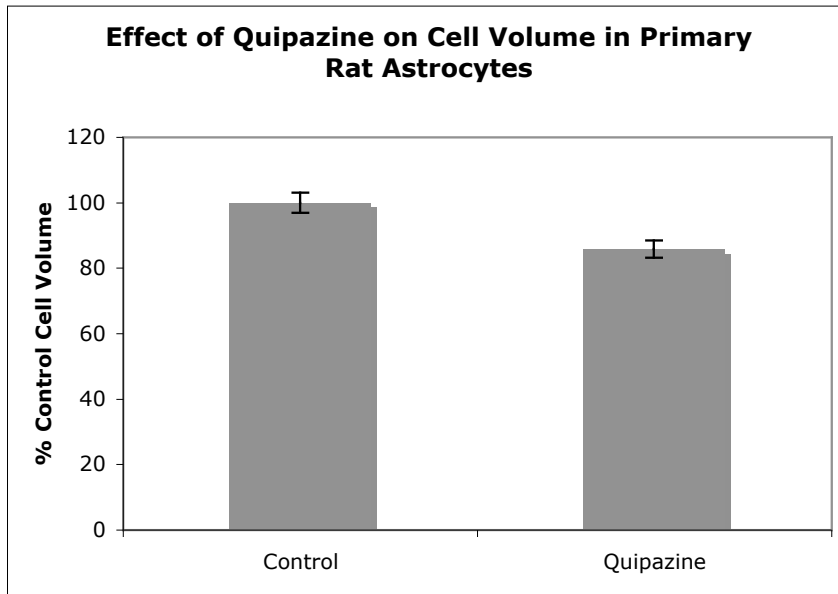


**Figure 31: Serotonergic Effect on Cell Volume of Primary Astrocytes**

The effect of 5HT 2/3R ligand quipazine on the cell volume in rat primary astrocyte cultures. Changes in cell volume were assessed by the uptake of [<sup>3</sup>H]-OMG in astrocytes treated with quipazine and astrocytes not treated as control. Treatment with quipazine resulted in a significant reduction in cell volume versus control 85.9±2.6% vs. 100±3.1% (p< 0.02)

Determination of 5HTR Expression in Primary Rat Astrocytes

Although there have been a number of efforts to characterize 5HTR expression for astrocytes in the in vivo setting, little has been done to study these receptors in primary cell culture of rat astrocytes. This is problematic because the cell culture setting provides a significant model for evaluating serotonin’s functional physiology and pharmacology. To begin the process of characterizing serotonin receptors in primary rat astrocytes, we exposed cultures to varying concentrations of [<sup>3</sup>H]-5HT using an experimental design parallel to that used for the [<sup>3</sup>H]-8-OH-DPAT experiments that comprise the bulk of this dissertation.



Membrane preparations of these astrocytes yielded data for specific [<sup>3</sup>H]-5HT binding that can be divided into two major components when the experiments are conducted in the presence or absence of cold 8-OH-DPAT. Figure 32, represented in double-reciprocal format, shows these two components as DPAT-dependent or independent binding. The DPAT-dependent binding comprises only about 5% of total [<sup>3</sup>H]-5HT binding. This component can also be called the high affinity component of binding as the K<sub>d</sub> for [<sup>3</sup>H]-5HT is in the low nanomolar range (about 1.4 nM).

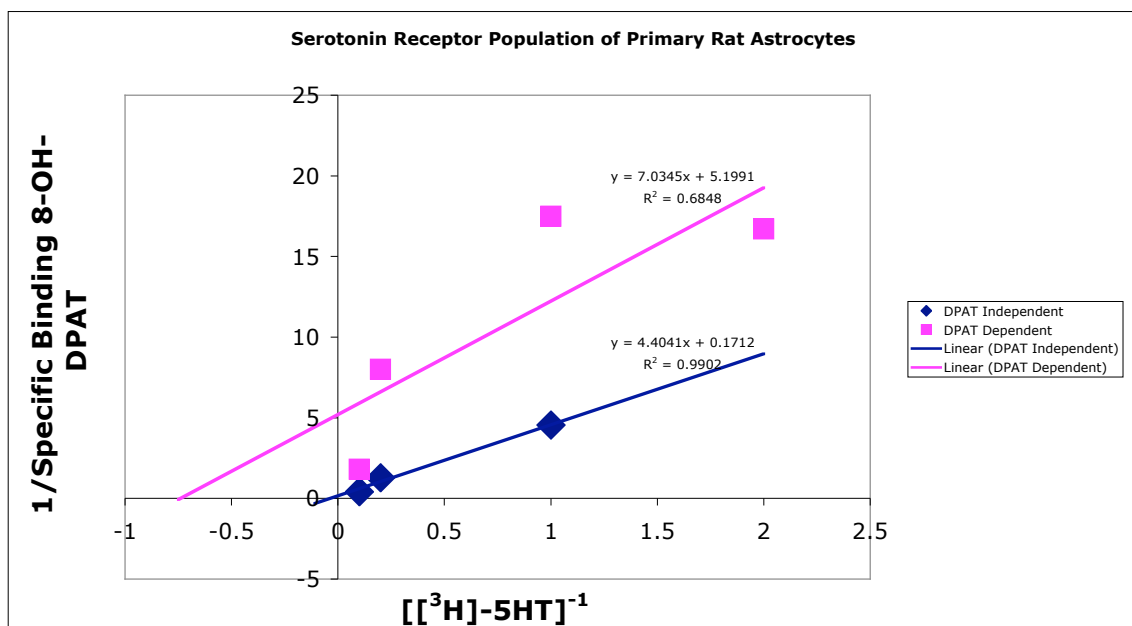


**Figure 32:** Serotonin Receptor Population of Primary Rat Astrocytes Ligand binding assay of [<sup>3</sup>H]-5HT in primary rat astrocytes. The upper line (square shape) is the 8-OH-DPAT dependent line (for receptors 5HT1a and 5HT7). The lower line (diamond shape) represents 8-OH-DPAT independent binding.

In additional preliminary investigations, we designed experiments to further subdivide the high and low affinity components of [<sup>3</sup>H]-5HT binding. Even though 8-OH-DPAT is typically described as specific for the 5HT<sub>1a</sub>R, like any drug, it is imperfectly discrete. It also has activity at the 5HT<sub>7</sub>R. The agent carbamidotryptamine is reasonably selective for the 5HT<sub>7</sub>R compared to 5HT<sub>1a</sub>R. Thus, if experiments are conducted with the high affinity, 8-OH-DPAT-dependent component of [<sup>3</sup>H]-5HT binding either in the presence or absence of carbamidotryptamine, an estimate of the ratio of 5HT<sub>1a</sub>R/5HT<sub>7</sub>R presence can be made. These experiments were conducted, with the following result: approximately 20% of the high affinity binding is due to 5HT<sub>1a</sub>R and about 70% is contributed by the 5HT<sub>7</sub>R (data not shown); another 10% is either in the realm of experimental error or to some other, unknown high affinity receptor.

Recall that only 5% of total [<sup>3</sup>H]-5HT binding is in the high affinity realm; thus, 95% of the binding is lower affinity. What had been previously known about primary cultured rat astrocytes was that the 5HT<sub>2a</sub>R is expressed in these cells (Deecher et al., 1993). Our preliminary studies with quipazine in the cell volume functional assay fit this observation, but quipazine also is not completely specific. It has been demonstrated to possess both 5HT<sub>2a</sub>R and 5HT<sub>3</sub>R activity. Thus, we hypothesized that the low affinity binding component in these cells could also have a 5HT<sub>3</sub>R component. To test this hypothesis, we conducted two sets of low affinity (high [3H] 5-HT conc.) experiments, one in the presence of ketanserin, a modestly specific 5HT<sub>2a</sub> antagonist, and one in the presence of ondansetron, a fairly specific 5HT<sub>3</sub>R antagonist. The preliminary results

suggest that about 30% of the low affinity binding is due to the 5HT3R and about 70% is represented by the 5HT2aR (data not shown).

These early experiments suggest that primary cultured rat astrocytes express four different serotonin receptors: 5HT1a, 5HT7, 5HT2a, and 5HT3. The initial nature of these results must be verified by additional repetition of the experiments and direct testing for the various receptor sub-types by using labeled specific analogues such as [3H]-8-OH-DPAT, [3H]-odansetron, etc. These exciting experiments, however, are beyond the temporal scope of this dissertation project. The expression of these receptor subtypes can be confirmed by RTPCR, which measures translation of genes to mRNA. However, this does not guarantee expression of the protein of interest.

#### Determination of 5HT1aR Expression in MKC Cells

We wanted to test specificity of the 5HT effect on cell volume (especially regarding 5HT1aR) by conducting additional experiments in cells known to express or not express 5HTR. There have been no published reports of the 5HT1aR being expressed in MKC cells. To determine if the receptor is present, we employed ligand binding experiments with the 5HT1aR ligand [<sup>3</sup>H]-8-OH-DPAT. In membrane preparations of MKC, a concentration dependent increase in specific binding of [<sup>3</sup>H]-8-OH-DPAT was observed versus control (Figure 33). To determine if the receptor is actually expressed and our data is not an artifact, RTPCR and specific antibodies for the 5HT1aR can be utilized in future studies.

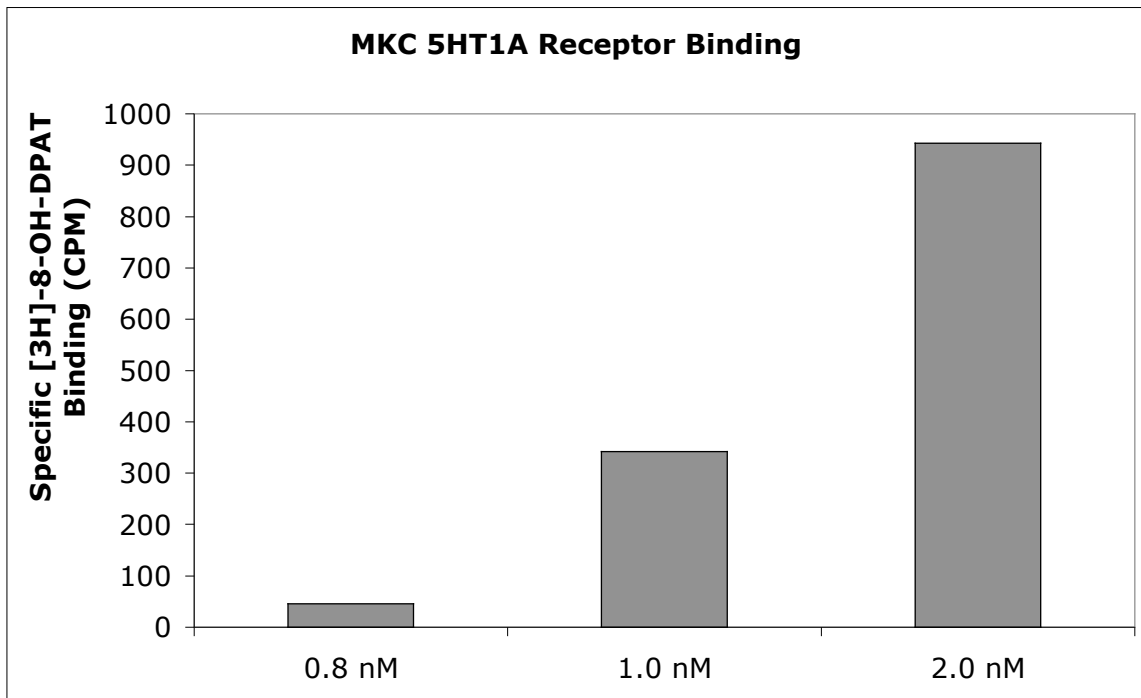


**Figure 33:** MKC 5HT1a Receptor Binding

A binding assay with the radiolabeled 5HT1aR ligand [<sup>3</sup>H]-8-OH-DPAT shows a concentration dependent (x-axis) increase in specific binding, suggesting that the MKCs do indeed express the 5HT1aR. Specific binding is total minus non-specific (NS) binding of triplicates. NS binding is conducted in the presence of 10 μM 5HT.

### Buspirone Affect on MKC volume

The addition of 500 nM buspirone to MKC followed by [<sup>3</sup>H]-OMG incubation showed a small decrease in cell volume as a percent of control (Figure 34). The change in cell volume was 94±4% for buspirone treated cells versus 100±5% for control. While not significant, this effect hints that a similar result to that seen in the primary rat astrocytes could occur upon optimization of experimental conditions. To further test the hypothesis that 5HT1aR agonists like buspirone, reduce cell volume in cells containing 5HT1aR, but not in cells lacking the receptor, we conducted experiments in the CHO cells containing cloned H5HT1aR. Buspirone reduced cell volume by 7% (data not shown). The volume reduction effect is blocked by the 5HT1aR specific antagonist NAN-190 (data not shown). While this effect is small, it should be noted that this activity occurs in cells that have not been challenged. It is anticipated that cells challenged with an agent causing cell swelling (like ammonia) will show a larger response to 5HT1aR agonists. Additional experiments were run in wild type CHO cells (that do not express 5HT1aR) and in 3T3 fibroblasts that express 5HT2aR. Buspirone had no effect on cell volume in these cells (data not shown).

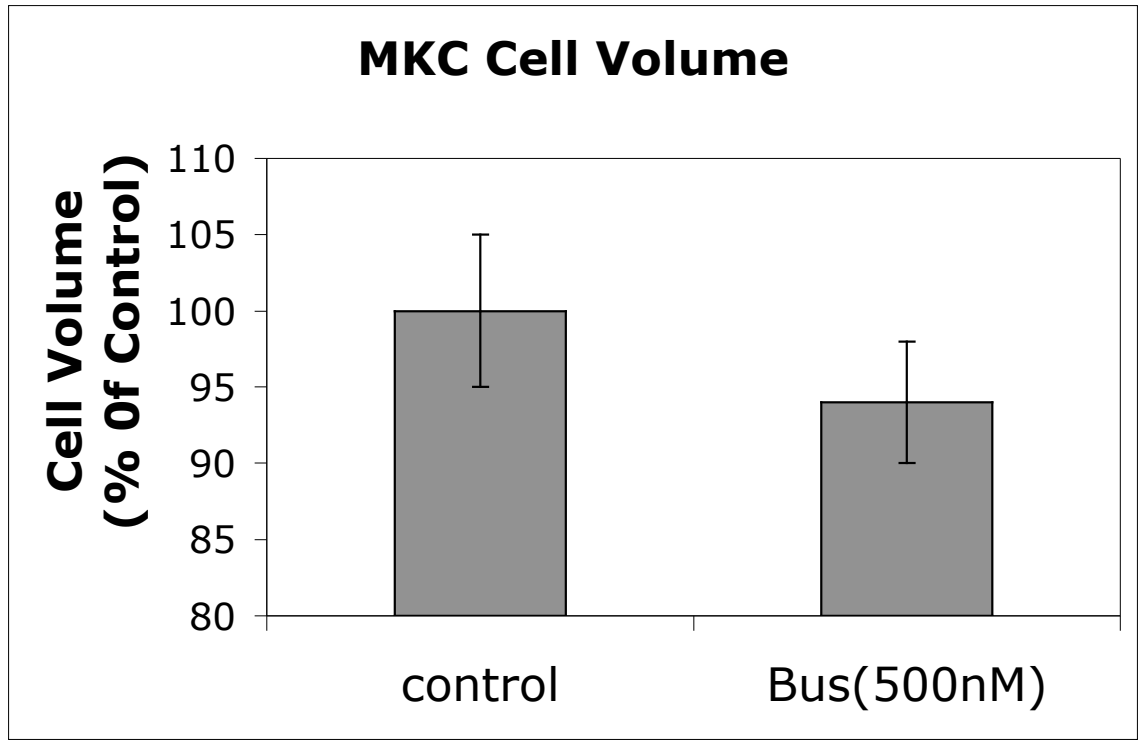


**Figure 34:** Buspirone Effect on MCK Cell Volume

500 nM Buspirone was able to reduce the cell volume of monkey kidney cells relative to control. Cell volume was assessed by cellular uptake of [<sup>3</sup>H]-OMG by MKC cells. MKCs have not been reported to express the 5HT1aR. 94±4% for buspirone treated cells versus 100±5% for control.

## Cell Volume Discussion

It is noteworthy that the MKC cell line has a nearly identical response to buspirone as the CHO line transfected with H5HT1aR and the cultured rat primary astrocytes; the results presented here are, to the best of our knowledge, the first demonstration of 5HT1aR agonist binding and effect in this cell line and in the primary astrocyte cultures. The effect of the 5HT1a partial agonist buspirone seems to be specific as cells that either do not express 5HT1aR or express some other 5HTR are unresponsive to the agent.

These initial studies set the stage for further work examining the mechanisms of 5HT1aR-linked changes in cell volume. Of particular interest will be development of a cell damage model, expansion of dose-responsiveness and ligand specificities, and extension of the work into coupling of the receptor activation to signal transduction networks. It should be pointed out though, that cell volume regulation in rat astrocyte culture does not seem to be a function of 5HT1aR alone. Since the cultured astrocytes also express 5HT7R, 5HT2aR, and 5HT3R, and at the very least, 5HT3R seems to be functional (quipazine reduction of cell volume; Figure 31), 5HT regulation of cell volume needs to be explored in the context of multiple 5HTR. These initial investigations promise a series of potentially meaningful projects in the future.

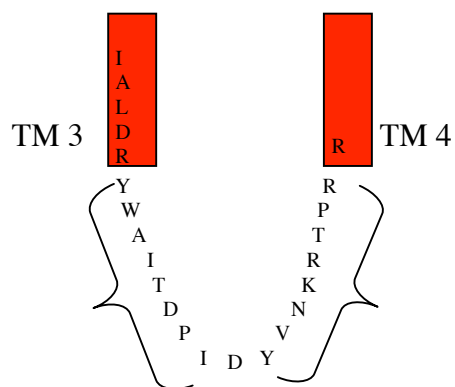


**Figure 35:** Intracellular Loop 2 (ic2) of 5HT1aR

A pictographic representation of the 17 amino acid second intracellular loop 2 of the 5HT1aR. The first amino acid shown in transmembrane domain 3 (TM 3) I is the first amino acid residue in the peptide mimic P11. The last amino acid residue shown in transmembrane domain 4 (TM 4) R is the final amino acid residue in ic2 peptide mimic P27.

Compound	Sequence
P11	IALDRYWAITD
P21	LDRYWAITDP
P22	RYWAITDPID
P23	WAITDPIDYV
P24	ITDPIDYVNK
P25	DPIDYVNKRT
P26	IDYVNKRTPR
P27	YVNKRTPRPR